Julius-Maximilians-Universität Würzburg
Graduate School of Science and Technology

Doctoral thesis / Dissertation

for the doctoral degree / *zur Erlangung des Doktorgrads*

Doctor rerum naturalium (Dr. rer. nat.)

Modelling Carbon Sequestration of Agroforestry Systems in West Africa using Remote Sensing

Modellierung der Kohlenstoffbindung von agroforstwirtschaftlichen Systemen in Westafrika mittels Fernerkundung

Submitted by

KANMEGNE TAMGA Dan Emmanuel

From Yaoundé, Cameroon

Würzburg, 2023

Submitted on: …….

Stamp Graduate School

Members of thesis committee

Chairperson: ……..…….

1. Reviewer and Examiner: Prof. Dr. Tobias Ullmann

2. Reviewer and Examiner: Prof. Dr Roland Baumhauer

3. Examiner: PD Dr. Hooman Latifi

Day of thesis defense: …….

To my son

GABISSI KANMEGNE Kenan Misericorde

Table of contents

List of Figures

List of Tables

List of Appendices

List of abbreviations

AFP	Agroforestry Practices
AFS	Agroforestry Systems
AGB	Aboveground Biomass
ALOS	Advanced Land Observation Satellite
AUC	Area Under the Curve
BGB	Belowground Biomass
BI	Biodiversity Index
CDM	Clean Development Mechanism
CIFOR	Centre for International Forestry Research
CO_2	Carbon dioxide
COP	Conference of Parties
ECOWAS	Economic Community of West African States
ER	Certified Emission Reduction
ESA	European Space Agency
EU	European Union
EVI	Enhanced Vegetation Index
FAO	Food and Agriculture Organization of the United Nations
FRL	Forest Reference Level
GEDI L4A	level 4A product of GEDI
GEDI	Global Ecosystem Dynamics Investigation
GEE	Google Earth Engine
GHG	Greenhouse Gas
GLCM	Grey-Level Co-Occurrence Matrix
GLI	Green Leaf Index
GPG	Good Practice Guidance
GWR	Geographically Weighted Regression
ICRAF	World agroforestry Centre

IDRC	International Development Research Centre
IPCC	Intergovernmental Panel on Climate Change
IR	Infrared Radiation
LiDAR	Light Detection and Range
LULUCF	Land Use, Land Use Change and Forestry
ML	Machine Learning
MRV	Measurement Reporting and Verification
MSAVI	Modified Soil Adjusted Vegetation Index
NDCs	National Determined Contributions
NDVI	Normalized Difference Vegetation Index
NICFI	Norway's International Climate and Forest Initiative
OA	Overall Accuracy
PA	Producer's Accuracy
PALSAR	Phased Array L-band Synthetic Aperture Radar
ppm	parts per million
REDD+	Reduction of Emissions from Deforestation and Forest Degradation
RMSE	Root Mean Square Error
ROI	Region of Interest
RS	Remote Sensing
SAR	Synthetic Aperture Radar
SAVI	Soil Adjusted Vegetation Index
SI	Simpson Index
SLAR	Side-looking Airborne Radar
SOC	Soil Organic Carbon
SVM	Support Vector Machine
TCARI	Transformed Chlorophyll Absorption in Reflectance Index
TNP	Taï National Park
UA	User's Accuracy
UAV	Unmanned aerial vehicle

UNESCO	United Nations Educational, Scientific and Cultural Organization
UNFCCC	United Nations Framework Convention on Climate Change
VARI	Visible Atmospherically Resistance
VSURF	Variable Selection Using Random Forest

Abstract

The production of commodities such as cocoa, rubber, oil palm and cashew, is the main driver of deforestation in West Africa (WA). The practiced production systems correspond to a land management approach referred to as agroforestry systems (AFS), which consist of managing trees and crops on the same unit of land. Because of the ubiquity of trees, AFS reported as viable solution for climate mitigation; the carbon sequestrated by the trees could be estimated with remote sensing (RS) data and methods and reported as emission reduction efforts. However, the diversity in AFS in relation to their composition, structure and spatial distribution makes it challenging for an accurate monitoring of carbon stocks using RS. Therefore, the aim of this research is to propose a RS-based approach for the estimation of carbon sequestration in AFS across the climatic regions of WA. The main objectives were to (i) provide an accurate classification map of AFS by modelling the spatial distribution of the classification error; (ii) estimate the carbon stock of AFS in the main climatic regions of WA using RS data; (iii) evaluate the dynamic of carbon stocks within AFS across WA. Three regions of interest (ROI) were defined in Cote d'Ivoire and Burkina Faso, one in each climatic region of WA namely the Guineo-Congolian, Guinean and Sudanian, and three field campaigns were carried out for data collection. The collected data consisted of reference points for image classification, biometric tree measurements (diameter, height, species) for biomass estimation. A total of 261 samples were collected in 12 AFS across WA. For the RS data, yearly composite images from Sentinel-1 and -2 (S1 and S2), ALOS-PALSAR and GEDI data were used. A supervised classification using random forest (RF) was implemented and the classification error was assessed using the Shannon entropy generated form the class probabilities. For carbon estimation, different RS data, machine learning algorithms and carbon reference sources were compared for the prediction of the aboveground biomass in AFS. The assessment of the carbon dynamic was carried between 2017 and 2021. An average carbon map was generated and use as reference for the comparison of annual carbon estimations, using the standard deviation as threshold. As far as the results are concerned, the classification accuracy was higher than 0.9 in all the ROIs, and AFS were mainly represented by rubber (38.9%), cocoa (36.4%), palm (10.8%) in the ROI-1, mango (15.2%) and cashew (13.4%) in ROI-2, shea tree (55.7) and African locust bean (28.1%) in ROI-3. However, evidence of misclassification was found in cocoa, mango, and shea butter. The assessment of the classification error suggested that the error level was higher in

the ROI-3 and ROI-1. The error generated from the entropy was able reduced the level of misclassification by 63% with 11% of loss of information. Moreover, the approach was able to accurately detect encroachment in protected areas. On carbon estimation, the highest prediction accuracy ($R^2 \geq 0.8$) was obtained for a RF model using the combination of S1 and S2 and AGB derived from field measurements. Predictions from GEDI could only be used as reference in the ROI-1 but resulted in a prediction error about 9 times higher than when using field measurements. It was found that the prediction error was higher in cashew, mango, rubber and cocoa plantations, and the carbon stock level was higher in African locust beans (43.9 t/ha), shea butter (15t/ha), cashew (13.8 t/ha), mango (12.8 t/ha), cocoa (7.51 t/ha) and rubber (7.33 t/ha). The analysis showed that carbon stock is determined mainly by the diameter ($R^2=0.45$) and height ($R^2=0.13$) of trees. It was found that crop plantations had the lowest biodiversity level, and no significant relationship was found between the considered biodiversity indices and carbon stock levels. The assessment of the spatial distribution of carbon sources and sinks showed that cashew plantations are carbon emitters due to firewood collection, while cocoa plantations showed the highest potential for carbon sequestration. The study revealed that Sentinel data could be used to support a RS based approach for modelling carbon sequestration in AFS. Entropy could be used to map crop plantations and to monitor encroachment in protected areas. Moreover, field measurements with appropriate allometric models could ensure an accurate estimation of carbon stocks in AFS. Even though AFS in the Sudanian region had the highest carbon stocks level, there is a high potential to increase the carbon level in cocoa plantations by integrating and/or maintaining forest trees.

Zusammenfassung

Die Produktion von Rohstoffen wie Kakao, Kautschuk, Ölpalmen und Cashew ist die Hauptursache für die Entwaldung in Westafrika (WA). Die verwendeten Produktionssysteme entsprechen einem Landbewirtschaftungskonzept, welches als Agroforstsysteme (AFS) bezeichnet wird und darin besteht, Bäume und Nutzpflanzen auf der gleichen Landeinheit zu bewirtschaften. Aufgrund der kohlenstoffbindung durch Bäumen sind AFS als praktikable Lösung für den Klimaschutz anerkannt, und der von den Bäume sind AFS als praktikable Lösung für den Klimaschutz anerkannt, die Vielfalt der AFS in Bezug auf ihre Zusammensetzung, Struktur und räumliche Verteilung erschwert jedoch eine genaue Schätzung der Kohlenstoffvorräte. Hier können Daten und Methoden der satellitenbasierten Erdbeobachtung ansetzten. Ziel dieser Forschungsarbeit ist es daher, einen fernerkundungs-basierten Ansatz für die Schätzung der Kohlenstoffbindung in AFS in den Klimaregionen von WA vorzuschlagen. Die Hauptziele waren (i) die Erstellung einer genauen Klassifizierungskarte von AFS durch Modellierung der räumlichen Verteilung des Klassifizierungsfehlers; (ii) die Schätzung des Kohlenstoffbestands von AFS in den wichtigsten Klimaregionen von WA unter Verwendung von Fernerkundungs-daten (RS); (iii) die Bewertung der räumlichen Verteilung von Kohlenstoffquellen und -senken innerhalb von AFS in ganz WA. Für jede Klimaregion in Westafrika wurden drei Regionen von Interesse (ROI) festgelegt, nämlich die guineisch-kongolesische (ROI 1), die guineische (ROI 2) und die sudanesische Region (ROI 3) in Côte d'Ivoire und Burkina Faso, und es wurden drei Feldkampagnen zur Datenerhebung durchgeführt. Die gesammelten Daten bestanden aus Referenzpunkten für die Bildklassifizierung und biometrischen Messungen (Durchmesser, Höhe, Artname) zur Schätzung der Biomasse. Insgesamt wurden 261 Proben in 12 AFS in ganz WA gesammelt. Für die RS-Daten wurden jährliche Komposite von Sentinel-1 und -2 (S1 und S2), ALOS-PALSAR und GEDI-Daten verwendet. Es wurde eine überwachte Klassifizierung mit Random Forest (RF) Algorithmus durchgeführt, und der Klassifizierungsfehler wurde anhand der aus den Klassenwahrscheinlichkeiten generierten Shannon-Entropie bewertet. Für die Kohlenstoffschätzung wurden verschiedene RS-Daten, Algorithmen für maschinelles Lernen und Kohlenstoff-Referenzquellen für die Vorhersage des Kohlenstoffs in AFS verglichen. Die Bewertung der räumlichen Verteilung von Kohlenstoffsenken und -quellen basierte auf der Bewertung von Anomalien in der Kohlenstoffdynamik zwischen 2017 und 2021. Es wurde eine

Karte zum durchschnittliche gebundenen Kohlenstoff erstellt, und die jährliche Differenz wurde verwendet, um Kohlenstoffsenken und -quellen zu identifizieren. Die Klassifizierungsgenauigkeit war in allen ROI höher als 0,9, und in der Region dominierten Kautschuk (38,9 %), Kakao (36,4 %), Palme (10,8 %) in ROI-1, Mango (15,2 %) und Cashew (13,4 %) in ROI-2, Sheabaum (55,7) und Johannisbrot (28,1 %) in ROI-3. Hinweise auf eine Fehlklassifizierung wurden vor allem bei Kakao, Mango und Sheabutter gefunden. Die Bewertung des Klassifizierungsfehlers ergab, dass das Fehlerniveau in ROI-3 und ROI-1 höher war. Der aus der Entropie generierte Fehler konnte das Ausmaß der Fehlklassifizierung reduzieren, ohne die gut klassifizierten Pixel zu beeinträchtigen. Außerdem war der Ansatz in der Lage, Eingriffe in Schutzgebiete zuverlässig und akkurat zu erkennen. Was die Kohlenstoffschätzung betrifft, so wurde die höchste Vorhersagegenauigkeit ($R^2 \geq 0,8$) bei der Kombination von S1 und S2 mit Random Forest und AGB aus Feldmessungen erzielt. Vorhersagen von GEDI konnten nur als Referenz in der ROI-1 verwendet werden, führten aber zu einem Vorhersagefehler, der etwa 9-mal höher war als bei der Verwendung von Feldmessungen. Es wurde festgestellt, dass der Vorhersagefehler bei Cashew-, Mango-, Kautschuk- und Kakaoplantagen höher war und der Kohlenstoffbestand bei Johannisbrot (43,9 t/ha), Sheabutter (15 t/ha), Cashew (13,8 t/ha), Mango (12,8 t/ha), Kakao (7,51 t/ha) und Kautschuk (7,33 t/ha) höher war. Die Analyse zeigte, dass der Kohlenstoffbestand hauptsächlich durch den Durchmesser ($R^2=0,45$) und die Höhe ($R^2=0,13$) der Bäume beeinflusst wird. Zudem wurde festgestellt, dass Plantagenkulturen die geringste Biodiversität aufweisen, und es wurde kein signifikanter Zusammenhang zwischen Biodiversitätsindizes und Kohlenstoffvorräten festgestellt. Die Bewertung der räumlichen Verteilung von Kohlenstoffquellen und -senken zeigte, dass Cashew ein Kohlenstoffemittent ist, da in dieser Region Brennholz gesammelt wird, während Kakaoplantagen wichtige Kohlenstoffsenken sind. Die Studie ergab zudem, dass Sentinel-Daten zur Unterstützung eines RS-basierten Ansatzes für die Modellierung der Kohlenstoffbindung in AFS verwendet werden könnten. Die Entropie könnte zur Kartierung von Anbauplantagen und zur Überwachung von Schutzgebiete verwendet werden. Darüber hinaus gewährleisten Feldmessungen mit geeigneten allometrischen Modellen eine genaue Schätzung der Kohlenstoffvorräte in AFS. Die AFS in der sudanesischen Region weisen die höchsten Kohlenstoffvorräte auf, aber es besteht die Möglichkeit, den Kohlenstoffgehalt in Kakaoplantagen durch die Integration und/oder Erhaltung von Waldbäumen zu erhöhen.

Chapter 1
Introduction

1.1 Carbon on earth

Carbon is a nonmetallic chemical element widely distributed in nature just like oxygen, hydrogen or Aluminum. His symbol in the periodic table is C, and it has an atomic number of 6. The atoms of carbon can bond to one another in different ways to from various allotropes of C, which refers to the property of some chemical elements to exist in two or more different forms in the same physical state. Some of the well-known allotropes of C include graphite which are used in pencils and electrodes, and diamond. Carbon is the 15^{th} most abundant element in the earth crust and the fourth most abundant element in the universe by mass after hydrogen, helium and oxygen.

Atoms of C can bond also to the five main chemical elements that make up all living things namely hydrogen, nitrogen, oxygen, phosphorus and sulfur (commonly known as CHNOPS) to form complex biological molecules. By mass, C is the second most abundant element in plants (12%) and animals (19%) after oxygen, and is found in carbohydrates, lipids, nucleic acids and proteins (Fischer et al., 2020). Because of its abundance, its unique diversity of organic compounds, and its ability to form polymers at temperatures commonly encountered on earth, C is the primary component of all known life on earth and is stored in the form of biomass and coal, often referred to as solid or sequestrated carbon. Such forms of carbon have a high energy density and is up to date the main source of energy for human activities including industries, transportation and electricity. Through combustion, sequestrated carbon is realized in the atmosphere following the equation below.

$$\text{Solid carbon} + O_2 \longrightarrow CO_2 + H_2O$$

C is also found in the atmosphere in the form of carbon dioxide (CO_2) and represents about 0.04% of its composition. CO_2 plays an important role in the atmosphere by regulating the temperature on earth, but is also the most important element for the development of photosynthetic plants. They are the first layer in maintaining life on earth by producing oxygen according to the equation below where $C_6H_{12}O_6$ represent sugar, a form of solid carbon.

$$6\,CO_2 + 6\,H_2O \xrightarrow[Sunlight]{Chlorophyll} C_6H_{12}O_6 + 6O_2$$

In the atmosphere and at the surface of oceans, CO_2 can react with water to form carbonic acid. Carbon is incorporated into water causing an acidification of the solution (reducing the pH). The process is represented in the equation below where H_2CO_3 stands for carbonic acid.

$$CO_2 + H_2O \rightleftharpoons H_2CO_3$$

A consequence of the relationship between CO2 and water is that, higher concentrations of carbon in the atmosphere will lead to more acid surface water on earth, which has negative impact on the biodiversity (Widdicombe & Spicer, 2008).

1.1.1 Carbon cycle

Under terrestrial conditions, the conversion of one chemical element to another is very rare. Therefore, the total amount of C on earth is constant, moving between the atmosphere, biosphere, hydrosphere and lithosphere. The paths of carbon in the environment is known as carbon cycle (Figure 1). The process goes as follow: carbon in the atmosphere is absorbed by plants during photosynthesis. It is a process by which plants and other organisms convert light energy into chemical energy using CO_2 and water. The synthesized chemical energy could be used to fuel the organism's activity or could be stored as biomass and/or starches. The carbon goes from the atmosphere to the biosphere through photosynthesis, and from the biosphere through the atmosphere through respiration, decomposition and/or combustion (a wild fire for example). Carbon is stored in the biosphere in the form of forest biomass. The carbon stored in plants is transferred to all links in the food chain. The energy will flow from plants to herbivores, carnivores and finally decomposers. The carbon is transferred from the biosphere to the lithosphere (soil) through decomposition in the form of dead organisms and animal waste. Carbon in the soil is not transferred in the biosphere, and can be stored for a long time: therefore, they are referred to as carbon sinks or carbon reservoirs. However, the carbon could be released in the atmosphere through fires, or poor agricultural practices (ploughing and erosion for instance). Under specific conditions, soil organic carbon could be transformed into rocks fossils and fossil fuels. Ocean also play a significant role in the carbon cycle as it is the largest carbon sink, followed by soils and forests. It is estimate that the amount of CO_2 in the oceans is about 50 times greater than the amount in the atmosphere (Bopp et al., 2002). Surface waters exchange gases with the atmosphere partly through phytoplankton and their photosynthetic activities, but also because CO_2 can dissolve in

ambient seawater that is not saturated. The dissolved carbon increases the pH and cause an increase in water density via the solute density effect and is stored in the form of calcium carbonate (Morgado & Esteves, 2014).

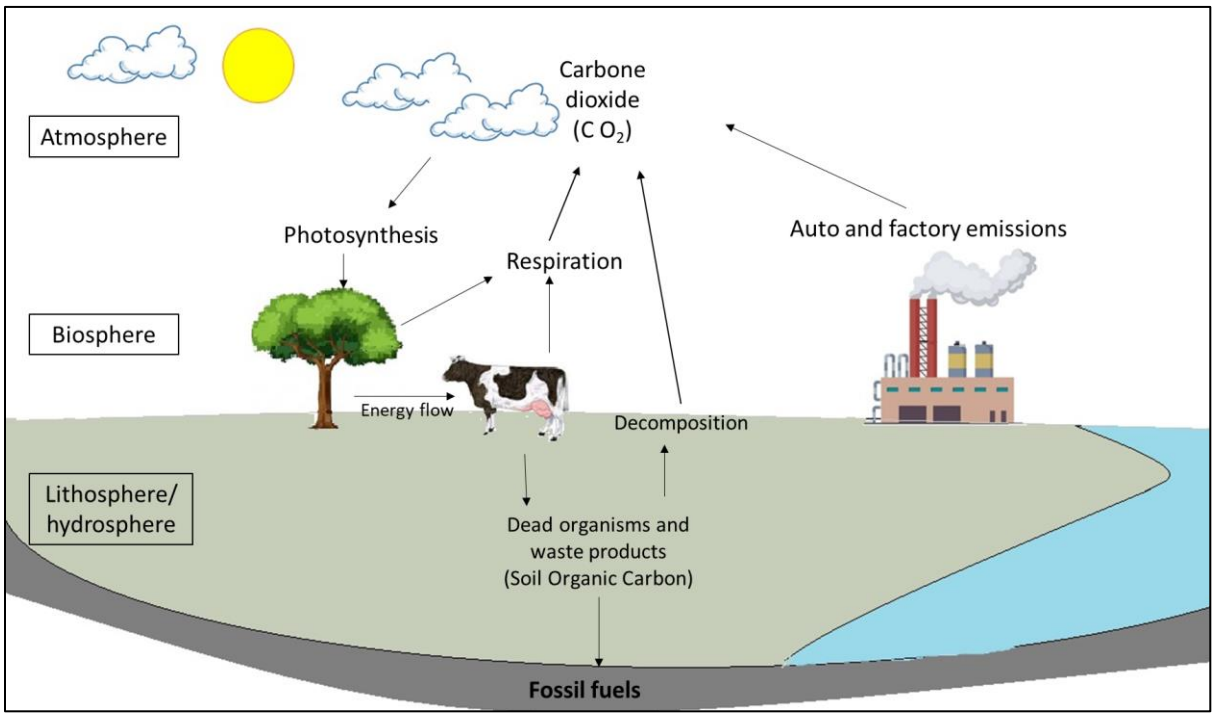

Figure 1:Carbon cycle on earth (created by the author).

C stored in stable forms such as forest biomass, soil organic carbon and/or fossil fuels is said to be sequestrated, and the process of collecting atmospheric carbon and storing it in the form of biomass is called carbon sequestration. On the other hand, releasing stored carbon in the atmosphere through combustion and/or land cover change (deforestation) is referred to as carbon emissions. Both of these processes have a significant effect on one of the most important natural phenomena known as the greenhouse effect.

1.1.2 Greenhouse effect

Greenhouse effect is the process by which heat is trapped close to the earth's surface by greenhouse gases (GHG) to maintain a favorable temperature for life on earth. Without this, the global average temperature would be -18°C. The main GHG include water vapor and clouds (36-72%). Water vapor is the most abundant greenhouse gas in the atmosphere, but human activities have only small

direct influence on its atmospheric concentration (Table 1). However other GHG are produced and emitted through human activities associated with industrialization.

Table 1: Greenhouse gases and their contribution to the greenhouse effect

Compound	Formula	Concentration in the atmosphere (ppm)	Contribution (%)
Water vapor and clouds	H_2O	10- 50000	36 - 72
Carbon dioxide	CO_2	~400	9 - 26
Methane	CH_4	~1.8	4 - 9
Ozone	O_3	2 - 8	3 - 7

When the sun emits radiation towards the earth, not all the energy reaches the earth surface: a portion of the emitted radiation is reflected back into space by the top of the atmosphere. The proportion of solar energy that reaches the surface of the earth is often referred to as incident radiation. At the top of the earth, a portion of the incident radiation is also reflected back in the atmosphere by different materials on the earth surface and some of the incident radiation is absorbed. The absorbed energy is converted into heat, and is radiated in the atmosphere in the form of infrared (IR). A portion of the IR radiation will go through the atmosphere into space, while some the rest will be trapped by GHG and reflect back to the earth surface. This phenomenon is called the greenhouse effect. It is crucial to maintain an optimal temperature for life on earth. The average global temperature for the 20^{th} century was 13.9°C instead of -18°C if there were no greenhouse gases.

However, changes of the landcover as well as of the concentration of the GHG in the atmosphere could lead to the accentuation of the greenhouse effect. Tree canopies filter in-coming solar radiation, by reflecting about 86 -97% of the incident radiation in the tropics depending on the tree species and leaf density (Shahidan et al., 2006). Trees reduce the energy reaching the ground, resulting in reduced IR radiation levels. Therefore, the microclimate is modified through the cooling effect of trees which is acknowledged to have a significant effect on reducing land surface temperature (Schwaab et al., 2021). On the contrary, the conversion of forest into bare soil and cities increases the surface of incident radiation absorption, leading to a higher level of IR radiation, resulting in increase in the average temperature.

Moreover, it is recorded that the global atmospheric concentrations of CO_2, CH_4, NO and certain manufactured GHG have risen significantly over the last few hundred years. Also, the concentration of CO_2 has increased substantially (48%) since the beginning of the industrial era, rising from an annual average of 280 ppm in the late 1700s to 414 ppm in 2021 (EPA, 2022). This has a direct impact on increasing the global land-Ocean temperatures (Lin et al., 2023). In a nutshell, the land cover change combined with the increased concentration of GHG in the atmosphere contribute to the accentuation of the greenhouse effect, resulting in the increase of the land surface temperature: this situation is often referred to as global warming.

1.2 Global warming and climate change

Several definitions are proposed for global warming: on Wikipedia, global warming is presented as the long-term heating of earth's surface observed since the pre-industrial period (between 1850 and 1900) due to human activities, primarily fossil fuel burning, which increases heat-trapping GHG levels in the atmosphere. In the IPCC special report, it is defined as the estimated increase in global mean surface temperature averaged over a 30-year period (IPCC, 2018). Global warming is different from climate change even though both terms are often used interchangeably. Climate change refers to a change in the state of the climate that can be identified (using statistical test for example) by changes in the mean and/or the variability of its properties and that persists for an extended period, typically decades or longer. Climate change may be due to natural internal processes or external forcing such as modulations of the solar cycles, volcanic eruptions and persistent anthropogenic changes in the composition of the atmosphere or in land use (IPCC, 2018). The United Nations Framework Convention on Climate Change (UNFCCC), in its article 1 defines climate change as "a change of climate which is attributed directly or indirectly to human activity that alters the composition of the global atmosphere and climate variability attributable to natural causes".

There is a high confidence that human induced global warming has increased the global mean surface temperature to approximately 1°C above pre-industrial values, and if the current warming rate continues, it will reach 1.5°C by 2040, with major impacts on natural and human systems (IPCC, 2018). Glaciers and sea ice melting are important indicators of global warming because their physical changes (growing or shrinking, advancing or receding) provide evidence of changes

in temperature and precipitation. They also act as reservoirs of freshwater, and provide water to ecosystems when melting. Under global warming, glaciers melt faster and increase sea levels, which in turn increases coastal erosion and elevates storm surge as warming air and ocean temperatures create more frequent and intense coastal storms like hurricanes and typhoons (Collins & Walsh, 2017). Glaciers melting also cause the loss of terrestrial and aquatic species as glaciers are natural habitats for endangered species including polar bears, artic fox and narwhal but also modifies the chemical composition of oceans which affects the aquatic biosphere. This process will also result in less freshwater available to support natural and human ecosystems including less water for consumption, lower hydroelectric energy generation capacity and less water available for irrigation. Finally, glaciers melting contribute to climate change as it slows the ocean currents which play a fundamental role in shaping the climatic zones on earth (Marsh & van Sebille, 2021). In fact, ocean currents help counteract the uneven distribution of solar radiation that reaches the earth's surface by transporting warm water and precipitations from the equator toward the poles and cold water from the poles back to the tropics. Without ocean currents (or with slowed ocean currents), regional temperatures will be more extremes with very high temperatures at the equator and very low temperatures towards the poles.

On land, the frequency and intensity of heavy precipitations are expected to increase under global warming, with fewer rainy days and shifted rainy seasons especially in tropical Africa (Deque et al., 2017). This will increase the risk of flooding events as the precipitation will exceed the infiltration rate in certain region. Moreover, heavy rainfall will increase soil erosion and runoffs especially in slope land, therefore decreasing soil fertility with severe effects on agricultural and livestock activities (Meng et al., 2021). Increasing temperatures combined with fewer rainy days results in increasing evapotranspiration which affects water availability in ecosystem (Zhao et al., 2022). In fact, under higher temperature, water in plants and in the top layers of the soil evaporates causing acute stress on plants especially in dry seasons, increasing the risk of desertification in natural area and lowering the productivity of agriculture systems. Another impact is the frequent occurrence of severe drought events, heatwaves and natural fires especially in the Mediterranean region and West Africa (IPCC, 2013).

Beyond natural systems, climate change also affects human systems including water availability, energy and health. In many areas, people's demand for drinking water as well as water for

agricultural activities will increase, while water availability is likely to decrease as a response to climate change. Due to frequent hazard events such as flooding and runoffs, water quality is expected to be affected because of nutrients and sediments pollution. In Coastal areas, the advancing of salty water into the land due to increase of sea level is likely to contaminate fresh waterbodies and causing important stress on water infrastructures according to the projections under an increase of 2°C above pre-industrial time (IPCC, 2018). Moreover, it is reported that global warming increases the risk of epidemic and infectious diseases. Over half of the know human pathogenic diseases is likely to be aggravated by climate change as climatic hazards contributes to their transmission (Zhao et al., 2022). The lifecycles of the pathogens, their spatial distribution and the animals that carry them are influenced by global warming and changes in the seasonal patterns. Also, habitat degradation through deforestation and other anthropogenic-induced activities increases the contact between humans and animals increasing the risk of disease transfer.

1.3 Responses to climate change

The beginning of the history of climate change could be traced back to the year 1824 when the French physicist Joseph Fourier first described the greenhouse effect, which is responsible of maintaining the earth warm. Few years later in 1896, the Swedish chemist Svante Arrhenius suggested that industrial-age coal burning will enhance the natural greenhouse effect. In 1900, the finding of Knut Angstrom revealed that even at lower concentrations, CO_2 in the atmosphere strongly absorbs parts of the infrared spectrum emitted from the earth, thus showing that the increasing concentration of certain gas in the atmosphere could increase the greenhouse effect. It was in 1938 that British engineer Guy Callendar demonstrated that the temperature had risen compared to the previous century, as a response to the increased concentrations of CO_2 in the atmosphere, pointing at CO_2 as the cause of global warming. In 1988, the UN general assembly endorsed the establishment of the Intergovernmental Panel on Climate Change (IPCC) with the initial task of collecting and evaluating the state of knowledge of the science of climate change, its social, environmental and economic impact, and potential response elements for future international convention on climate.

United Nations Framework on Climate Change (UNFCCC)

In 1992, many countries joined the United Nations Framework on Climate Change (UNFCCC), which is an international treaty acting as the foundational framework for international cooperation and negotiations to combat climate change. The aim is to limit the average global temperature increases and the resulting climate change, and coping with the inevitable impacts. The negotiations between countries towards a strong response to climate change led to the adoption of the Kyoto protocol in 1997. The Kyoto protocol operationalizes the UNFCCC by committing industrialized countries (Annex B parties) to limit and/or reduce their GHG emissions in accordance to the agreed targets. These goals should be reached through the adoption of policies and measures on mitigation which has to be reported periodically. An important element of the Kyoto protocol is the establishment of flexible market mechanisms based on the trade of emissions permits. Therefore, countries have to meet their target of allowed emissions by national measures, but also through additional market-based mechanisms including (i) International Emissions Trading (article 17 of the protocol) which allows countries that have emissions less than their target to sell the "unused" emissions to countries that are over their targets; (ii) Clean Development Mechanism (CDM) (article 12 of the protocol) allows a country with emission reduction commitment (Annex B parties) to implement an emission reduction project in developing countries from which it can earn certified emission reduction (CER) credits. These credits can be counted as effort towards meeting the emission targets. Examples of projects include rural electrification project with solar panels or installation of more energy-efficient infrastructures (cooking stoves, boilers); and (iii) Joint Implementation (article 6 of the protocol) which allows a country from the Annex B to earn emission reduction units from an emission reduction project in another Annex B party. It offers a flexible and cost-efficient means to reach the emission reduction targets while the host country benefits from foreign investment and technology transfer.

Paris agreement

The Paris agreement (COP21) is the latest step in the evolution of the UN climate change conference. It is a legally binding international treaty on climate change adopted in 2015 in Paris and its overarching goal is to keep the increase in the global average temperature to well below 2°C above pre-industrial levels, and purse the effort to limit the temperature increase to 1.5°C

above pre-industrial levels. To reach this ambitious goal, social and economic transformation are required to face the existing and upcoming climate change problems based on the best scientific knowledge available. The Paris agreement works on a five-year cycle: since 2020, countries have been submitting their Nationally Determined Contributions (NDCs) or Intended NDCs, which indicate climate actions by each country to reduce national emissions and to build resilience to adapt to the impacts of climate change (Article 4 of the Paris agreement). Every five years, countries are required to prepare, communicate (submission to the UNFCCC secretariat) and maintain successful NDCs to be achieved. Moreover, the Paris agreement also provides a framework for financial, technical and capacity building support to countries who need it. Developed countries are encouraged to provide financial assistance to vulnerable ones to support mitigation and adaptation to climate change which require large investments and significant financial resources. Also, technology development transfer and climate related capacity building are emphasized to provide guidance and sufficient capacities to deal with the challenges initiated by climate change. Under the enhanced transparency framework establish by the Paris agreement, countries will report on actions taken and progress in climate change mitigation and adaptation measures starting in 2024.

REDD+

In 2013 during COP 19 in Warsaw, UNFCCC member states developed a holistic framework for climate action to strengthen the protection and sustainable management of forests known as Reduction of Emissions from Deforestation and forest Degradation (REDD+). REDD+ activities address not only deforestation but also relevant social, policy and environmental aspects to help conserving forest through five activities including reducing emissions from deforestation, reducing emissions from forest degradation, conservation of forest carbon stocks, sustainable management of forests and enhancement of forest carbon stocks. REDD+ is implemented in phases which can overlap, allowing countries to start at different points and at their own pace based on their national circumstances. The phases include (i) development of national strategy or action plan, policies, measures and capacity building also known as readiness phase, (ii) implementation of the national policies, measures and strategies and results-based demonstration activities, (iii) evolution into results-based actions that are measured, reported and verified, enabling countries to seek and obtain results-based payments. To receive those payments, countries are required to provide (i) a

national REDD+ strategy or action plan specifying how the drivers of deforestation and forest degradation will be addressed, (ii) the assessment of the forest reference level (FRL) by independent forest experts through two separate verification processes including the technical assessment of the FRL as the baseline for REDD+ activities and the technical analysis of the submitted REDD+ results; (iii) information on how the REDD+ safeguards have been addresses and respected in the REDD+ activities. These safeguards include among others the consistency of the actions to the objectives of the national programs and international conventions, respect for the knowledge and rights of indigenous people, full and effective participation of relevant stakeholders and actions to reduce the displacement of emissions (Hirata et al., 2012) (iv) National forest monitoring that provide data and information that are transparent, consistent and appropriate for Measurement, Reporting and Verification (MRV) built on existing systems and allowing for improvement over time.

Deforestation-free supply chain

Sustainable forest management is one of the most important aspects of climate change mitigation since deforestation accounts for 11% of GHG emissions (Hirata et al., 2012). Tropical countries including Brazil, Indonesia and DR Congo are associated with the highest deforestation rate in the world (Hirata et al., 2012). Agriculture have been identified as the main cause, and it is responsible of about 90% of the deforestation the main commodities linked with a high risk of deforestation include cocoa, cattle, coffee, palm oil, rubber and soya. They are cash crops mainly produced by smallholder farmers to supply the world's demand. About 1/3 of the globally traded agricultural products are imported to and/or consumed by the EU market, representing about 10% of the global deforestation between 1990 to 2008 (EU, 2022).

As a response, the European commission, council and parliament agreed on an innovative regulation (EUDR) which aims to limit placing of deforestation-linked products on the EU market. The law will enter into force later in the year 2023 and will limit the importation of products containing or made from commodities that were produced on land that have been subjected to deforestation after December 2020. The regulation requires economic operators to provide evidence (a due diligence statement) that the commodities and products they wish to introduce on the EU market have not contributed to deforestation. In addition to the legal documents, the

operators should provide the geographical coordinates of the farms where the commodities were produced (Article 9 and 31). The regulation will be extended to other relevant ecosystems including wetlands and savannas as well as natural systems with high levels of carbon stocks or high biodiversity such as grasslands and peatlands (Article 32).

The EUDR is not a legally binding agreement between countries, rather it applies only to operators involved in importing to- and/or exporting commodities from the EU market. Those actors should provide evidence to competent authorities that their products are legal and have not contributed to deforestation in the country of production. The regulation will require an existing, functioning and updated national forest monitoring systems to provide near-real time information on the status of the forest areas especially around deforestation hotspots. The implementation of this regulation is expected to improve deforestation monitoring by providing accurate data on the locations production plots. These data could be reported in NDCs or MRV as avoided deforestation.

1.4 Carbon stock estimation

The goal of the Paris agreement to limit temperature increases below 1.5°C before pre-industrial times could be reached speedily through the sustainable management of forests. For this purpose, reports on emission reduction efforts under the Paris agreement (NDCs) and/or REDD+ (MRV) require that the amount of sequestrated carbon in different carbon pools should be accurately estimated over a given period of time. These estimations are demonstrations of countries' contributions to fight climate change, and could be used as proof for financial gratifications. Moreover, the carbon stock of an ecosystem is an indicator its contribution to climate change because it represents not only the amount of CO_2 that has been removed from the atmosphere, but also the quantity of carbon that will be released if the system is subjected to perturbations such as wildfire or deforestation (Somarriba et al., 2013). The main terrestrial carbon sequestration pools include aboveground or standing biomass (AGB), belowground biomass (BGB), soil organic carbon (SOC), litter and deadwood (Gytarsky et al., 2015; Kayler, Janowiak & Swanston, 2017). Considering the importance of the information it conveys, methodological approaches for the estimation of carbon stocks constitute a key aspect of terrestrial ecosystems monitoring (Covey et al., 2012). Several methodologies for carbon stock estimation are reported in the literature based on the ecosystem, the carbon pool and the spatial scale (Brahma et al., 2021; Nayak et al., 2019;

Qureshi, et al., 2012). The commonalities between the existing approaches are that they are based on direct (soil, litter samples) and/or indirect (diameter, height) field measurements from which carbon stocks are derived by laboratory analysis or using allometric models. To be generalized over a larger geographic region, studies often rely on geo-technologies including geo-statistics and remote sensing. However, the precision of the estimations is affected by the measurement techniques and the size and heterogeneity of the study area. The reporting of carbon stock estimations by countries in the framework of climate change mitigation require the methodologies to be accurate, transparent and documented following the good practice guidance (GPG).

Good practice guidance (GPG)

The GPG was proposed by IPCC as framework for carbon estimation and reporting which ensures the minimization of under – or overestimations and the quantification of uncertainties (IPCC, 2019). For large scale studies (subnational or national levels), a good practice for carbon estimation in a given ecosystem is to use a combination of direct field measurements from field campaigns and remote sensing. In woodlands ecosystems including forests, savannas and wetlands, diameter and height are reported as the most important parameters from which the AGB and BGB could be derived (Brahma et al., 2021). To convert biometric parameters of trees into carbon stock, a good practice is to use appropriate allometric equations, i.e transfer models which have been developed in the region of interest, with tree species that are present in that region. Often such models are not available, especially in the tropics. Therefore, a pan-tropical multi-specie allometric model such as the one developed by Chave et al. (2014) is accepted as good practice in locations where no region-specific allometric models are available (IPCC, 2019). Field measurements and the derived estimations of carbon stocks are crucial for generalization over larger areas because they are used as reference data inputs for the development of transfer models including machine learning models. Because of their nature, field campaigns cannot be carried over large area and for all carbon pools even though they provide accurate carbon estimations. In fact, field campaigns are laborious, costly in terms of time, financial and human resources. Moreover, field campaigns are spatially limited since it is often impossible in certain part of the globe because of insecurity or unreachability. Therefore, indirect measurement methods are used because they allow to collect relevant property of the ecosystem without direct contact. Spaceborne remote sensing (RS) has

emerged as the most cost-effective tool for ecosystem monitoring globally because it consistently provides data of the earth surface at different spatial, temporal and spectral resolutions.

Remote sensing

The history of remote sensing began with the invention of photography (Table 2), when the first permanent photograph was taken in 1826 by the French inventor Nicéphore Niépce (NFI, 2023). In 1858, Gaspard Tournachon took the first aerial photo of a village near Paris from a balloon at an altitude of about 365 m. This picture was the start of the era of earth observation and his example was soon followed by other people worldwide. In fact, aerial photography from balloons played an important role to reveal defence positions in Virginia during the civil war of 1860 in the US. This war time speeded the development of photography, lenses and airborne-use of this technology. During world war I, aeroplanes were used on a large scale for photo reconnaissance, and aircraft was found to be more reliable and more stable platform than balloons. After WWII and the application of non-visible part of the electromagnetic spectrum, aerial photograph started to be available for civil research in field such as geology, forestry and agriculture. This led to improved cameras with near-infrared, thermal and radar sensors. In the 1950s, two type of radar was developed: side-looking airborne radar (SLAR) and synthetic aperture radar (SAR).

In the early 1960s, the US started the space era of remote sensing with the first meteorological satellite TIROS (Television Infrared Observation satellite). About a decade later, ERTS-1 (Earth Resources Technology Satellite) later renamed in 1975 as Landsat was the first satellite specifically designed to collect data of the earth's surface and its resources. The collected images established remote sensing as a valuable technology worldwide, capable of providing repetitive high-quality images at low cost with multispectral coverage and minimal image distortion. Following the success of ERTS-1 and the Landsat program, other successful earth observation missions have been launched and continue to be launched across the world as presented in Table 2. According to United Nations Office for Outer Space Affairs (UNOOSA) in 2022, there was 4852 active individual satellites orbiting the earth, providing different types of imagery data at different spectral, spatial and temporal resolutions for different applications (Mohanta, 2023).

Table 2: Milestone in the history of remote sensing

1800	Discovery of Infrared by Sir W. Herschel
1839	Beginning of practice of photography
1847	Infrared spectrum shown by J.B.L. Foucault
1859	Photography with balloons
1873	Theory of electromagnetic spectrum by Jc. Maxwell
1909	Photography from airplanes
1916	War war I: aerial reconnaissance
1935	Development of Radar in Germany
1940	WW II: Applications of non-visible part of the electromagnetic spectrum
1959	First space photograph of the earth (Explorer-6)
1960	First TIROS Meteorological Satellite launched
1972	Launch of Landsat-1 (ERST-1): MSS sensor
1982	Launch of Landsat-4: new generation of Landsat sensors: TM
1986	French commercial earth observation satellite SPOT
1991	Launch of the first radar satellite JERS-1 by Japan
1995	Launch of Radarat by Canada
1995	Launch of ERS-2 by ESA
1999	Launch of EOS: NASA earth observing mission “Terra” with MODIS and ASTER
1999	Launch of IKONOS, very high spatial resolution sensor system
2001	Launch of QuickBird, very high spatial resolution sensor system
2002	Launch of ‘Aqua” with MODIS by NASA
2006	Launch of Advanced Land Observing Satellite (ALOS)
2014	Launch of Sentinel-1 by ESA
2015	Launch of Sentinel 2A
2018	Launch Global Environment Dynamics Investigation (GEDI)

In the GPG, important criteria in the selection of RS data and products include adequate land use classification scheme, appropriate spatial and temporal resolution for estimating land use and carbon stock changes, availability of accuracy assessment, transparent methods applied in data acquisition and processing and consistency and availability over time (Gytarsky et al., 2015). Earliest carbon estimation studies using RS data were based on aerial photo interpretation to map forest biomass in combination with non-destructive field sampling. The approach was to develop regression models to predict in-situ biomass using in situ measurements including mean crown diameter, density and basal cover, and delineated crown cover on the aerial photo (Tiwari & Singh, 1984). RS was able to differentiate different forest types and provide and accurate estimation of in situ carbon stocks. In current biomass assessment studies, traditional aerial photographs are not used anymore. Photographs are mainly collected using unmanned aerial vehicles (UAV) and the

image interpretation and measurements are carried out using photogrammetry software such as pix4D or Regard3D. Carbon estimations using this approach are very accurate because UAVs provide a very high spatial resolution (up to 1.25 cm), and the overlapping of the photos allows the processing of 3D point clouds (Abdullah et al., 2021; Jones Kachamba et al., 2016; Maesano et al., 2022). However, the acquisition of aerial photo over large areas is costly, mainly because UAV are powered by batteries, therefore limiting the spatial extent that could be covered. Moreover, this approach is highly regulated and is limited by the weather. Another type of RS data acknowledged in the GPG include optical imagery data, which consist of spectral bands on the visible and near infrared spectrum, used to describe the vegetation. Optical imagery could be freely accessed, and the Copernicus Sentinel-2 mission from the European Space Agency (ESA) provides relatively high-resolution image (10 m resolution) globally every 5 days. The methodology for biomass estimation that consists of linking field measurements and vegetations indices derived from the original spectral bands, have been successfully used in different terrestrial ecosystems including forest, savannah, wetlands and agriculture (Bousbih et al., 2018; Forkuor et al., 2020; Malhi et al., 2022; Wang et al., 2020; Zhang et al., 2019). Even if high prediction accuracies have been obtained using Sentinel-2 data, there are some limitations associated with optical data for biomass studies such as (i) the sensitivity to atmospheric conditions. In fact, optical sensors capture the emitted radiations of objects which are exposed to the sun. therefore, optical sensors could provide data in the night or if there are clouds, which is always the case in tropical regions. (ii) Another limitation is that the optical spectral reflectance saturates at high biomass levels (Shao & Zhang, 2016). Consequently, optical data could not differentiate ecosystems (mainly forests) over a certain biomass level, resulting in poor carbon estimation in forests. To solve the issue associated with optical imagery, Synthetic Aperture Radar (SAR) data are used, as they can collect data regardless of the weather or time of day. Also their ability to penetrate the targeted object allows to accurately modelled the biomass as it reported that SAR data are more sensitive to higher biomass (El Hajj et al., 2018; Huang et al., 2018; Lone et al., 2018; Naidoo et al., 2015). SAR data could be freely accessible from the Sentinel-1 mission of ESA, which provides C-band SAR data at 10 m resolution. Sentinel-1 have been successfully used for biomass estimations in several ecosystems, but the prediction of the SAR data is always lower than optical data (GFOI, 2018; Ghosh & Behera, 2021). A better prediction accuracy is obtained when combining optical and

SAR data. This combination allowed accurate estimations of biomass in tropical humid and dry forests (Forkuor et al., 2020; Tadese, Soromessa et al., 2019), the detection of encroachments in protected areas (Abu et al., 2021; Knauer et al., 2017), the delineation of complex landscape such as agroforests and small size mixed crop (Aguilar et al., 2018; Numbisi et al., 2019) and monitoring deforestation and forest degradation (Gao et al., 2020; Mitchell et al., 2017).

Land Use, Land Use Change and Forestry (LULUCF)

Deforestation is taking place at an alarming rate, predominantly in tropical countries. According to FAO, this process is defined as "the conversion of forest area to another land use -such as arable land, urban use, logged area or wasteland-, or the long-term reduction of tree canopy cover below the 10% threshold" (FAO, 2020). In the same report, a forest is defined as a piece of land with a minimal area of 0.5 ha, with trees that could reach at least five meters at maturity, with a crown cover of at least 10%. In the last decades, the forest cover in Africa has decreased by 24.4%, which correspond to an average loss of 4.4 million hectares of forest per year (Mongabay, 2020). The annual deforestation in Africa is an import source of greenhouse gas emissions corresponding to about 11% of the global emissions (Friedlingstein et al., 2022). Deforestation occurs as the result of the pressure for agriculture lands which is driven by the global demand for commodities such as cocoa, rubber, oil palm. In west Africa, cash production, especially cocoa farming expansion was reported as the main driver of land use change. In Côte d'Ivoire for instance -the world largest producer of cocoa beans-, cocoa expansion was responsible of the loss of more than 80% of the forest cover in the country between 1960 and 2000 (Sabas et al., 2020). Agriculture plays an important role in the region as it is the major activity which employs about 80% of the active population and represents an important source of income for countries. In west Africa, the exports of cocoa represent about 5% of the income of producer countries and support the livelihood of more than two million farmers (ECOWAS, 2016). Beyond its negative effect on the environment, the intensification of the production of commodities (cash crop agriculture) is acknowledged as a potential solution for poverty alleviation and could be beneficial for the environment as it involve the long term management of perennial trees also known as agroforestry (Boeckx, Bauters, & Dewettinck, 2020; Nair, Kumar, & Nair, 2009; Owusu, Anglaaere, & Abugre, 2018; Thangata & Hildebrand, 2012).

1.5 Agroforestry systems

Agroforestry refers to a land management practice at the interface between agriculture and forestry. It brings into a given agricultural production system the socioeconomic and environmental benefits of forestry, such as soil fertility restoration, firewood, food and medicine (Tschora & Cherubini, 2020). Agroforestry is the oldest land management practice and is often refers to as "a new name for an old practice". Originally it was define as a suitable land management system which increases the yield of the land, combines the production of crops (including tree crops) and forest plants and/or animals simultaneously or sequentially on the same unit of land, and applies management practices that are compatible with the cultural practices of the local population (Howard & Nair, 1988). It was the main land management approach in Europe and Asia until the middle ages, and is still the dominant practice in the tropics. It consisted of clearing a piece of land in combination with fire to burn the slash after what agricultural crops were established. This land use sequence is no longer existing in Europe, but I was still used in Finland and in Germany until the end of the 1920 (Steppler & Nair, 1987). A different kind of shifting cultivation was practised in Asia: In the process of cleaning the forest for agriculture (mostly rice production), certain trees were deliberately maintained on farm and by the end of the growing season, they would provide shade to protect the crops from excessive exposure to the sun. This function was crucial in period where soil moisture was more important than sunlight for the development and maturation of the grain. In addition to the protection function, the trees provided food and medicine (Steppler & Nair, 1987). In Africa, crops on farms have always been cultivated in combination with trees because of the desire to extract the maximum amount of resources from a given land unit. A well-known agroforestry system (AFS)- slash and burn agriculture- consists of removing unwanted forest trees prior to the establishment of high value crops on the land, often always followed by natural or improved fallows (Kanmegne, 2004).Until now, trees are perceived as an inexpensive way of combatting erosion and leaching, and of managing soil fertility.

History of agroforestry

In the tropics, agroforestry has emerged from the need to combat deforestation and forest degradation, and to implement sustainable practice in agriculture. The importance and worldwide notability of agroforestry as a land management system started with forest plantations around the

end of the nineteenth century. In fact, during the year 1806 in Myanmar (Burma) the *taungya* system was tested and proposed as "the most efficient way of planting teak trees". Initially designed for foresters, it is a way of establishing tree plantations (initially teak trees) where food crops are associated and managed with tree seedlings until canopy closure (Atangana et al., 2014). This system spread rapidly in different parts of the world and quickly was adopted by foresters as the most inexpensive way to establish forests and restore landscapes, and is still used throughout the tropics for different forest species. It was around 1974 that aid to the rural poor farmer was added as a new direction to the traditional areas of forestry development of agroforestry. Emphasis started to be put on the beneficial effects of trees and forests on agricultural production stressing the necessity of devising systems which would provide food and fuel and yet conserve the environment (Steppler & Nair, 1987). The acceptance of agroforestry as a sustainable and promising land use system on farms and forest was facilitated by some measures including the re-examination of policies by FAO, the deteriorating food supply in several developing countries, increase of deforestation and degradation of forest ecosystems in the tropics, the energy crisis of the 1970s leading to the increase in commodity prices and absence of fertilizers and the establishment of the International Development Research Centre (IDRC) of Canada which aimed at identifying research priorities for tropical forestry (Atangana et al., 2014). IDRC was faced with the problem of deforestation and forest degradation and its impact including soil degradation and fertility loss, with slash and burn agriculture as the main driver (Kanmegne, 2004). As a solution, production systems which integrate forestry, agriculture and animals was proposed as a response to slash and burn in the tropics; This is the mission of the International Council for Research in Agroforestry (ICRAF) nowadays known as World Agroforestry Centre which was created in 1977. In the beginning, ICRAF activities were focused on creating an inventory of existing agroforestry systems, collecting information and introducing new approaches and systems, fine-tuning existing agroforestry practices towards soil fertility management. Activities included alley cropping, fallow systems with nitrogen-fixing species (*Leucaena leucocephala, Calliandra calothyrsus Inga edulis* etc.), intercropping and development of agropastoral systems that are adapted to the tropics. Due to the limited impact on slowing deforestation and improving the livelihood of farmers, poverty-reduction strategies was included through a worldwide domestication program, which consisted of identifying and ranking priority species that farmer would like to plant on their farms (indigenous

tree species) and techniques for their production (Leakey, 2017). At the present time, research priorities of ICRAF include four categories: (i) Landscapes: improving governance of tree crop landscapes for resilient Green economies, climate change and sustainable environmental services; (ii) Soils: land health evaluation, restoration and investments decisions; (iii) Systems: Resilient productivity and profitability of agroforestry systems; and (iv) Trees: tree productivity and diversity – realising economic and ecological value from tree genetic resources (https://apps.worldagroforestry.org/research-areas access on May 30, 2023).

Classification of agroforestry systems

As mentioned previously, agroforestry is a generic name for land-use systems, practices or technologies where woody perennials are deliberately integrated with agricultural crops and/or animals in the same land management unit in some form of spatial arrangement or temporal sequence. As defined by Howard & Nair (1988) the key points of an agroforestry system are (i) presence and management of a woody perennial (shrubs, trees, bamboo etc.) in the system: it should be adapted to the locality and provide some benefits such as food, fodder, income, medicine, fertility restoration, protection in form of shade or windbreaks etc. and (ii) positive ecological and/or socioeconomical interactions between the components of the system since multiple production systems are managed on the same land unit. However, some agroforestry systems do not have a food crop component such as cocoa agroforests. As far as the classification is concerned, agroforestry systems are classified based on (i) the structural composition and the spatial arrangement of the component within the system including the temporal sequence of introducing different components in the system. Also, (ii) the function of the tree component in the system is considered (production or protection). Finally (iii) agroforestry systems are classified based on the level of inputs in the management of the system, which is different if the system is meant for food production or for commercial purposes (cocoa plantations and fruits trees on farmlands for example). It is worth noticing the difference between an agroforestry system (AFS) and an agroforestry practice (AFP): AFS involve the integrated production of trees and crops/animals characterized by the environment, plant species and their arrangement, management and socioeconomic functions while AFP reflects the distinct arrangement of components in space and time. Therefore, similar practices are found in different AFS under different conditions, however, both terms are often used interchangeably (Atangana, 2014). Hundreds of AFS have

been identified in the tropics for about 30 AFPs. One of the most popular AFP since mid-1990s is the participatory tree domestication of high value and multipurpose indigenous forest species. The most common AFS in the humid tropics include improved fallows, homegardens, perennial crop-based systems, farm wooldlots, alley cropping and plantation crops (Table 3).

Table 3: Main agroforestry systems in the tropics (adapted from Atangana et al. 2014)

	Agroforestry systems (AFS)	Description
1.	Improved fallow	Tree or shrub species planted and left to grow during the fallow phase.
2.	Taungya	Combined stand of woody and agricultural species during early stages of establishment of plantations
3.	Alley cropping	Woody species in hedges; agricultural species in alleys between hedges; micro-zonal or strip arrangement
4.	Multilayer tree gardens	Multispecies, multilayer, dense plant associations with no organized planting arrangements
5.	Multipurpose trees on croplands	Trees scattered in cropland (eg: maize in parkland) or according to some systematic patterns on bunds, terraces or plot fields boundaries
6.	Plantation crops combination	Integrated multi-storey mixture of plantation crops Mixtures of plantation crops in alternate or other regular arrangement
7.	Homegardens	Intimate, multi-storey combinations of various trees and crops around homesteads
8.	Irrigated agrisilviculture	Crop combination with fruit bearing woody perennials
9.	Fuelwood production	Interplanting firewood species on or around agricultural lands
10.	Herboforestry	High-value specialty herbs cultivated under woody perennials

11.	Mangrove management	Plantation establishment and rehabilitation of degraded mangrove formations to mitigate erosion and reduce flooding, protect fish and shrimp ponds
12.	Community forestry	Tree planting on common lands by local people

Because of the ubiquity of trees, AFS are acknowledged to have an interesting potential for carbon sequestration. In fact, it was found that AFS stored more carbon than other land cover; for example carbon stocks levels were higher in AFS compared to monocrop agricultural systems, although the amount of sequestrated carbon varied based on the AFS depending on the species and density of trees (Ali et al., 2022; Gomes et al., 2020). Feliciano et al. (2018) found that for sylvopastoral AFS (trees combined with animals), the carbon stocks were higher in the soil, whereas in sylviculture AFS such as cocoa plantations, carbon were predominant in the biomass. Moreover, AFS demonstrated their ability to regulate the temperature by creating a microclimate that is beneficial to other crops (Gomes et al., 2020). The potential of AFS to reduce fire risk and protect ecosystem was also reported, as areas where AFS were present had fewer wildfire incidents compared to forest, shrublands or grasslands (Damianidis et al., 2021). The integration of animals in the land management helped controlling the progression of grass which are easily flammable during the dry season. In addition to the economic benefits that are derived from AFS, the environmental impact in terms of emission reduction and avoid emissions could be rewarded under existing mechanism within the UNFCCC framework (REDD+), if those efforts are properly measured and monitored.

1.6 Problem statement

Mixed pixels

Freely available RS imagery including imagery data from the Sentinel mission have been extensively used for the detection and mapping of AFS in West Africa. For instance, the combination of Sentinel-1 and -2 data was successfully used for the detection of cocoa plantations encroachment in protected area (Abu et al., 2021). By applying machine learning techniques on time series images, it was possible to accurately estimate the extent of cocoa plantations in major producer countries namely Cote d'Ivoire and Ghana. Moreover, advanced processing techniques including deep learning approach was able to distinguish between full sun cocoa plantations from cocoa agroforests in West Africa (Ashiagbor et al., 2020). The availability of increasing computing resources combined with powerful algorithms and methodologies and increasing open-source data has improved the monitoring of AFS in the tropics. However, earth observation with open-source data remain challenging particularly for tropical AFS. One of the reasons is due to the fact that AFS are very heterogenous by nature. The composition and density of the elements within an AFS as well as the spatial arrangement of field create similar aspect across AFS. This often result in spectrally overlapping signals making it difficult for separate those AFS within that landscape (Filella, 2018). Another reason is related to the size of the plots. In fact, in Africa agricultural farms are small (generally less than 1ha) and are established next to each other. The combination of these reasons results in mixed pixels where more than one AFS is captured in a pixel. This led to high omission and commission errors during the classification which results in a very low overall accuracy. This phenomenon was observed in the classification of cocoa plantations in west Africa where high levels of confusion were recorded between cocoa and rubber plantations (Kanmegne Tamga et al., 2022a).

As a solution, high resolution imagery data are used in combination with open-source data. Optical data of very high resolution are often used to improve the classification and open-source SAR data could be considered as additional input variable. This methodology was implemented for the delineation of cocoa plantations in Cameroon, and was able to reduce the confusion between cocoa agroforests and secondary forests (Numbisi et al., 2019). Likewise, Aguilar et al. (2018) were able to accurately delineate different AFS in Mali, and captured the characteristics of small agroforestry

farms including different crops and planting-patterns. In most of the case, those very high-resolution images are not free, they are expensive, and their coverage is limited. In September 2020, the Norway's International Climate and Forest Initiative (NICFI) satellite data program has provided open access to planet's high-resolution data to help reduce and reverse the loss of tropical forest to support efforts to combat climate change. The available data consisted of monthly and quarterly analysis-ready mosaics of four bands (red, green, blue and near-infrared) at a spatial resolution of 4.77 meters. Since then, Planet-data have been used worldwide in different programmes including governmental projects, private sectors and university research. Because it is a composite, Planet-data are mainly used as reference data in classification and validation. It has been used to map tropical forest cover and deforestation, and was found to provide reference points with 'extremely high" accuracies (Vizzari, 2022; Wagner et al., 2023). Classification studies where Planet-data are considered used Sentinel data as input data for landcover classification. Planet-data is very useful to improve the assessment of the classification by providing reliable reference points, but is not able to deal with mixed pixel which is a major problem in the classification of complex landscapes including AFS. There is a need to propose a new approach to evaluate the classification capable of detecting mixed pixels which contribute to the classification error. This will allow the development of error maps alongside with the classification map resulting therefore in more robust and reliable maps of complex landscapes.

Spatial distribution of the classification error

The assessment of a classification map is based on the confusion matrix. Also known as error matrix, it is a table that is used to evaluate the performance of the classification algorithm and it shows the score of the predictions versus the reference/actual values. The values in the confusion matrix are used to calculate the producer's and user's accuracies of the classification as well as the overall accuracy. Other metrics such as precision, recall, F1 score and AUC ROC curve could also be calculated from the confusion matrix. Confusion matrix and the information it provides are essential to see the performance of a model and the type of error it is making, but it is criticised because it does not provide any information on the spatial distribution of the classification error on the map (Roodposhti et al., 2019). The assumption on existing maps is that the error is homogeneously distributed across the region of interest. Even if this assumption is valid in different terrestrial systems including forest, wetlands and agriculture, complex landscapes where

there is evidence of mixed pixels could not by evaluated on this basis. The combination of certain conditions related to the type of AFS and its spatial arrangement could result in higher classification error at given location on the map. A local form of spatial analysis known as Geographically weighted regression (GWR) was introduced and allowed the modelling of the relationships between the independent variables and the dependant variable to vary by locality. In the literature, GWR showed that the relation between biomass and vegetation indices were significantly spatially variable (Propastin, 2012). It revealed that certain drivers of deforestation (land ownership, altitude and slope) showed significant spatial variability, which facilitate and improved the understanding of the causes and mechanisms of deforestation in different regions (Pineda Jaimes et al., 2010). The application of GWR models in the classification of AFS is missing and there is a need to evaluate the relationship between the spatial distribution of the classification error and the independent variables across the map.

Methodologies for carbon estimation in AFS

AFS are acknowledged to have a great potential for climate mitigation. Because of the ubiquity of trees in their system, AFS have the ability to capture and store atmospheric carbon in the biomass of trees and in the soil (Nair et al., 2009). Several studies assessed the carbon stocks in different AFS in the tropics using RS, and revealed that the standing biomass is an important carbon pools (Nair et al., 2009; Nair et al., 2010; Vatandaşlar & Abdikan, 2022). Yet, methodologies for carbon estimations are criticized, mainly because of the lack of uniformity within AFS (Nair & Nair, 2014). The main argument is that the methodologies are based on assumptions which have been derived from forestry and implemented without any adaptation, resulting in unreliable estimations of carbon stocks in AFS. As a response, the GPG was proposed by IPCC as a framework to normalize methodologies for carbon estimation studies in terrestrial ecosystems. Despite these efforts, existing methodologies need to be adapted and fine-tuned to match with the specificities of AFS. One of the critics is about the selection of the allometric model: In the GPG it is accepted as good practice to use the pan-tropical allometric model such as the one developed by Chave et al. (2014). This allometric model gave accurate estimations in forestry, but not in AFS because the model was developed and validated in forest ecosystems, using forest species which are not always present in AFS. As a result, the biomass estimations are associated with high levels of uncertainties. There is a need to develop and/or used appropriate allometric equations for biomass

estimation, which have been developed and tested on agroforestry tree species. Also, the carbon fraction used in most studies are not appropriate. It is established in forestry half of the biomass is carbon. Nair & Nair (2014) demonstrated that in most case the proportion is less than 0.5 and is a function of the tree species, the environmental conditions and the management practice in the AFS. For instance, a different carbon fraction is used in biomass studies in Mozambique: in dry forest ecosystems 0.45 of the biomass is regarded as carbon (Negash & Kanninen, 2015). Therefore, it would be a better practice to present biomass levels instead of carbon stocks to limit estimations errors unless a reliable carbon fraction is applicable. Finally, the generalization of the carbon estimations often assumes AFS to be uniform across a given region and refer to them as a single agroforestry class. But, there is a high level of spatial heterogeneity within AFS depending on the management practices, their composition as well as the climatic regions. There is a need for a remote sensing-based approach for the estimation of carbon stocks in each of the main AFS in different climatic regions in the tropics. This will address the existing information gap related to the carbon sequestration potential of different AFS in the tropics, and their ability to address climate change.

Unevaluated remote sensing data

Field measurements play a crucial role in the estimation of carbon stocks, and it is required as a good practice when using RS data and methods. The measurements should be accurate, and the number of samples large enough to be representative of the region of interest. Generally, field campaigns consist of collecting biometric parameters on trees such as height, diameter at breast height, crown size etc. which are then input in allometric equations to get the biomass. By nature, it is a costly and exhausting task which could only cover a limited area. For larger areas, such information could be derived using Light Detection and Ranging data (LiDAR) which is a RS method that uses light in the form of pulsed laser to measure ranges to earth. LiDAR data provide information on the location and height of the target allowing 3D modelling of the earth surface. It has been used in biomass modelling studies and provide very accurate estimation of the standing biomass of terrestrial ecosystems (Anderson et al., 2016; da Costa et al., 2021; Musthafa & Singh, 2022; Pourshamsi et al., 2021). In 2018, the Global Ecosystem Dynamics Investigation (GEDI) mission was launch and it provides accurate 3D measurements of the earth surface. GEDI is the first satellite mission to provide high resolution LiDAR data designed for ecosystem monitoring.

It has successfully contributed to the accurate estimations of biomass in different wooded land (Duncanson et al., 2020; Milenković et al., 2022; Silva et al., 2021). Taking advantage of its precision for biomass modelling, predictions of aboveground biomass was generated using the 3D measurements of GEDI and ground truth data in different ecosystems, to create a biomass product known as GEDI level 4A (L4A) (Dubayah et al., 2020). GEDI L4A has been successfully used to monitor forest regrowth and carbon emissions from land use change (Houghton et al., 2012; Milenković et al., 2022). This could be a major contribution to carbon assessment methodologies as it could be used as a complement and/or a substitute to field campaigns especially in hostile areas. To this point, very limited studies have investigated the potential of GEDI L4A for biomass estimation and existing studies focused on forests and wetlands. There is a need to evaluate biomass predictions from GEDI L4A in AFS in comparison with field measurements.

1.7 Objectives of the research

Carbon sequestration is an important topic nowadays as it represents one of the main ways to mitigate climate change globally. Therefore, a lot of initiatives are financed to improve the state of the art by providing relevant information in the fight against climate change. In the tropics, agroforestry has contributed to global emissions through unsustainable agricultural practices such as slash and burn agriculture and crop plantations (mainly cocoa). Yet, agroforestry is acknowledged as a viable solution to address poverty, food security and climate change. Existing AFS could be integrated in emission reduction strategies at national level and/or could be eligible for financial compensation within international mechanisms such as REDD+. For that, accurate information, reliable data and applicable methodologies need to be provided. The aim of this study is to propose a methodological framework for the assessment of carbon sequestration in AFS of West Africa using remote sensing. More specifically, the objectives are:

1. Provide an accurate map of the different AFS in West Africa, by modelling the spatial distribution of the classification error (Kanmegne Tamga et al., 2022a). The main research questions are:
    a. How does the spatial distribution of the classification error vary across different AFS in west Africa?

   b. How does the input data from remote sensing affects the distribution of the classification in AFS?
2. Estimate the carbon stock of AFS in different climatic regions of West Africa using remote sensing (Kanmegne Tamga et al., 2022b). The research questions are:
   a. What is the best combination of remote sensing data (SAR, optical and LiDAR) for the estimation of the standing biomass in different AFS?
   b. How does the carbon stock level vary in different AFS across west Africa?
3. Assess the spatial dynamic of carbon stocks within AFS across West Africa. The research questions are:
   a. How does the aboveground biomass change between 2017 and 2021 in AFS of west Africa?
   b. How does the spatial distribution of carbon sources and sinks vary across the region of interest between 2017 and 2021?
   c. What are the main carbon sinks and carbon sources within the AFS in west Africa?

1.8 Structure of the thesis

The thesis is organized in five chapters: (i) Introduction where all the terms and concepts are defined. Here the state of the art, the research gaps and the objective of the study is presented. (ii) materials and methods where the methodological approach is presented. It starts with the presentation of the region of interest and the description of the data, their acquisition and processing. All the analysis are presented including formula and the workflow used to address the research questions. (iii) Results is the section where all the findings are presented. Maps, graphs, tables and statistics from the analysis are described. (iv) in the discussion, the results are put in context of the state of the art, and the findings of this research are discussed and compared with existing studies. Limitations of the proposed methodology are evaluated and further improvements are proposed. Finally (v) the conclusion presents the main findings of the study: answers to the initial research questions are presented and implications of the results are presented

Chapter 2

Materials and Methods

2.1 Study area

The study was carried in two west African countries of Côte d'Ivoire and Burkina Faso, located within the latitude 4.34° to 15.08° and the longitude -8.59° to 2.45° (Figure 2). Both are French speaking countries, and are part of the 16 members of the economic community of the west African states (ECOWAS). They are bordered by the Gulf of Guinea in the south, Liberia and Guinea in the west, Mali and Niger in the north, and Ghana, Togo and Benin in the east. Côte d'Ivoire is ranked as the 3rd richest country in West Africa after Nigeria and Ghana, while Burkina Faso is ranked 5th based on their GDP. The two countries are separated by a terrestrial border of 584 km which regulates most of the economic exchanges from one side to the other, using a common currency -the West African CFA franc.

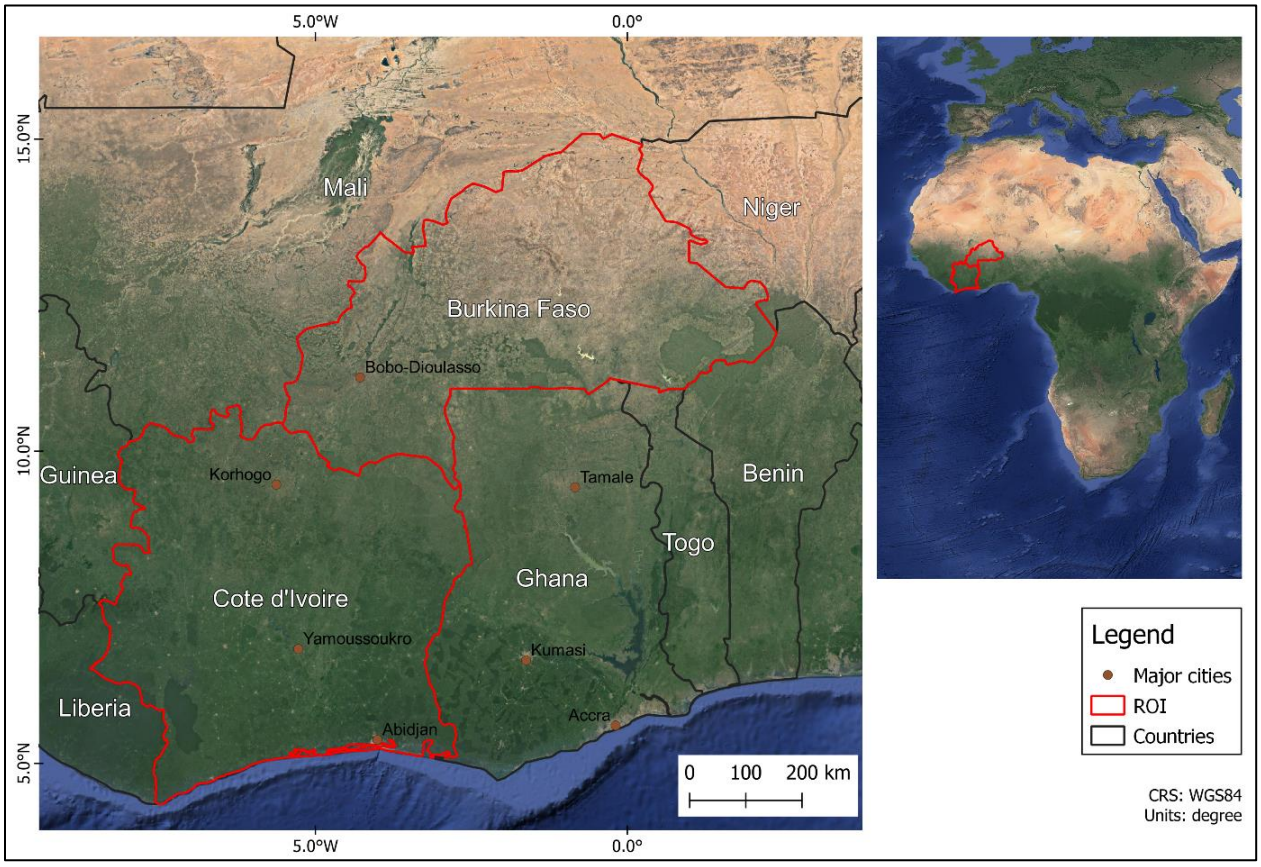

Figure 2: Area of interest (AOI) of the study

Côte d'Ivoire

The Republic of Côte d'Ivoire is a former French colony bordered by Liberia, Guinea, Mali, Burkina Faso and Ghana. The name is derived from the intensive trade of Ivory that took place in the coastal part of the country between the 15th to 17th centuries. The country has two capital cities: Yamoussoukro which is the official capital since 1983 and Abidjan which is the administrative capital but also the largest city of the country (around 6.3 million inhabitants). Another intriguing fact, it is not the "Republic of Ivory Coast"! Since 1986, the government changed the name and adopted the French name even though some media still use the former English translation. The country has five UNESCO world heritage sites. Among them, natural site includes the Comoe National Park, one of the largest protected areas in West Africa; the Taï National Park which has a rich and diverse natural flora and is home of threatened mammal species such as the pygmy hippotamus and also Mount Nimba Strict Nature Reserve which has a diverse flora and fauna such as viviparous toad and chimpanzees.

About 70% of the economy of Côte d'Ivoire comes from the exportation of agricultural products, As the country is the world largest producer of cocoa beans. In 2020, the production was over 2 million tons, which represented about 39% of the world's cocoa production (Shahbandeh, 2021). The exported commodities are mainly represented by cocoa products (49%), several nuts including coconuts and cashews (7%) and rubber (2%). Those products are mainly traded in Europe (Netherlands, Switzerland, and France), America (mainly the USA) and Asia (Malaysia) according to the report of the OEC (2020). Côte d'Ivoire is a relatively large country with a size of 322 460 km², associated with a population density of 85.2 inhabitants/km², with agriculture as the main activity. There, cocoa farming is by far the most important activity, providing employment and supporting the livelihood of more than two million small scale farmers (Boeckx et al., 2020). Although very few farmers live solely on revenues from cocoa and the question of child labour in the cocoa value chain, the sustainable intensification of cocoa production is acknowledged as an important pillar for poverty alleviation (Boeckx et al., 2020; Busquet et al., 2021; ILO, 2017; International Anti-slavery, 2004). In fact, global demand for cocoa beans is expected to increase by 7.3% in 2025, due to growing chocolate industries in emerging economies such as China and India (GVR, 2019). Next to cocoa, Côte d'Ivoire is also the world largest producer of raw cashew nuts, with 792.678 megatons in 2022 (WPR, 2023). Cashew nuts are mainly grown by small-scale

farmers in the middle and northern parts of the country, where cashew, cotton and mango are the main cash crops. The yield per tree is low (2 or 3 kg of raw cashew nuts per trees per year) because farms are managed extensively with low to no inputs, resulting therefore in low income. Most of the farmer sell their nuts to local traders, which will be sold to independent buyers and finally will be exported, mainly in India and Vietnam (Koné, 2010).

Burkina Faso

Burkina Faso is a landlocked country bordered by Mali, Niger, Benin, Togo, Ghana and Côte d'Ivoire. Similar to Côte d'Ivoire, it is a former French colony which was named Upper Volta after the independence in 1960. It was in 1984 that the current name was adopted which means "country of upright men" derived from the local language (Moré). The capital city of Burkina Faso is Ouagadougou, and the country is 274 200 km² for a population density of 80.6 inhabitants per km². Over 40 percent of its population was living below the poverty level, and the country was ranked 184th out of 191 countries between 2021-2022 according to the Human Development Index report of the United Nations Development Programme (UNDP, 2022). The main activity is agriculture, which represents about 80 percent of the workforce of the country. the land is exploited for food crop production (sorghum, millet, cowpea, and maize), but also for cash crop including cashew and cotton. Cotton is an important crop in Burkina Faso, to the extent that the country is the 3rd largest producer in Africa, behind Benin and Côte d'Ivoire, and the commodity represent about 5 percent of the income from exportations (OEC, 2020). Because of the extreme climatic conditions associated with the Sahel, most agricultural activities are carried out in the southern and western parts of the country. The north is part of the Sahel region, where the low rainfall level supports a landscape mostly appropriate for livestock. The Northern part of the country has been facing terrorist attacks from military rebels based in Burkina Faso, Mali, and Niger. The first attack was recorded in April 2015, and since then, the instability in the country has increased to the point of having two *coup d'états* in 2022. Despite the political instability and the associated insecurity on the one hand, and the extreme climatic conditions on the other hand, the country showed interesting results on the adoption and the impact of agroforestry not only by improving the local economy (shea butter value chains), but also by contributing to climate change adaptation through the improvement of soil organic carbon in agricultural farms (Coulibaly et al., 2017).

2.2 Climatic regions

West Africa is bordered in the south by the Golf of guinea which opens to the Atlantic Ocean, and the Sahara Desert in the North (Figure 3). These two regions generate two different air masses: a hot, dry continental air masses from the Sahara Desert known as Harmattan, and a moist equatorial air masses from the Atlantic Ocean known as Monsoon, and their interactions regulate the precipitation regime and the temperature in West Africa (CILSS, 2016). The interactions of the Harmattan and Monsoon have defined several climatic regions going from a wet climate in the south characterized by high precipitations, and dryer conditions with fewer rainfall in the north.

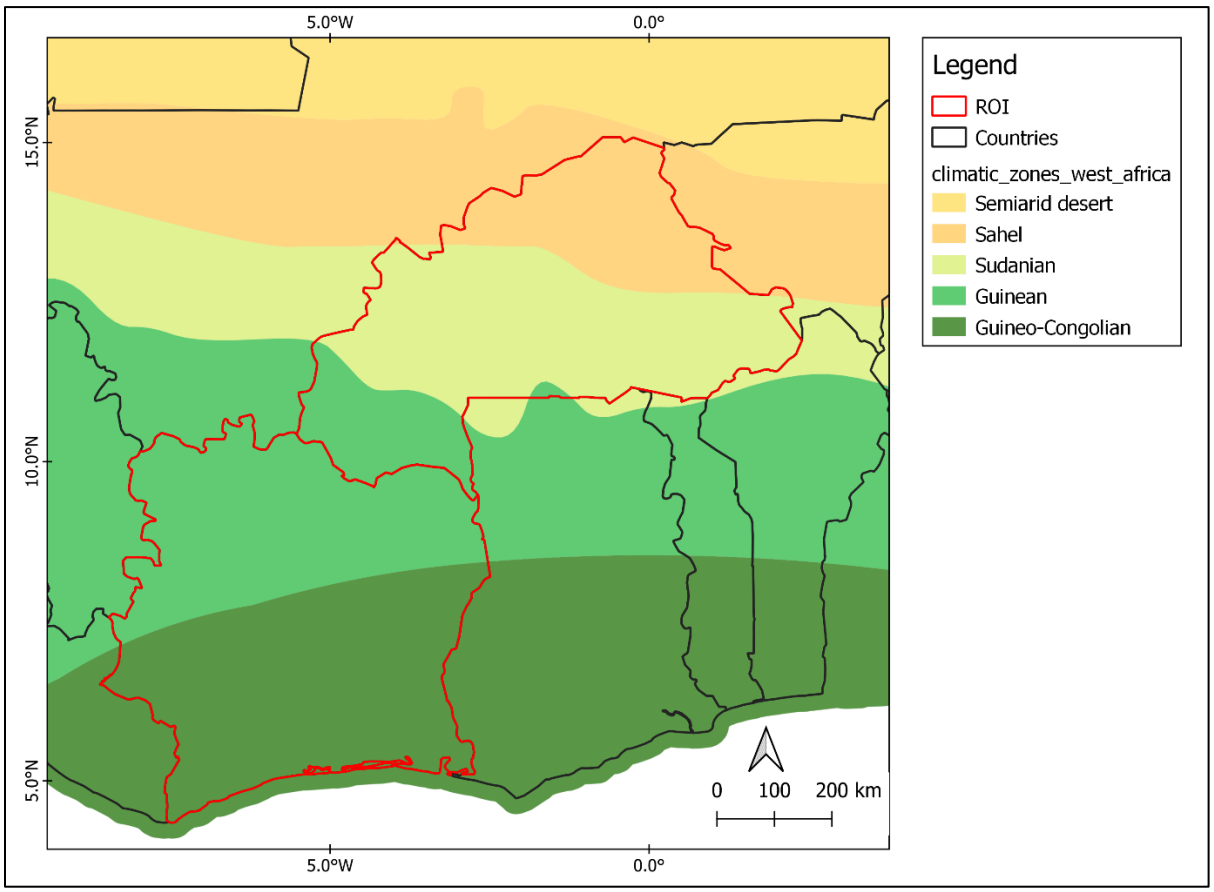

Figure 3: Main climatic regions in the study area

The study area covered four climatic regions in West Africa namely: (i) Guineo-Congolian, (ii) Guinea, (iii) Sudanian and (iv) Sahel. For this study, the first three climatic regions were considered, and the Sahel was excluded from the region of interest. Aside from the insecurity in the northern part of Burkina Faso, and in the Sahel in general, the primary reason was the climatic

conditions which are not optimal for the establishment and management of AFS with a high potential for carbon sequestration. The selected climatic zone provides different conditions allowing the development of different AFS across West Africa.

2.2.1 The Guineo-Congolian region

It is the largest climatic region of the study area, which covers the southern half of Côte d'Ivoire. It is also the wettest region in West Africa, with an annual rainfall between 2200 and 5000 mm and a temperature between 24 and 28°C. The precipitation regime is bimodal characterized by a long raining season of four months from April to July, and a short one of 2-3 months between September and November. The region has 4-5 dry months per year organised in two dry seasons, following each of the rainy seasons. In response to the increased concentration of GHG in the atmosphere, the temperature in the region is projected to rise between 1.7 to 3.7°C (very likely) by 2080 (BMZ, 2020). The sea level is expected to rise as a response to temperature increases, which could end up in flooding and intrusion of sea water into groundwater reservoirs, compromising therefore the availability of freshwater. Also, heavy precipitation events are expected to be more intense, posing a risk for food crop production and risk of flooding. BMZ (2020) reported that a change in the rainfall pattern will have a negative impact on the yield of maize, while rice and cassava are projected to gain from climate change.

The climatic conditions of the Guineo-Congolian region correspond to the tropical rainforest. However, the forests in Côte d'Ivoire have been reduced to small patches mainly due to cash crop expansion, including cocoa, rubber, and oil palm. Cocoa beans and rubber are often sold to independent buyers for exportations, while oil palm is included in the diet, and portion is sold in the local market, mainly in major cities like Abidjan and Yamoussoukro. Food crops are mainly represented by maize, cassava, yam, plantain, and rice which is cultivated mainly for family consumption. It is often produced on small farms (generally less than 2 ha).

2.2.2 The Guinean region

This climatic region covers the northern part of Côte d'Ivoire and is characterized by a monomodal precipitation regime. The mean annual rainfall ranges between 1200 and 2200 mm, distributed between March/April and October, with the wettest months in July to September. The rainy season is followed by a long dry season of 4-7 months. The temperature in the region varies between 27

to 34°C, the hottest months being March and April. The impact of climate change will be more severe in the Guinean region, where an increase in temperature would increase the risk of droughts. Consequently, crop yields are projected to decline as a response to the increased exposure of crops to drought. Moreover, the frequency of wildfires will increase, and their intensity will increase with the availability of dry biomass, increasing the risk for infrastructure and human lives.

The vegetation in the Guinean region corresponds to the semi-deciduous forest and wooded savannas, with trees reaching up to 20 m. The region is severely affected by anthropic activities including fire management as a tool for soil preparation or to renew the pasture before the raining season, but also cash crop agriculture including cotton, mango, and cashew. Cash crop production is the main income for small scale farmers in the northern Côte d'Ivoire. After the harvest, raw cashew nuts are sold to local buyers at a very low price compared to the official price of 1.29 US$. For mango, often the price is agreed upon in advance, and the harvest is then made by the buyer. Aside from cash crop, farmers grow food, mainly maize, sorghum and millet together with several vegetables depending on the season.

2.2.3 The sudanian region

In the study area, the region is a belt located in the middle of Burkina Faso, bordered in the south by the Guinean region, and in the north by the Sahel. The region is dryer with the annual rainfall between 600 and 1200 mm. The precipitation region is monomodal with a rainy season between June and September, with August being the wettest month. The dry season starts in October, and last for 7 to 8 months. The average temperature varies between 26 to 40°C, and the picks are observed between March and April. The impact of climate change will be catastrophic for the country because agriculture is the main activity (over 80% of the active population which depends mainly on climatic conditions. Following the current trend of the increase in temperature an increase of about 1.4 to 1.6°C is expected by 2050 (ICRC, 2021). The precipitation levels are expected to change, and intense rainfall could be more frequent and more severe, even though the projections on the precipitations are associated with a high level of uncertainty in this region.

In the region, the main cash crop is cotton. It represents the main income of small-scale farmers, and it is often associated with oil seed production such as shea butter. In such farms, shea trees are introduced or maintained, and managed together as an AFS. The fruit are often processed by

women, and the derived oil is used in the diet or as cosmetic. Because of its fat content, shea butter is a valuable product for the cosmetic industry, and the demand is increasing both nationally and internationally. The local food crops include maize, millet, and cowpea, which is managed at the farm level in association with cattle to produce milk, meat, and derivatives.

2.3 Regions of interest

To capture the climatic effect of the different climatic region on the AFS in West Africa, three regions of interest (ROIs) were defined, one in each climatic region. In Côte d'Ivoire, 02 ROIs were defined, one in south and one in the north, and 01 ROI was defined in Burkina Faso. In the Guineo-Congolian region, the ROI was defined around the municipalities of Soubré, Buyo and Gueyo (Figure 4). Two field campaigns were carried out for data collection in March 2020 and November 202 in the municipality of Gueyo and Buyo, in the vicinity of the Taï national park (TNP). The TNP is one of the most important forest reserves in Côte d'Ivoire, together with the Comoe national park. It was created in 1926 as a forest reserve and was promoted to national park status in 1972. Because of the flora and fauna diversity of the TNP, it was recognized as a UNESCO biosphere reserve in 1978, and added to the world heritage site in 1982. It is nowadays one of the last areas of primary rainforest in West Africa (Riezebos et al., 1994). From a management point of view, the TNP is assumed to be intact, and available reports confirmed its integrity and no human activities within the boundary of the park (GIZ, 2020). The TNP was not investigated during this study, and field measurements from the park were not considered in the analysis. However, due to the rapid extension of cocoa plantations in the surrounding of the park, the ability of remote sensing to detect encroachment was tested.

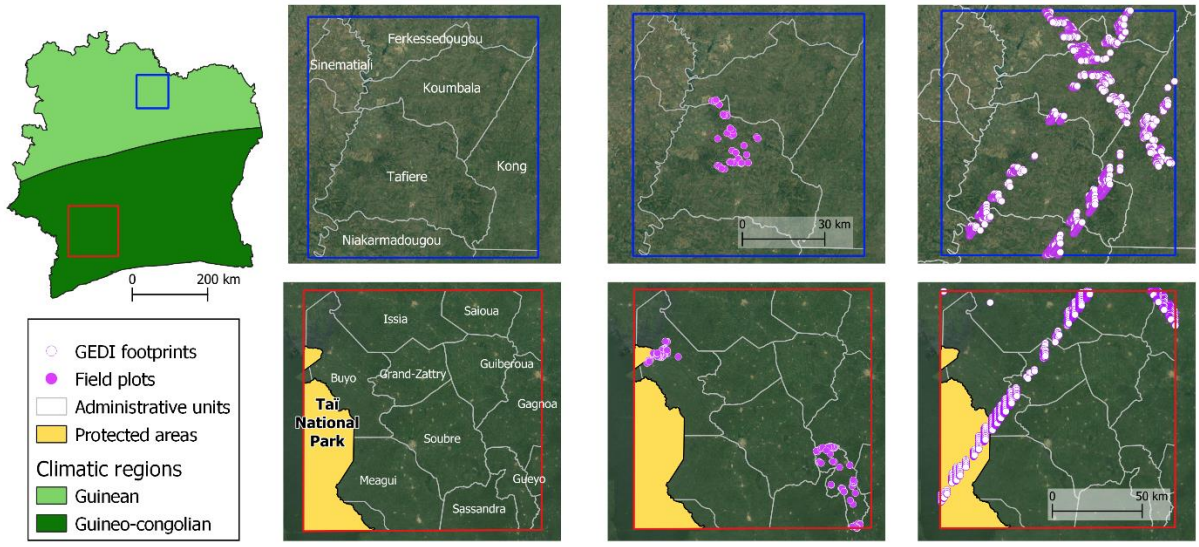

Figure 4: Region of interest in Côte d'Ivoire showing the distribution of the field plots and the footprints from GEDI (Background image: google earth)

For the Guinean region, a ROI was defined around the municipality of Tafiere, in the northern part of Côte d'Ivoire. Like the activities in the south of the country, two field campaigns were carried out in the same period. The field activities were limited in the sub-division of Tafiere because of the constraint due to transportation. Motorbike was the only practicable way to reach farms for data collection mainly due to the road, and the daily distances to the sites were limited to about 10 to 20 km.

The third ROI was defined in Burkina Faso. (Figure 5). Here, only one field campaign was possible, and the data collection was carried in 04 municipalities: Pa, Pompoï, Yaho and Boromo, in June 2021. The defined ROI contained several protected areas, which consisted of six classified forests located in the municipality of Pa, Bouahoun, Bounou, Tui, Bansié and Nossébou. The investigation on the ground showed that the protected areas that were referenced at forest were severely deforested, mainly due to overgrazing of livestock and bush fires. Certain areas have been converted for cotton production, but the main areas associated with protected areas were managed in the form of agroforestry parklands dominated by *Parkia biglobosa*. The tree gives a fruit commonly known as African locust bean (nere in French), which is appreciated for its pulp and seeds which is used as food and medicine both for humans and for the cattle.

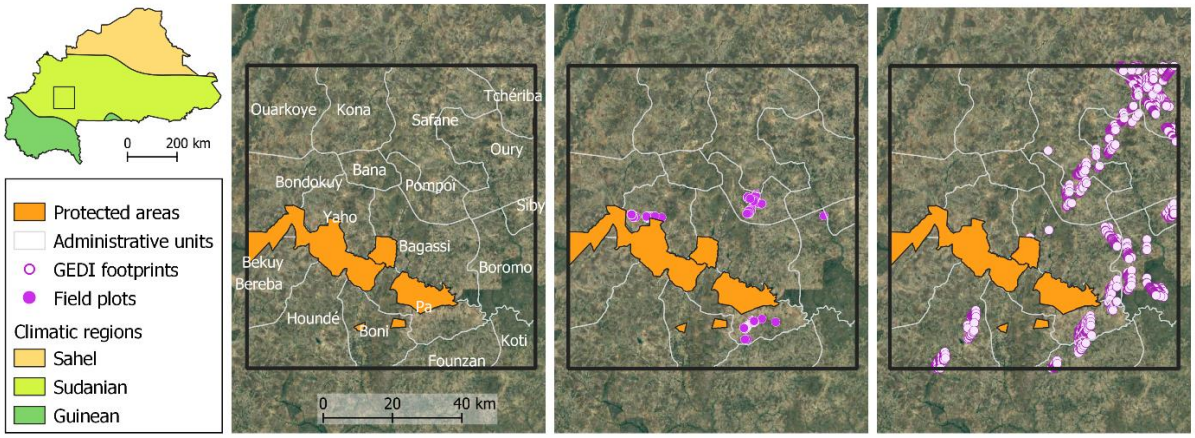

Figure 5: Region of interest in Burkina Faso showing the distribution of the field plots and the footprints from GEDI (Background image: google earth view)

2.4 Agroforestry systems

Agroforestry systems (AFS) is a collective term for land-use systems, practices, or technologies, where woody perennials (trees, shrubs, bamboo etc.) are deliberately integrated with agricultural crops and/or animals in the same land management unit in some form of spatial arrangement or temporal sequence (Lundgren et al., 1983). AFS is not a revolutionary land management approach, rather it has been always present throughout the history of mankind. In fact, it is often said to be "a new name for an old practice". The tree component is central for AFS and its composition and/or arrangement is used to determine the typology of a system. The three major aspects considered in the definition and classification of AFS were described by Atangana et al. (2014) and included:

i. The structural composition and spatial arrangement of the trees in the system: here, AFS will be differentiated based on a vertical stratification as it is the case for shade trees, or if the trees/shrubs are the same size as the crop, as it is the case in alley cropping. Also, the spatial arrangement is important and helps distinguish systems where trees are used as windbreaks or living fences. Furthermore, some AFS show trees with no spatial arrangement, where trees are randomly distributed on a farm for example. This is the case for fruit trees or trees with medicinal properties, which are actively maintained on farmlands.
ii. The temporal sequence of the woody component: A popular system here is the fallow, or improved fallow, where trees and/or shrubs are allowed to grow in the process of

regenerating the soil fertility. In the case of improved fallow, nitrogen fixing shrubs are often introduced, as an efficient way to reduce the length of the fallow. An older system is referred to as the Taungya. It is a reforestation approach which consists of associating the seedlings of trees with agricultural crops. The seedlings benefit from the treatment applied on crops (pesticides, fertilisers), and the crops are reduced as the tree grows. The same is applied in Côte d'Ivoire for cocoa plantations. At their early stage, cocoa seedlings and banana trees are managed simultaneously. Until the cocoa trees are big enough, they benefit from the shade from banana trees.

iii. The functions of the woody perennials in the system: among the functions, production refers to direct product generated by the trees. This could be fruits, edible leaves, bark and roots, medicine. Another function is service including firewood, timber for construction, fodder to feed the cattle, production of by-products such as honey and edible insects. Another function could be social as some trees are sacred and some parts used in rituals and traditional ceremonies such as marriage and funerals. A function could be environmental. This includes soil protection, fertility restoration, wind protection, improvement of the microclimate and carbon sequestration.

In this study, four AFS were considered, mainly agri-silvicultural systems, where the woody perennials are associated with agricultural crops. The main AFS identified in the ROIs were presented and described in Table 4. Homegardens, Improved fallow and multipurpose trees on croplands were referred to as farms, and plantations crop combinations were identified by the main cash crop of the system (cocoa, rubber, oil palm, mango, and cashew). In the Sudanian region, since all the AFS in the ROI were in the form of multipurpose trees on croplands (associated mainly with Cotton and sesame), the AFS classification was based on the composition of the tree species. The name of the most abundant tree species in an agroforestry farm was used as the name of the AFS.

Table 4: AFS identified in West Africa, and their description (adapted from Atangana et al., 2014)

AFS	Description
1. Homegardens	Combination of trees and crops around farmer's house. The woody components are often fruit trees.
2. Improved fallow	Perennial planted or left to grow during fallow. The woody components are fast-growing leguminous tree species
3. Multipurpose trees on croplands	Trees scattered in cropland. The perennial components are multipurpose trees (fruits, medicine, fodder, firewood etc.)
4. Plantation crop combinations	Mixture of trees and cash crop such as cocoa, rubber, mango, and cashew. The associated tree species are often forest tree species.

2.4.1 Plantation crop combination

The plantation crops were mainly found in the Côte d'Ivoire. Cocoa, rubber, and oil palm plantations were identified in the Guineo-Congolian region, whereas cashew and mango plantations were mostly located in the Guinean region. The plantation crops were often installed at the expense of forest or old fallows, especially for cocoa. The selected plantations were at least 10 years old, with at least 1 production cycle (Figure 6). The tree components in the oil palm plantations were managed sequentially in the form of a long rotation that could be up to 25 years. In the Guinean region, mango and cashew are established on previous agricultural farms. Most of the plantation crops in the region were established in the early 2000, mainly for the farmer to multiply and diversify sources of income. From the discussion with farmer on the ground, a future land use change was not planned. The sequence could therefore be summarized as follow: a forest or old fallow is cleared for agriculture including cotton production. The land is then converted to mango or cashew plantation. In the Guineo-Congolian region, the sequence is a bit different: a forest or old fallow is converted to cocoa, rubber, or oil palm plantation. The land conversion is

triggered by the yield level. When the farm is no longer economically viable, the land is converted to agricultural farms which eventually will be converted to fallow.

Figure 6: Plantation crops combination in Côte d'Ivoire. From left to right, first row: oil palm, rubber, cocoa; second row: mango and cashew plantations. (Source: author, Côte d'Ivoire, March 2020)

2.4.2 Farms

Farms are mainly managed for food production, for consumption at the family level, or for the market. The AFS referred to as farms also include homegardens, and fallows (Figure 7). The main agricultural crops in West Africa include:

- Cassava (*Manihot esculenta*) which is used to manufacture *Atieké,* the main local food of the country.
- Rice (*Oriza sativa*) which is also a major component of the daily diet. The rice is mainly cultivated in lowlands throughout the year, but there is also a variety of rainfed rice for the rainy season.

Figure 7:Agroforestry farms in West Africa. From left to right: homegardens, multipurpose trees on crop lands and improved fallow (from where firewood is often collected). (Source: author, Côte d'Ivoire, March 2020).

- Yam (*Dioscorea alata*) is an important food crop cultivated mainly on very fertile lands. The edible tubers are pounded often in combination with banana-plantain, to make a very appreciated meal referred to as *futu*. However, the main purpose of yam production is the commercialization in urban areas.
- Plantain or banana (*Musa sp*) is a major crop in the region. It is often established at the early stage of cocoa plantations. Since cocoa trees are mainly grown on pure stands (without associated trees), the shade they need at their early stage is often provided by banana trees. The production is part of the local consumption, but the surplus is destined to the local and international market.
- Maize (*Zea mays*) is one of the most important crops in the country. Because of its short cycle, it is one of the most cultivated crops both in high and lowlands. In the Guinean region, it was found as the main element of the diet of farmers. The residuals from maize are used as fodder for the cattle during the dry season. Also, maize is used as input for processing local beer.
- Cotton (*Gossypium sp*) is the first cash crop in the Guinean and Sudanian region of West Africa. It has a cycle of about 3 months, and it is the main source of income for farmers in that region. The yield was estimated at 473 kg/ha in Côte d'Ivoire and about 385 kg/ha in Burkina Faso.
- Sesame (*Sesamum indicum*) is an important crop in the Sudanian, and Burkina Faso is the 6th world largest producer with about 374.7 tonnes in 2019. Sesame is preferably established on old fallows, where they are managed in combination with other trees.

African locust bean trees and shea trees (*Parkia sp* and *Vitellaria sp*) are often associated with cash crop.

2.5 In situ data

During the field campaign two types of data were collected: (i) reference points for the image classification and (ii) biophysical parameters of trees for carbon estimation.

2.5.1 Data collection

The same data collection approach was applied in each of the ROIs. In each site, sample plots of 40 × 40 m were defined in plantations (cocoa, rubber, oil palm, mango, and cashew) (Figure 8). The plot was defined in the middle of the considered AFS, at least 100 m away from the main road. A condition of minimum five trees in the sample plot was observed in each AFS. When the previous conditions were fulfilled, the coordinates of the four corners of the plot were recorded using a GPS, and the centre of the field plot was also registered and labelled.

Figure 8:Establishment of a field plot in an agroforestry farm (Source: author, Burkina Faso, June 2021)

Each tree in the defined sample plot was identified by its name (common name and or local name) with the help of field assistants. For trees that were not directly identifiable in the field, pictures, and some parts of the trees (leaves and/or fruits) were collected for a post-field identification by a botanist. Another challenge was to find the correct scientific names of trees species from their local names, as the local name is associated with the local language. Therefore, local names were recorded with the corresponding dialect, and the corresponding picture. Additionally, to the name of the tree, biometric parameters of the tree were collected including the height of the tree, and the diameter at breast height (Figure 9). The height was measured by an altimeter, which provided a ready-to-use measurement in metres. The DBH was measured using a diameter tape, which returned the diameter of the tree from the diameter.

Figure 9:Collection of biophysical parameters of trees in AFS (Source: author, Côte d'Ivoire, March 2020).

from left to right: diameter measurement using diameter tape; species identification; and height measurement with an altimeter. (Picture from the field campaign, Côte d'Ivoire, March 2020).

The collected sample plots in West Africa were summarized in Table 5. It shows (i) 122 samples in the Guineo-Congolian region including 62 plots in farms, 30 plots in cocoa plantations, 16 plots in oil palm and 31 plots in rubber plantations. (ii) 66 samples were collected in the Guinean region: 21 plots in cashew, 22 plots in mango plantations and 23 plots in farms, and finally (iii) 56 samples in the Sudanian region, in different crop farms (Sesame, cotton and maize) managed as AFS.

Table 5: Summary of the number of samples collected in West Africa

Climatic regions	AFS	Number of samples
Guineo-Congolian	Cocoa	30
	Rubber	31
	Oil palm	16
	farm	62
Guinean	Mango	21
	Cashew	22
	farm	23
Sudanian	Miscellaneous AFS	56

2.5.2 Data preparation

The collected data were reported and organized in MS Excel. it included quantitative data gathered through in situ measurements and qualitative data collected using questionnaire. The main elements of the qualitative data included information related to the age of the AFS, the management practices and a description of the land cover supported by pictures.

2.6 Carbon estimation

The estimation of carbon stocks in a given ecosystem summarizes the carbon stocks of five different carbon pools namely: aboveground biomass (AGB), belowground biomass, dead wood, litter and soils (Gytarsky et al., 2015). In Agri-silviculture, it was reported that aboveground carbon sequestration rates were higher in farms (improved fallows and multipurpose trees on crops lands) compared with any other AFS, while soil carbon sequestration rates were higher in crop plantations (Feliciano et al., 2018). In this study, AGB was considered the most important carbon pool, since it is the only pool that could be used for a consistent monitoring of carbon sequestration across AFS using remote sensing. Therefore, the aboveground parameters collected on trees were used to

determine the standing biomass in each plot. For each tree, the species name was used to retrieve the wood density from the ICRAF's database (Carsan et al., 2012). For trees that were not found in the database (*Ficus gnaphalocarpa* for example), the wood density of a tree from the same family was used (*Ficus trachyphylla* in this case).

$$\mathbf{AGB=0.0580 \times \sigma \times (D^2 \times H)^{0.999}}$$

The wood density of the species (σ), the height (H) and the diameter (D) of the tree were compiled to determine the AGB using the allometric equation proposed by Aabeyir et al. (2020) equation 1). This allometric equation is a mixed-species model for the estimations of AGB in the tropical woodlands of West Africa, which was found to be equivalent to the pantropical model proposed by Chave et al. (2014) within ±10% of their mean prediction. The model was appropriate for this study, as all the tree species that were identified in the AFS were present in the list of species used to develop the allometric model. This ensured that the prediction of the model was more accurate than the prediction from the pantropical model of Chave et al. (2014), as suggested by the study. The AGB estimations of all the trees in a sample plot were averaged to get an estimation for the sample plot.

2.7 Remote sensing data

2.7.1 Data description

Three data sources were considered and used during this research: (i) the C-band Radar and Optical data from the Sentinel missions; (ii) the L-band Radar data from the Advanced Land Observation Satellite-2 (ALOS-2) and (iii) the LiDAR data from the Global Ecosystem Dynamics Investigation (GEDI).

2.7.1.1 Sentinel mission

Sentinel mission is an earth observation mission developed by the European Space Agency, and was created with the aim of replacing older earth observation missions such as ERS and Envisat missions, to ensure a continuity of data (ESA, 2022). Sentinel has seven missions, each one observing different aspects of the earth surface including atmosphere (Sentinel-4, -5, -5P), oceans (Sentinel-1, -3, -6), and land (Sentinel-1, -2). In the research, Sentinel-1 (S1) and Sentinel-2 (S2) data were considered.

S1 was first launched in April 2014 and is composed of two polar-orbiting satellites (S1A and S1B) operating day and night, to provide VH/VV polarization for the C-band Synthetic Aperture Radar data (SAR), enabling the observation of the earth surface regardless of the weather conditions. Figure 10 illustrates an overview of the S1 data over the AOI in the Guineo-Congolian region. SAR refers to a technique for producing fine-resolution images from a resolution-limited radar system, requiring the radar to be moving in a straight line, from the space platform (NISAR, n.d.). The constellation (S1A and S1B) covers the entire world with a revisit time of six days.

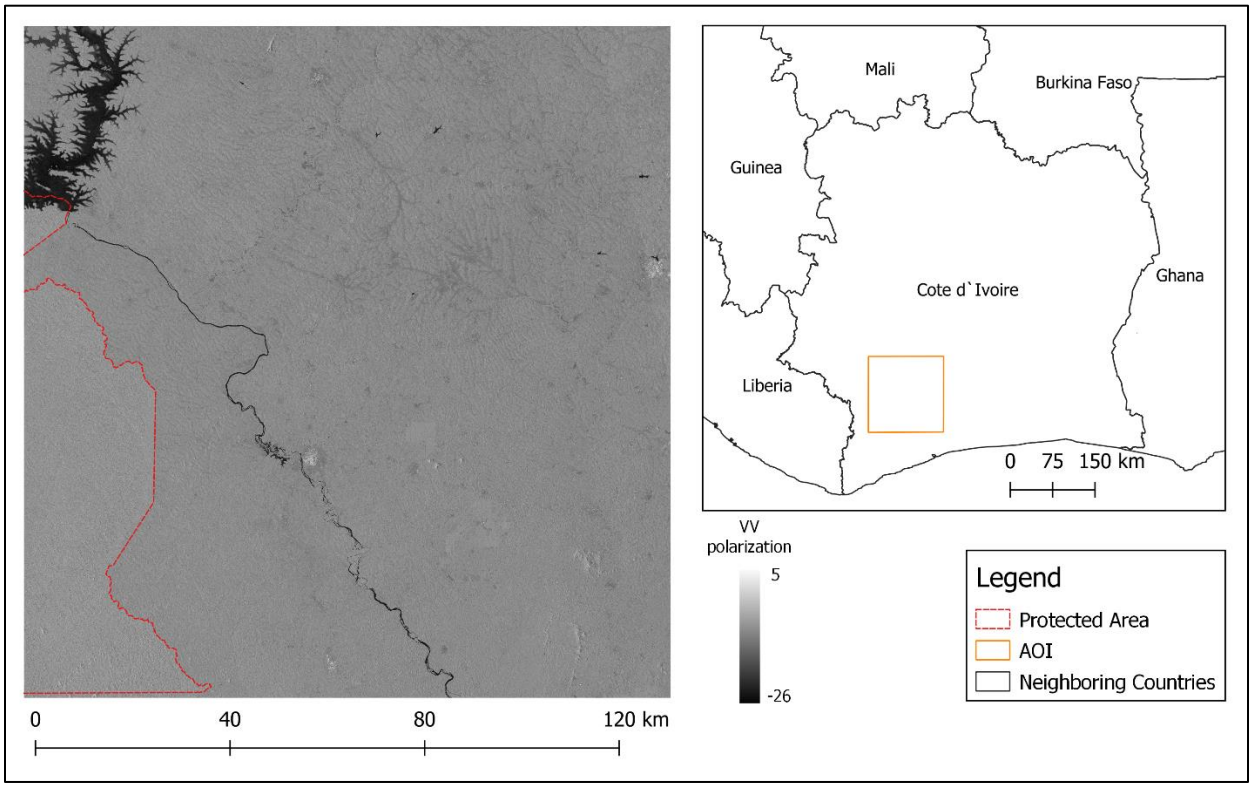

Figure 10: Sentinel-1 image (VV polarization) of the ROI in the Guineo-Congolian region

S2 is a constellation of two polar-orbiting satellites (S2A and S2B) placed in the same sun-synchronous orbit, phased at 180° to each other, that was first launched in June 2015. The constellation offers a revisit time of 5 days and a spatial resolution of 10 m for the visible-Near infrared bands including red, green, blue, and near-infrared and 20 m for the red-edge band. S2 data are sensitive to clouds, since they are passive sensors, which makes it harder to monitor tropical landscapes. Figure 11 shows and overview of a false colour display of S2 data in the Guinean region.

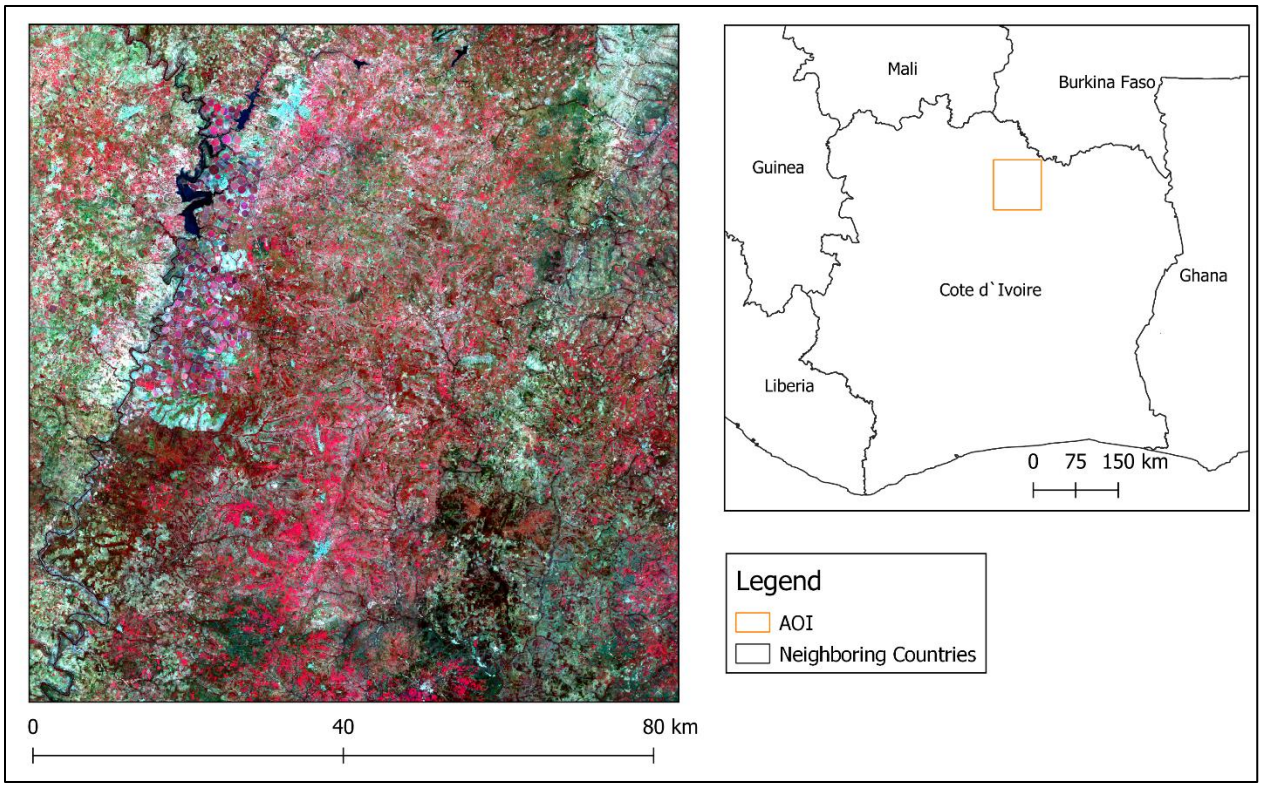

Figure 11: Sentinel-2 image (false colour) of the ROI in the Guinean region

2.7.1.2 ALOS-2

The spacecraft ALOS-2 also known as DAICHI-2 was launched in May 2014 and provides Phased Array L-band Synthetic Aperture Radar (PALSAR) data. PALSAR data were reported to be successful for the effective monitoring of cultivated areas and for the identification of carbon sinks. ALOS-2 has a revisit time of 14 days and can observe the earth surface day and night in all weather conditions. The data is available at a single polarization (HH or VV) but the cross polarization (HH/VV) was used (PALSAR, 2022). Figure 12 gives an overview of the VH polarization of the ALOS PALSAR data in the Sudanian region.

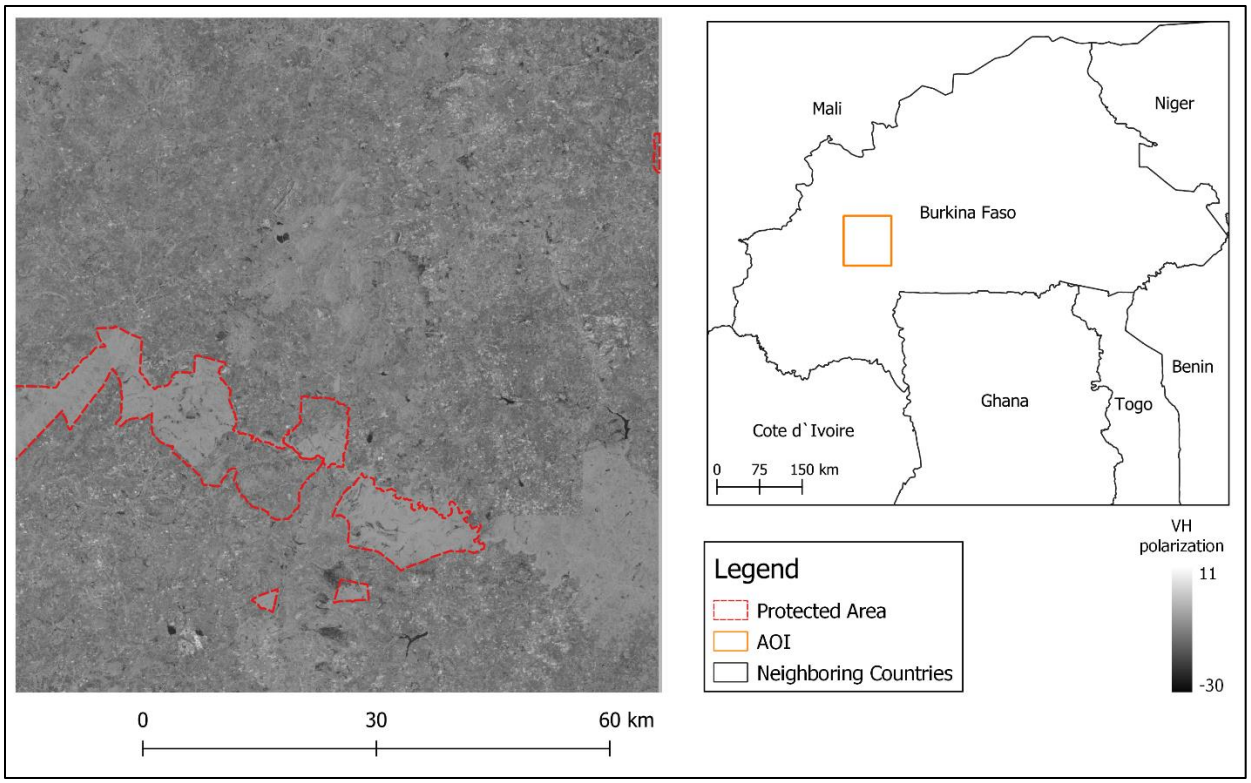

Figure 12: ALOS-2 PALSAR image (HH polarization) of the AOI in west Africa

2.7.1.3 GEDI

GEDI is a full waveform lidar instrument, which uses pulses of laser light to measure the 3D structure of the earth surface. It is the first high resolution laser ranging observation instrument to study the earth surface. It was launched on SpaceX-16 on December 5th, 2018. GEDI started collecting scientific data on March 25th, 2019, and will continue until 2023. The applications of GEDI are numerous and diverse, and some of the domains include water resource management, weather prediction, geomorphometry and forest management. It provides accurate measurements of the forest canopy height, the canopy vertical structure and the surface elevation, which has radically improved the estimations of carbon stocks. The LiDAR system of GEDI is made of three lasers that produce eight parallel tracks of observations. Each laser is emitted at a frequency of 242 Hz to illuminate a 25 m footprint where the 3D structure is measured. Each footprint is separated by 60 m along the track and 600m across-track distance. From the measured 3D structure, several products have been derived including relative height (level 2A), canopy cover fraction (level 2B) and aboveground biomass (level 4A). The level 4A product (GEDI L4A) contains aboveground

biomass predictions and the associated uncertainties which has been derived from level 2A combined with field measurements (Dubayah et al., 2020).

2.7.2 Data acquisition

All the satellite data were accessed via Google Earth Engine (GEE), and a mosaic image for each region of interest was generated. For S2 data, a composite image was used as a solution to the cloud issue. The image collection from January to December was filtered, and only scenes with a maximum cloud percentage of 5% were selected. A median image was then generated for five bands (blue, green, red, red-edge and near-infrared). For S1, the Sentinel global backscatter model (S1GBM) was used, where the VH/VV polarizations was acquired by the interferometric wide swath mode, which is mostly used for land monitoring since it satisfies most of the current service requirements such as preserving the revisit performance (Bauer-Marschallinger et al., 2021; Copernicus, 2022). Only the yearly composites of the ALOS-2 data were available on GEE. Average images of the HH/VV polarization were generated over the past three year (2019 to 2021) to reduce the noise on the image. GEDI L4A data were downloaded from the Earth Data platform, and the footprints were extracted as shapefile for each region of interest. The footprints were filtered based on the quality of prediction as described in the metadata. Only footprints associated with a good quality (high accuracy and low error) was selected.

2.7.3 Data preparation

The five optical bands from S2 were combined to generate seven vegetation indices including NDVI, GLI, EVI, SAVI, MSAVI, TCARI and VARI (Table 6). The five bands and the seven derived indices were stacked together to represent S2 data input.

Each of the HH/VV and VH/VV polarizations from ALOS-2 and S1 respectively were used to generate texture parameters. The Grey Level Co-occurrence Matrix (GLCM) was used to generate the texture parameters. GLCM is a tabulation of how often different combinations of pixel brightness values (grey levels) occur in an image (Hall-Beyer, 2017). GLCM texture considers the relation between two pixels at the same time, called the reference and the neighbour pixel. It returns the probability of the reference pixel to have the same grey level with its neighbour, in specific direction, and the result textures metrics are based on those probabilities. For the calculation, all direction was considered, within one pixel offset (a reference pixel and its immediate neighbour).

Table 6: Vegetation indices and formulae

Vegetation indices	**Formula**
1. Normalized Difference Vegetation Index (NDVI)	(NIR – R) / (NIR + R)
2. Green Leaf Index (GLI)	(2 × G – R – B) / (2 × G + R + B)
3. Enhanced Vegetation Index (EVI)	2.5 × (NIR – R) / (NIR + 6 × R – 7.5 × B + 1)
4. Soil Adjusted Vegetation index (SAVI)	(1 + L) × (NIR – R) / (NIR + R + 0.5)
5. Modified Soil Adjusted Vegetation Index (MSAVI)	0.5 × (2 × NIR + 1 – sqrt ((2 × NIR + 1)² - 8 × (NIR – R))
6. Transformed Chlorophyll Absorption in Reflectance Index (TCARI)	3 × ((RE – R) - 0.2 × (RE - G) × (RE / R))
7. Visible Atmospherically Resistance Index (VARI)	(G - R) / (G + R - B)

* sqrt = square root, (bands B: blue, G: green, R: red, RE: red-edge, NIR: near infra-red).

The GLCM values were used to calculate eight texture parameters for each polarization, using a window size of five-by-five pixels and the default number of 32 grey levels. The parameters were computed using the glcm R package version 1.6.5 (Zvoleff, 2020). The formula of the different GLCM parameters and their explanation is presented in Table 7.

Table 7: GLCM texture parameters (Hall-Beyer, 2017)

Texture measures	**Formula**	**Explanation**
Entropy	$\sum -\ln(P_{ij})\, P_{ij}$	Smaller P_{ij} leads to higher entropy value
Contrast	$\sum P_{ij}\,(i-j)^2$	Express difference as an exponential function
Variance	$\sum P_{ij}\,(i-\mu_i)^2$	Describe the variance of GLCM values
Correlation	$\sum P_{ij}\,[(i-\mu_i)\,(j-\mu_i) / \sigma^2]$	Describe the correlation of GLCM values
Mean	$\sum P_{ij} / N$	Describe the mean of the GLCM values
Homogeneity	$\sum P_{ij} / (1+(i-j))^2$	Express difference as an inverted exponential function
Dissymmetry	$\sum(\sum(\lvert i-j\rvert\, P_{ij}))$	Express difference as a linear function
Second moment	$\sum(\sum(P_{ij})^2)$	Return the max value when all pixels are identical

where (i): reference pixel; .(j) : neighbour pixel; P_{ij}: GLCM expressed as a probability of having a pair of pixels with a specific value in a specific spatial relationship , μ: mean -and σ: standard deviation within GLCM in the specified window size.

2.8 Data processing

2.8.1 Overview of data processing

The approach for the data analysis was organized in three steps (Figure 13):

(ii) Mapping the different AFS: This step consisted of training a random forest algorithm (RF) using field data, for the classification of the satellite data using a supervised classification approach. From the trained model, the probability map of each feature class was generated and used as input to generate an entropy map. The entropy map was used to analyse the heterogeneity at pixel level using predefined threshold values. Different entropy threshold values which were used to differentiate mixed- from unmixed pixels on the classification

map, were defined and compared. An improved classification map was obtained by removing mixed pixels from the initial classification map.

(iii) Estimating carbon stock in AFS: The analysis consisted of training and comparing the performance of seven machine learning regression models for the prediction of carbon stock based on two AGB reference sources: the first reference source was the carbon estimations derived from field measurements and the second one was the predictions obtained from the GEDI L4A product. The performance of the regression models was assessed and the model setting with the best performance was used to generate the carbon map in each ROI. Based on the carbon estimation generated with field measurements, the uncertainties at plot level was quantified and a RMSE map was generated. Using the improved AFS map from step (i), the carbon and RMSE maps per AFS were generated.

(iv) Evaluating the carbon dynamic in different climatic regions: in this section, the spatial distribution of carbon source and carbon pools were detected, and the amount of emitted/stored was estimated using yearly estimations of carbon storage of AFS between 2017 to 2021. The carbon time series was summarized by producing an average carbon map and the corresponding standard deviation map. Yearly anomaly maps were returned from the difference between the annual estimation and the average, and the standard deviation map was used as threshold to detect significant changes in the carbon stocks. The detected changes and the improved AFS classification were used to describe the carbon flux in the AFS of West Africa.

2.8.2 Image classification

2.8.2.1 Random forest classification

RF was trained in R using the package random forest (Breiman, 2001). Pixels values from the satellite images were extracted using the labelled field plots. The resulting data was divided in two parts: 3/4 was used to train the model and 1/4 as a test set. The model was trained using a cross validation approach of 10 folds and 10 repetitions. The hyperparameter tuning routine was implemented to find out the optimal number of variables to be sampled at each split. The model was then used for the classification of the AFS, and three parameters were extracted: the overall accuracy (OA); the producer and user accuracies (PA and UA respectively). To reduce the salt and

pepper effect on the map, a probability pass filter of 3 by 3 pixels was applied on the classified map.

2.8.2.2 Spatial error assessment (entropy and GWR)

Probability maps of each feature class were generated from the trained model, showing the likelihood of each pixel to belong to the corresponding AFS. The Shannon entropy was calculated to assess the heterogeneity at each pixel by returning a value between 0 and 1, where 0 correspond to a low level of heterogeneity referred to as "pure pixels" in this study, and 1 correspond to high heterogeneity referred to as "mixed pixels". The entropy threshold values used to distinguish pure from mixed pixels were 0.2, 0.3, 0.4 and 0.5. Each of those values were compared with the AFS' entropy threshold values derived from the entropy map using the field plots. The entropy map was then classified into pure pixels and mixed pixels, referred to as good and error pixels respectively.

$$\mathbf{H(x) = -\sum P(x)_i \log P(x)}$$

Where H(x) represents the Entropy values for the pixel (x), and $P(x)_i$ the probability value of the pixel (x) to belong in the AFS class i.

Before using the error pixels, their spatial distribution was assessed to check for spatial autocorrelation in the study area using a geographically weighted regression (GWR). GWR is a technique to model spatial heterogeneities on the map when the relationship between variables varies as a function of spatial location (Brunsdon et al., 1996).

$$\mathbf{Y_i = \beta_{i0} + \sum \beta_{ik} X_{ik} + \varepsilon_i}$$

Where Yi corresponds to the pixel label (good/error pixels) at location i; β_{i0} is the intercept variable at location i; β_{ik} is the regression coefficient for variable k at location i; X_{ik} is the independent variable k at location i, and ε_i is the residual error at location i.

To implement the GWR, 500 random points were used to extract pixel's values across the study area. The values were taken from the satellite images and the entropy map (good/error pixels). The relevant features to explain the distribution of the error pixels were selected using a stepwise logistic regression based on the Akaike information criterion (AIC). The spatial autocorrelation in the residuals was tested using the Moran's I statistic

$$\mathbf{I = n \sum\sum w_{ij} Z_i Z_j (S_0 \sum Z_i^2)^{-1}}$$

Where Zi represents the deviation to the mean for feature i; w_{ij} is the spatial weight between feature i and j. n represents the number of features and S_0 is the aggregate of all the spatial weights (ArcGIS, 2005)

In case of no evidence of spatial autocorrelation, the relationship between the predictors and the error pixels was assumed to be constant across the map, thus a GWR was not applicable. However, if there was evidence of spatial autocorrelation in the residuals, a multiscale GWR was applied, and the residuals were tested for spatial autocorrelation. Depending on the scale at which each variable affected the distribution of the error (local or global) on the one hand, and the result of the spatial autocorrelation test on the other hand, a variant of the GWR was applied as described by Comber et al. (2020). After the spatial assessment of the classification error, the error pixels were removed from the classified map, returning an improved classification map of the AFS in the study area.

2.8.3 Carbon estimation

2.8.3.1 Model training

For the carbon estimation, two carbon reference sources (field measurements and GEDI L4A) were compared. The pixel values extracted from the input images using the field plots and the GEDI footprints were used separately to train a set of models. Several models were considered including:

i. a linear regression model with three regularization techniques namely Ridge, Lasso and ElasticNet (Kirkland et al., 2015).
ii. a RF model was considered, and the model was trained using a cross validation approach of 10 folds and 10 repetitions. The model was tuned to determine the optimal number of variables to be sampled at each split. The model used to generate a carbon map from the satellite data.
iii. the variable selection using random forest model (VSURF) which is based on reducing the correlation within predictors by removing redundant variables and identifying the most relevant variable for the prediction and interpretation (Genuer et al., 2015).
iv. a support vector machine classifier (SVM) which is aimed at minimizing the margin between two classes to distinguish them (Genuer et al., 2015)

The coefficient of determination (R^2) and the root mean square error (RMSE) were used to assess the prediction performance of the AGB models in the study area. The combination of satellite data and the model that showed the highest performance was selected to generate the AGB map in each region of interest. The improved classification of the AFS was then used to describe the carbon stock for different AFS in West Africa.

$$\mathbf{RMSE} = \sqrt{\frac{\sum (\hat{y}\mathbf{i} - \mathbf{yi})^2}{\boldsymbol{n}}}$$

$$\mathbf{R^2} = \mathbf{1} - \frac{\sum (\hat{y}\mathbf{i} - \mathbf{yi})^2}{\sum (\mathbf{yi} - \bar{y})^2}$$

Where $\hat{y}_i$ represents the predicted carbon stock value at the pixel i ; y_i is the measured carbon stock value at pixel i; n is the number of pixels; $\bar{y}$ is the average carbon stock value of the field plot.

2.8.3.2 Uncertainties estimations

The carbon estimations were compared with the measured value to capture the spatial distribution of the prediction uncertainties. The prediction was compared to the measured values of carbon stocks for each pixel, and the RMSE was estimated for each plot. Using the RMSE value at the plot level as a target, a RF algorithm was used to generate an uncertainty map from the satellite input data. The RMSE value from the carbon stock estimation model was used as a threshold to identify pixels with higher or lower RMSE value. Pixels with an uncertainty lower than the RMSE of the model were considered to have a lower error, whereas pixels with a predicted uncertainty higher than the RMSE of the model was considered to have a higher error. The uncertainty map was presented alongside the carbon map to show the spatial distribution of the uncertainties in the estimation of the carbon stock in AFS.

2.8.4 AGB dynamic in AFS

2.8.4.1 AGB time series mapping (2017-2021)

Yearly AGB maps were generated between 2017 and 2021 for each ROI. The predictions were generated using the model that was trained using the field measurements as reference. Since the reference data were only available for the year 2021, the evaluation of the yearly AGB predictions was not possible. The main assumption was that the variation of the carbon level in the sample plots was minimal during the time frame. Consequently, the R^2 and the RMSE were not calculated

for that period, and the error was assumed to be consistent from one year to the other. The yearly AGB maps were summarized using a raster calculator to generate an average AGB map and a standard deviation map over the period 2017 – 2021.

2.8.4.2 Anomaly detection in the AGB

To capture the dynamic of AGB stocks in West Africa, the yearly anomaly maps were returned from the difference between the yearly AGB estimation and the average AGB level. By showing the difference of the AGB estimation of a given year to the average AGB level, the anomaly map provides the spatial distribution of carbon source and carbon sinks, where carbon source was defined as the portion of the map which emits carbon. It corresponded to the area where the yearly estimation is below the average. On the other hand, a carbon sink was defined as the portion of the map which stored carbon. It represented locations where the yearly AGB estimation was higher than the average.

The values from the anomaly map of a given year was assessed for significance using the standard deviation map. The standard deviation was used as a threshold to separate non-significant changes from significant changes. If the values from the anomaly maps were lower than the standard deviation (in absolute value), the difference between the yearly AGB estimation and the average AGB level was not significant for that location. On the contrary, if the values of the anomaly map were superior to the standard deviation, the difference was significant, and the location was classified as carbon sink or carbon source, depending on the direction of the change.

The spatial distribution of carbon sinks and carbon sources was then used as a mask to remove areas where the carbon level was constant. The values from the anomaly maps, representing the amount of carbon stored or emitted, were used to quantify the contribution of the ROI to climate change. Finally, the AFS map was used to rank AFS based on their level of emission and/or sequestration.

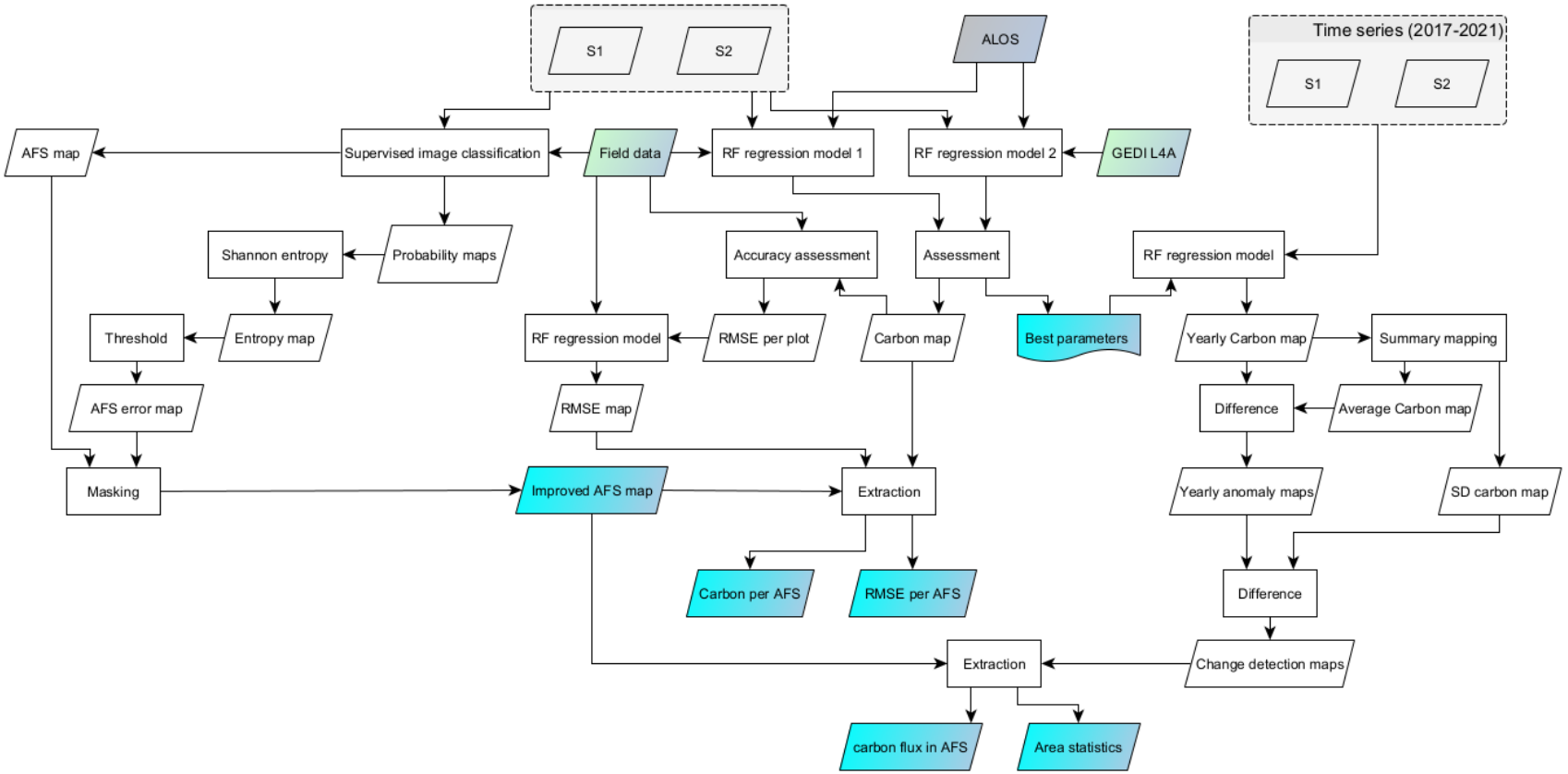

Figure 13: Flowchart of analysis: the boxes in green represent the carbon reference data sources; the boxes in blue correspond to the main outputs. The output best parameters correspond to the data combination and ML regression model that gives the best performance.

Chapter 3

Results

3.1 Mapping AFS in West Africa

Mapping AFS is a challenging task especially when using opensource RS imagery such as data from the Sentinel mission. The applied methodology aimed at providing a reliable classification map of the main AFS in West Africa by identifying the best feature combination of the predictors derived from optical and SAR data on the one hand, and also to model the spatial distribution of the classification error on the other hand. Some of the results presented in this section were organised and applied in Cote d'Ivoire to model the spatial distribution of the classification error in cocoa agroforestry systems (Kanmegne Tamga et al., 2022). This section was organised in way to present the AFS mapping for each of the main climatic regions in West Africa, including assessment of the classification model and the spatial error assessment.

3.1.1 Guineo-Congolian region

3.1.1.1 Feature importance and AFS classification

The classification of the AFS in the Guineo-Congolian region was carried by training a RF model on RS derived indices from Sentinel-1 and -2. Features derived from optical data, especially band B and G but also the vegetation index GLI, are the most important variables for mapping AFS (Figure 14). The figure also shows that S1 bands and the derived GLCM texture parameters are less important features regarding the mean decrease Gini value.

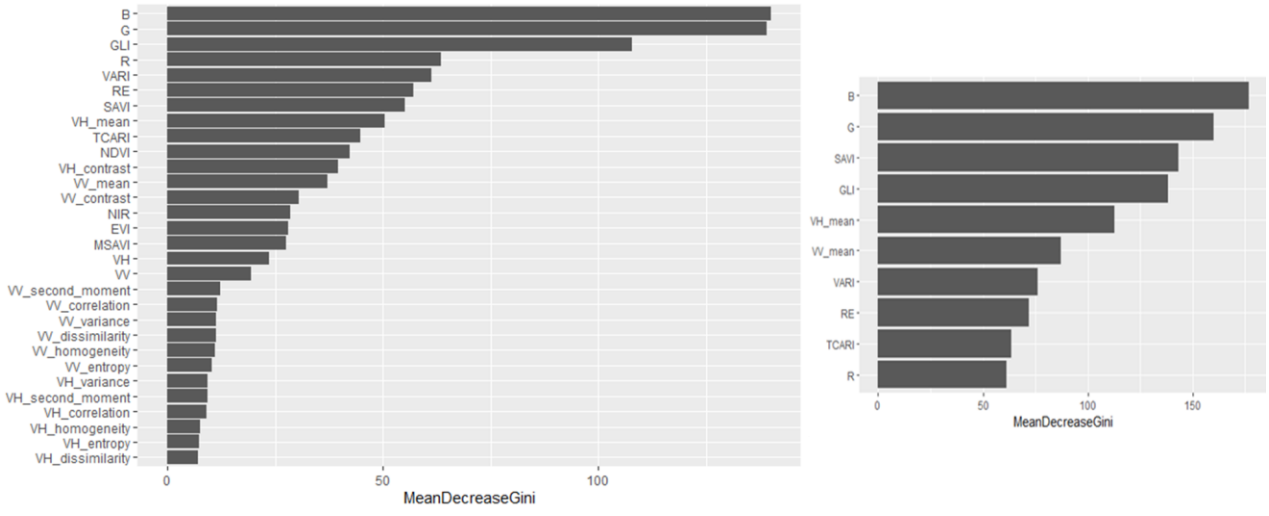

Figure 14: Feature importance (A) and the variable selection for the classification of AFS in the Guineo-Congolian region

The wide value range within the feature importance and the large proportion of unimportant features required a feature selection to identify the most important variables for the prediction of AFS using Sentinel data. The variable selection using random forest (VSURF) was used to return the list of variables for the prediction of AFS while minimizing the correlation between features. The VSURF shows only 10 features are required for mapping AFS in the Guineo-Congolian region: four optical bands, four vegetation indices and two GLCM texture parameters. The assessment of the variable's importance after the VSURF shows that significant variables for AFS mapping are derived from optical data.

Classification assessment

The selected variables were used to train a RF model for the classification of AFS. The assessment of the model suggested an overall accuracy OA = 0.89 (Kappa = 0.86). The confidence interval of the accuracy at 95% is between 0.86 and 0.92. The producer's and user's accuracies showed that the omission and commission errors are higher for farm (PA=0.85, UA=0.92), cocoa (PA=0.89, UA=0.84), rubber (PA=0.92, UA=0.94) and palm (PA=0.92, UA=0.89) respectively. These results were supported by the AUC for each of the feature class: farm (0.85), cocoa (0.89), rubber (0.96) and palm (0.98). Figure 15 shows the spatial distribution of the main AFS in the region and the area statistics suggested that rubber (38.9%) and cocoa plantations (36.4%) were dominant, followed by farms (13.8%) and oil palm (10.8%). The protected area corresponding to the Taï National Park (TNP) corresponded to a tropical dense forest. However, during the classification the area was not masked out, rather it was classified as an AFS. Only waterbodies, urban area and bare soil were removed. The TNP is mainly classified as cocoa plantations with intrusions of rubber and palm plantations which could help detected encroachments within the boundaries of the protected area.

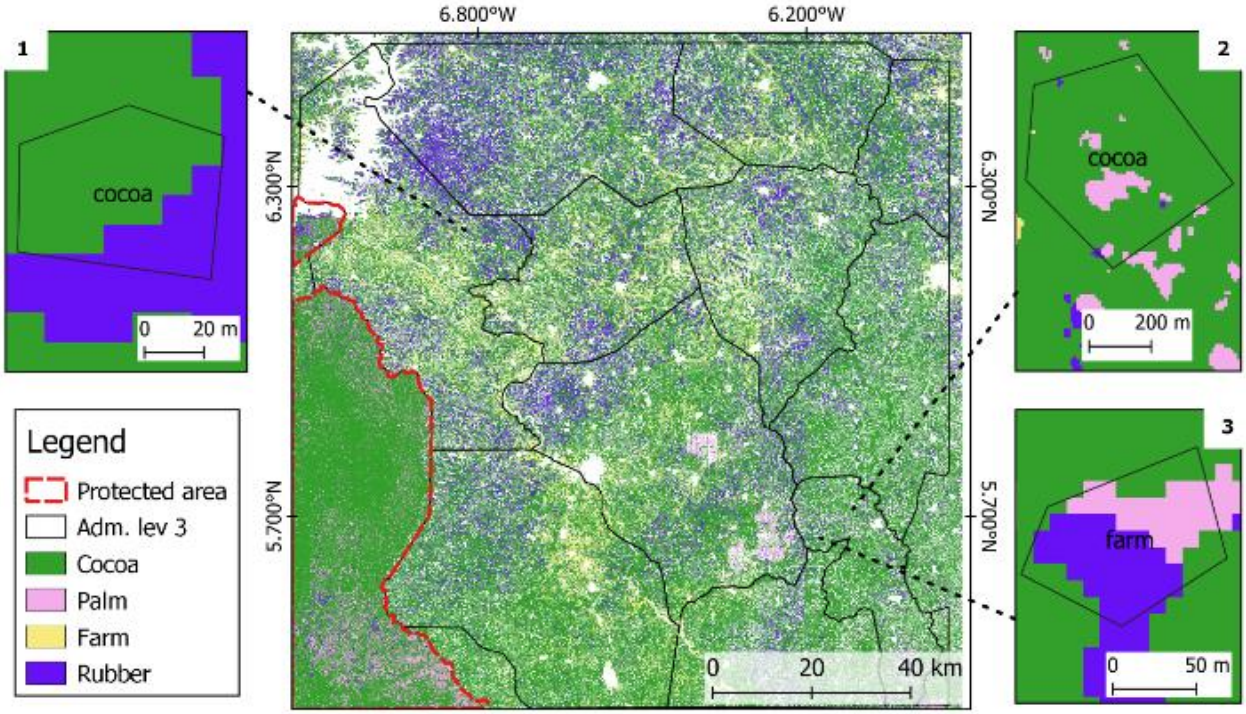

Figure 15: Classification map of the AFS in the Guineo-Congolian region of West Africa

A closer look at the classification map shows evidence of misclassification in cocoa plots as presented in figure 15-snippet 1 and snippet 2. Pixels within cocoa boundaries were misclassified as rubber or oil palm plantations. Also, some pixels corresponding to farm are falsely classified as rubber or palm plantations as presented in Figure 15-snippet 3.

3.1.1.2 Spatial error assessment

The probability maps that were derived from the classification showed that the spatial distribution of pixels with high probability of prediction for cocoa and rubber are overlapping in certain region, for example within the protected area (Figure 16).

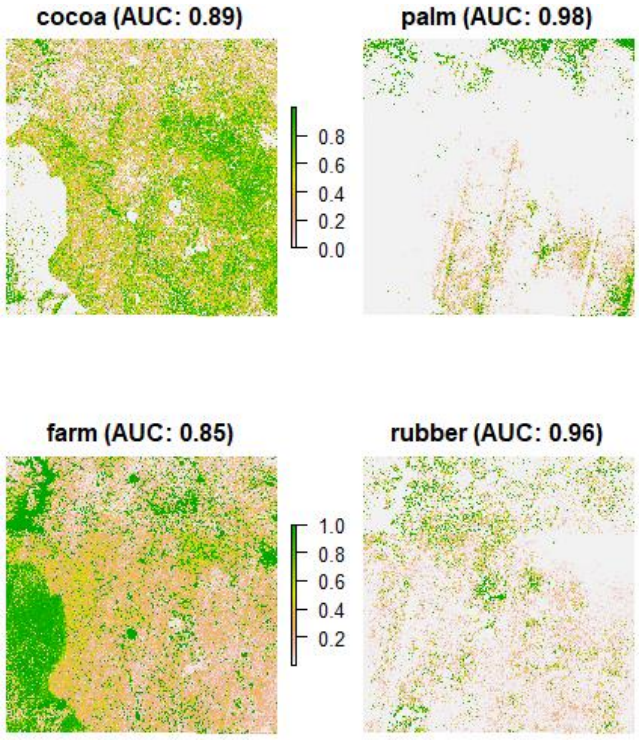

Figure 16: Probability maps of the AFS in the Guineo-Congolian region

In agreement with the information provided by the probability maps, the entropy map showed that pixels located within the boundaries of the protected areas were associated with a high level of heterogeneity (Figure 17). From the entropy map, different thresholds were used to generate the error maps. The common points between the error maps was that, for the different considered thresholds, the region corresponding to protected area was classified as error.

The error maps showing the spatial distribution of mixed pixels have been used to improve the classification map by removing pixels associated with error (Figure 18). All the pixels in the protected area were removed, however certain pixels were not considered as error, and could be regarded as encroachment within the protected areas. The analysis also showed that by removing the mixed pixels, there is an improvement of the classification at the plot level. In cocoa plantations for instance, the level of error within certain plots was significantly reduced (Figure 18-Snippet 2) but in region where cocoa plantations were established next to rubber, all the pixels were considered as error and therefore removed (Figure 18-Snippet 1). In agricultural land, the approach reduced the level of misclassified pixels, but the overall error level remains high (Figure 18-Snippet 3).

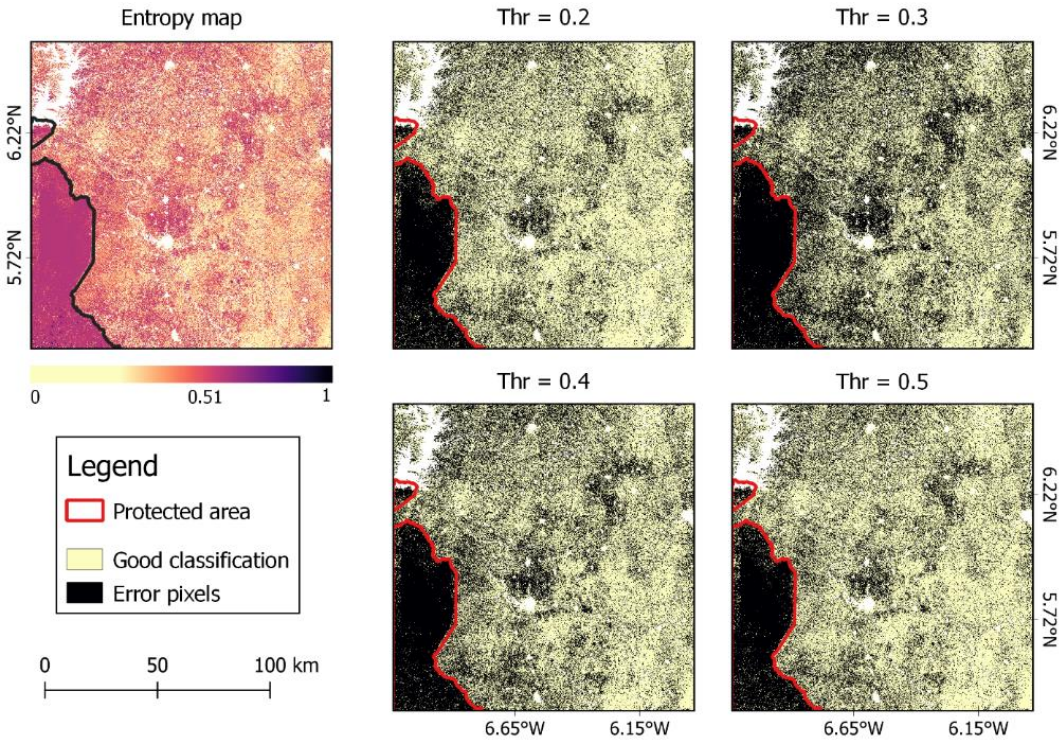

Figure 17: Entropy map and corresponding error maps at different threshold in the Guineo-Congolian region

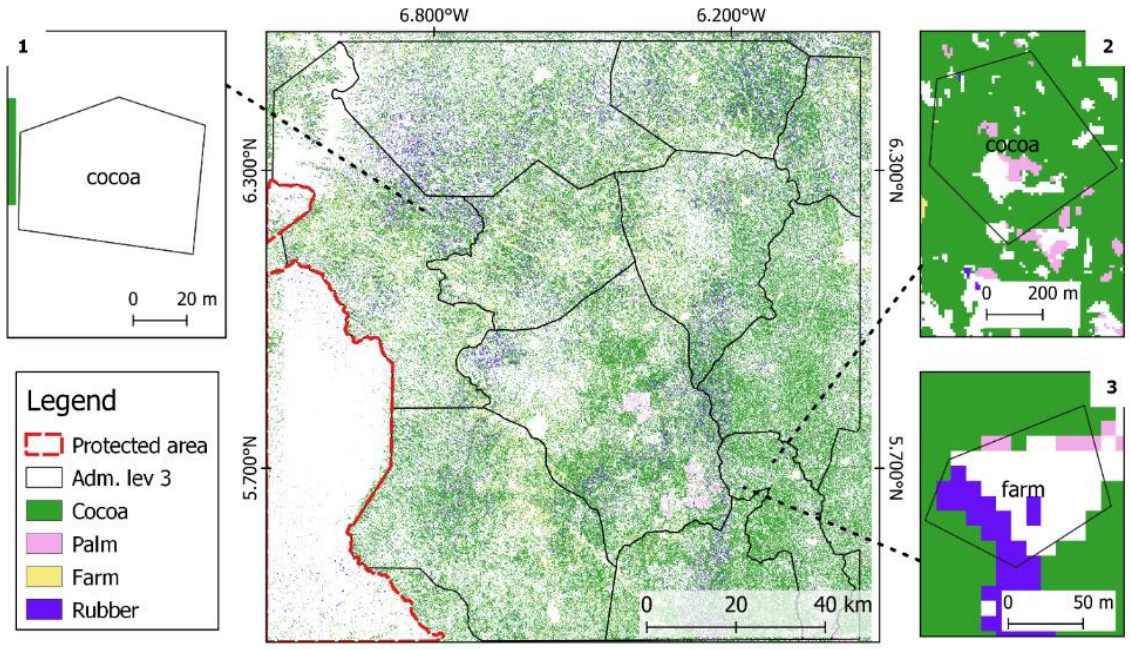

Figure 18: Improved classification of the AFS in the Guineo-Congolian region

Considering the improved AFS map, the estimation of the corresponding area is presented in Figure 19. The graph shows a comparison between areas estimated at different threshold and the reference threshold (derived from field measurement). It appears that farm, cocoa, rubber and palm had the largest area respectively at different threshold. In farms, a threshold under 0.4 underestimated the area, while above that threshold value, the area was overestimated. However, in cocoa rubber and palm, area estimations were lower than the reference value regardless of the threshold value.

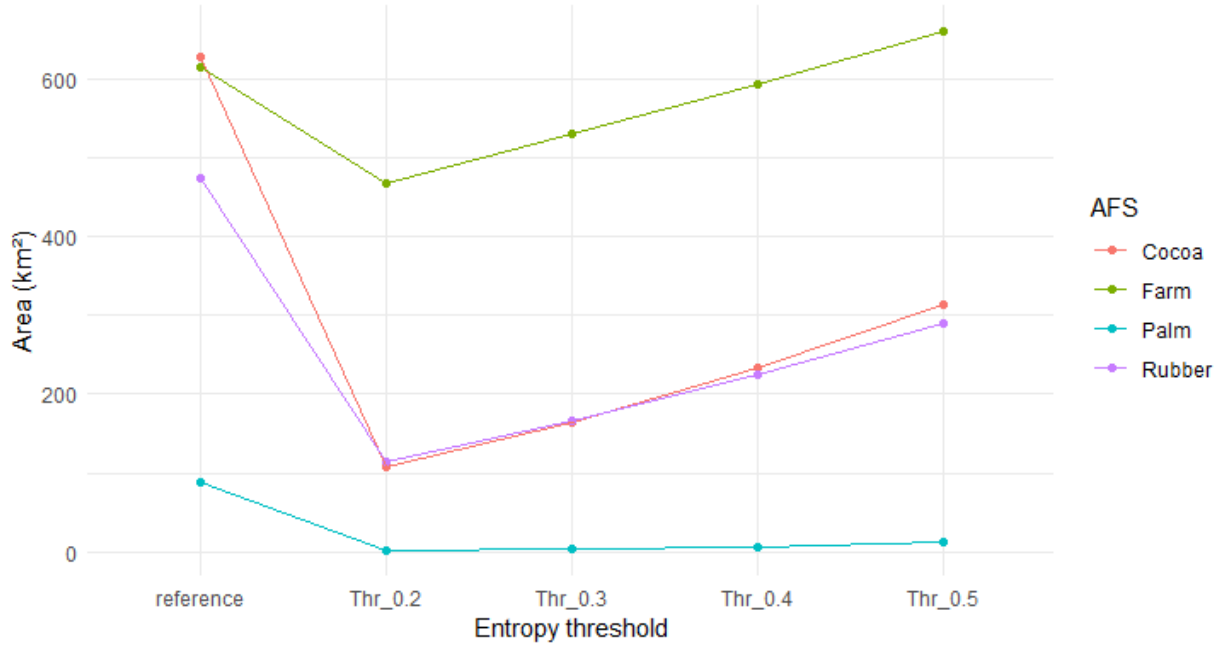

Figure 19: Area statistics of the main AFS in the Guineo-Congolian region

3.1.2 Guinean region

3.1.2.1 Feature importance and AFS classification

The feature importance in the Guinean region revealed the mean decrease Gini value decreased evenly from one feature to the other, in opposition to the Guineo-Congolian region some features were disproportionally more important than other. The graph shows that the most important features for AFS mapping in the region are represented by vegetation indices Figure 20 A. The VSURF shows that only eight features are required for the prediction of AFS in the region with four vegetation indices (GLI, SAVI, MSAVI and TCARI), three optical bands (B, NIR and B) and one texture parameter from S1 (Contrast from the VH polarization).

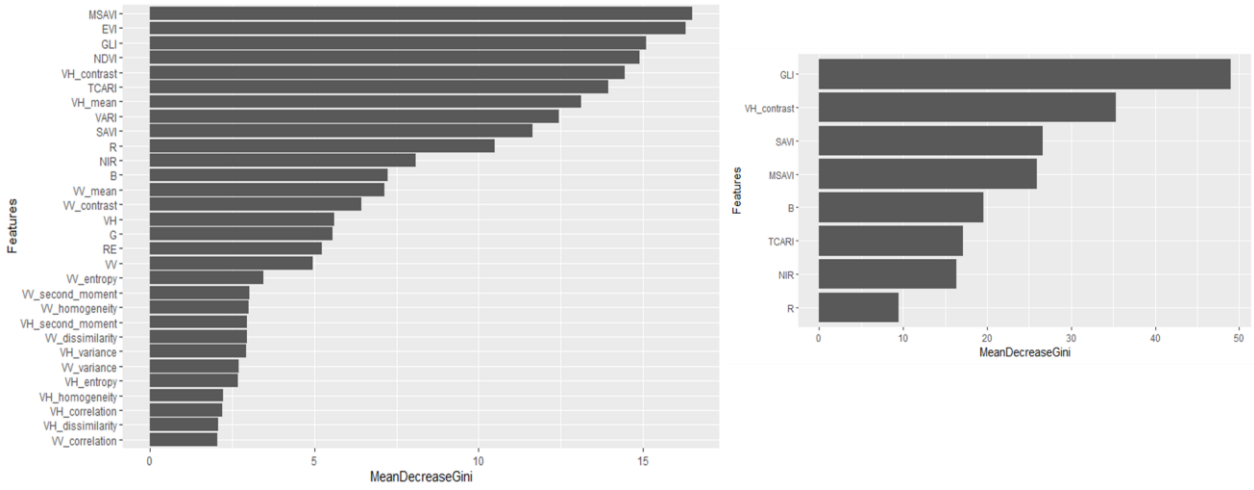

Figure 20: Feature importance (A) and variable selection (B) for the classification of AFS in the Guinean region

Classification assessment

The eight features were used as predictors for a supervised classification of the AFS in the Guinean region. The model returned an OA =0.91 (Kappa = 0.87), with a 95% confidence interval between 0.86 and 0.95. The area under the curve showed that for the three main AFS in the region (cashew, farm and mango), mango was the AFS class with the lowest error (AUC=0.96) followed by cashew (AUC=0.94) and farm (AUC=0.86). However, the producer's and user's accuracies showed that the higher commission error was associated with mango (PA=0.82, UA =0.91), cashew (PA=0.96, UA=0.9) and farm (PA=0.96, UA=0.92). The spatial distribution of the AFS in the region of interest is presented in (Figure 21). The map shows that in the region of Tafiere, which is located in the centre of the ROI, the main AFS is cashew and mango. Samples plots in that region showed that classification errors were located at the edges of farm plots when they were next to mango plantations (Figure 21-Snippet 1 and 3).

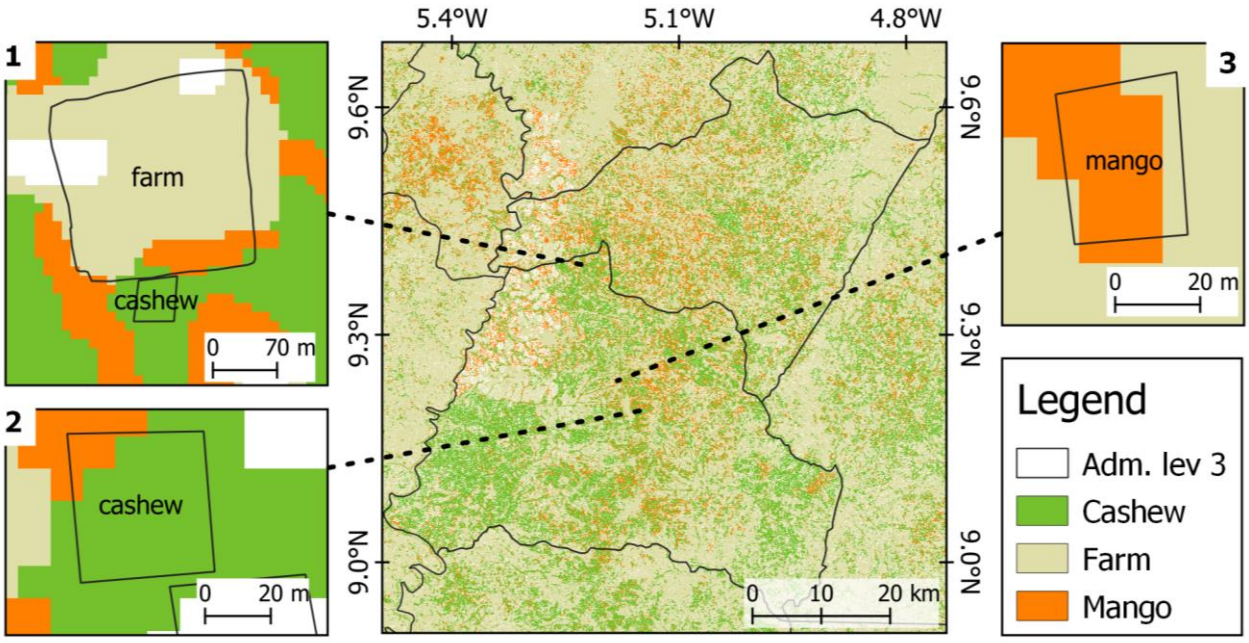

Figure 21: Classification map of the AFS in the Guinean region of west Africa

3.1.2.2 Spatial error assessment

Based on the classification map presented in Figure 21, the observation of the classification at field plot level reveals that the level of classification error is reduced in the Guinean region, compared to the Guineo-Congolian. The probability maps showed that farm was the AFS class with the highest probability level across the region. Only localised area in the central part has a higher probability of prediction of cashew and mango (Figure 22).

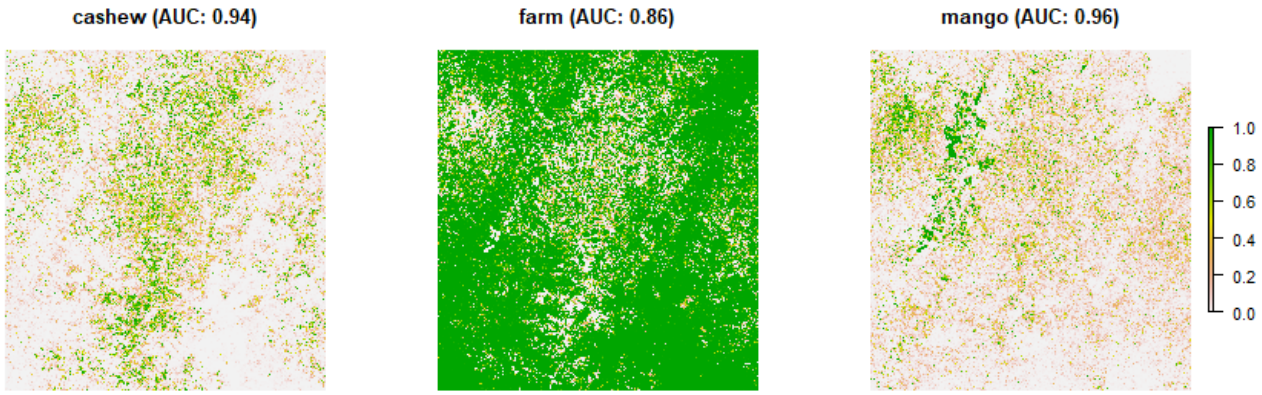

Figure 22: Probability map of the AFS classes in the Guinean region

The entropy map showed that the overall entropy level was below 0.51 suggesting a lower number of mixed pixels in the region of interest (Figure 23). The spatial distribution of the detected mixed pixels did not show any spatial configuration, rather are evenly distributed across the region. At different thresholds, it was found that the error level was comparable, and no large difference was observable from the map.

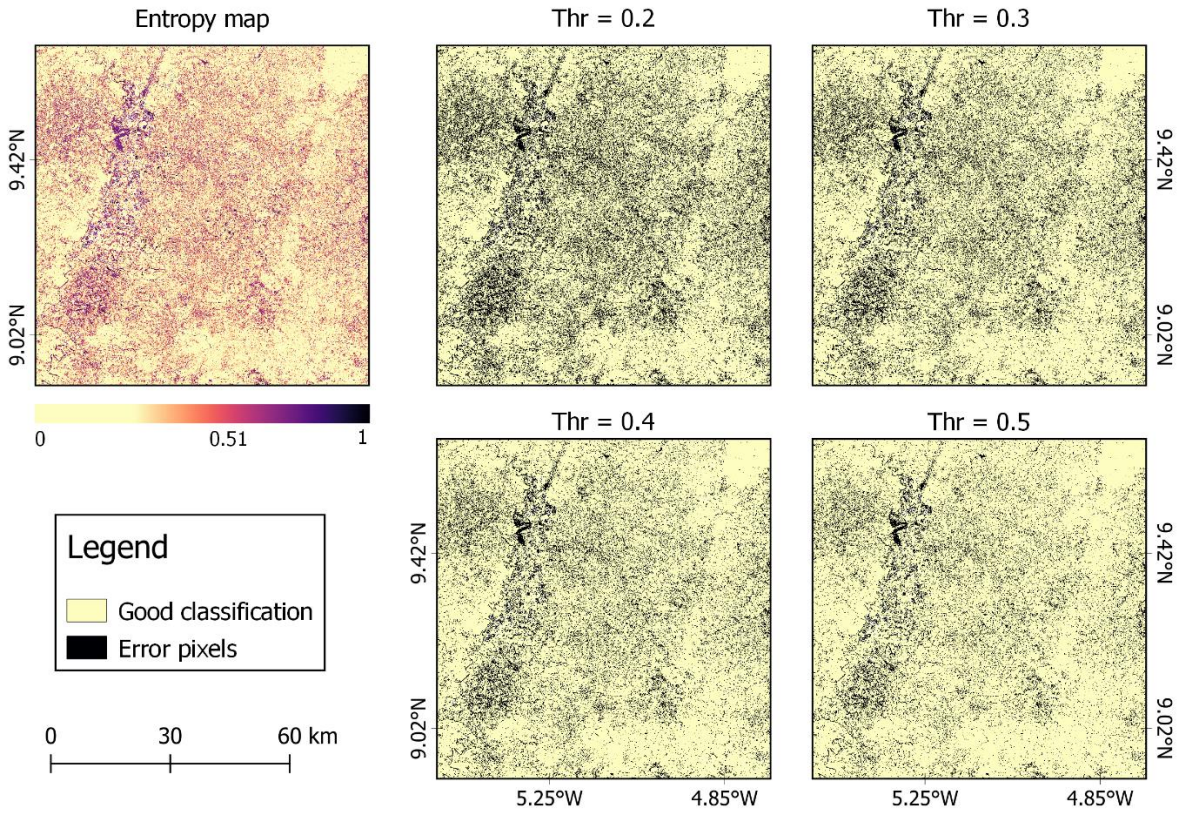

Figure 23: Entropy and error maps at different thresholds in the Guinean region

The AFS resulting from the improvement of the classification of AFS in the Guinea region showed few and localised changes in the ROI (Figure 24). As presented in Figure 24-Snippet 1, the approach was able to efficiently remove misclassified farm, providing a more reliable area for farm. However, the approach was not able to deal efficiently with cashew and mango. For Cashew, the detection was mixed cashew pixels resulted in loss of information while in mango plantation, no changes were observed.

The area statistics derived from the improved AFS map in the Guinean region showed that, in the ROI, farm was the main AFS in term of area (71.4% of the total area) followed by mango and

cashew with 15.2% and 13.4% km² respectively. They also showed that the spatial assessment in the region resulted in an underestimation of the area of the different feature classes (Figure 25). As the threshold increased, the estimated area approximated more and more the real area value. However, Farm was more sensitive to threshold setting compared to mango and cashew respectively. It was also found that for all the threshold values considered in the study, the area estimation was always lower than the estimation based on field measurement.

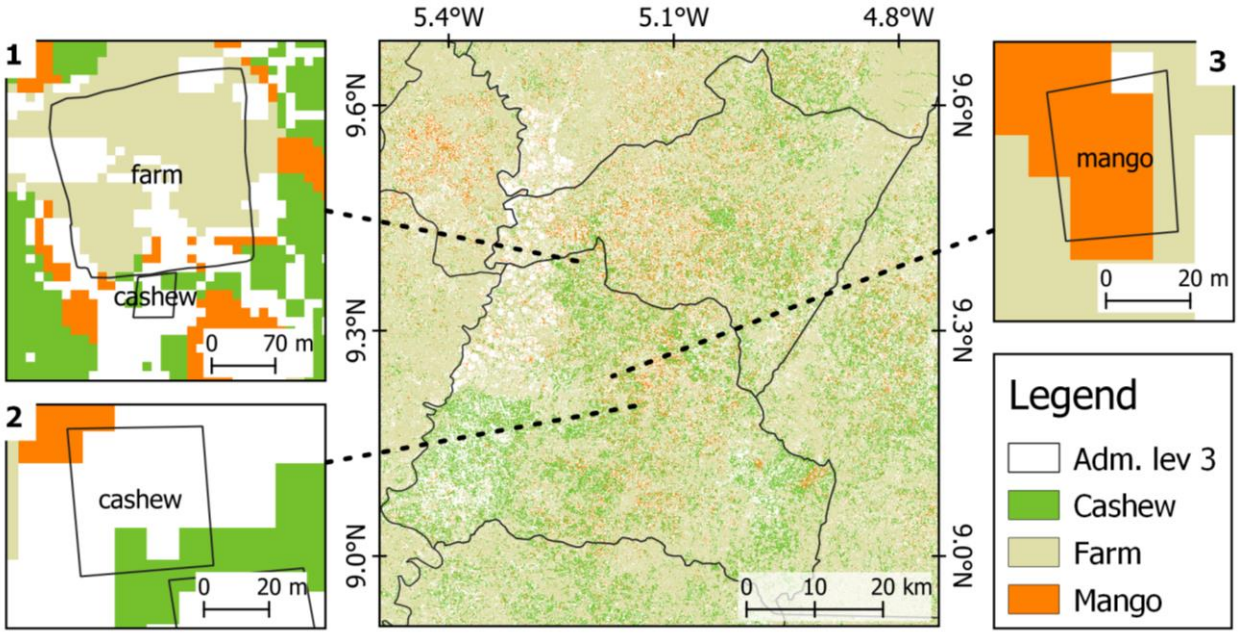

Figure 24: Improved AFS map in the Guinean region

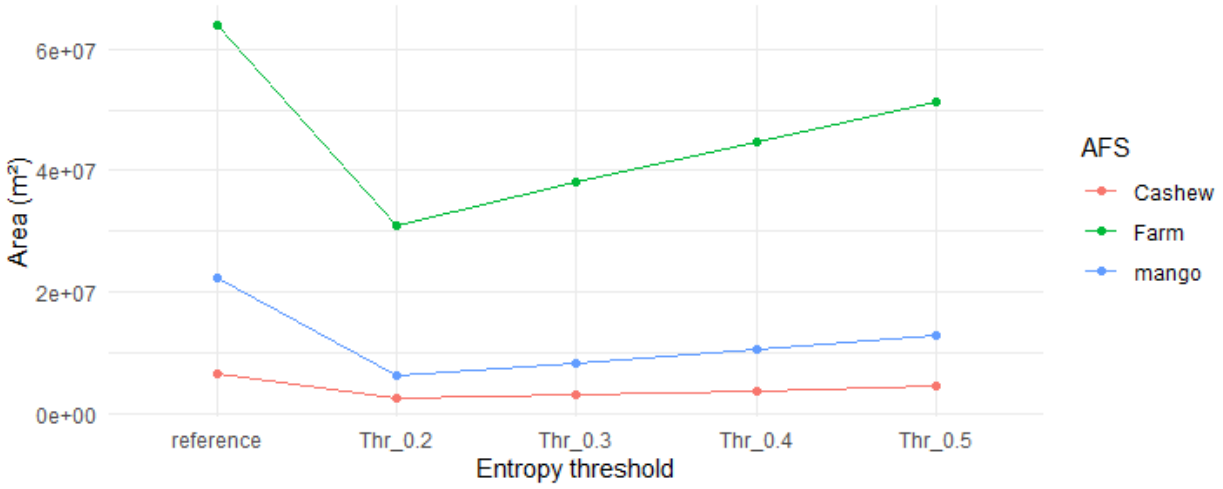

Figure 25: Area statistics of the main AFS in the Guinean region

3.1.3 The Sudanian region

3.1.3.1 Feature importance and AFS classification

The classification of AFS in the sudanian region relied mainly on predictors derived from optical data. The feature analysis showed that the most important features for the classification vegetation indices were mainly VARI and GLI and optical bands (Figure 26 A). The contribution of SAR data as well as the derived GLCM texture parameters was significantly low. The variable selection was then carried on to identify the most relevant features for the classification of AFS. The VSURF reveals that 12 out of the 30 initial predictors were significantly important for the classification of AFS in the ROI. Four textures parameters from the VH polarization namely entropy, mean, contrast and homogeneity were reported relevant for class prediction. Five vegetation indices and three optical bands were also included (Figure 26-B)

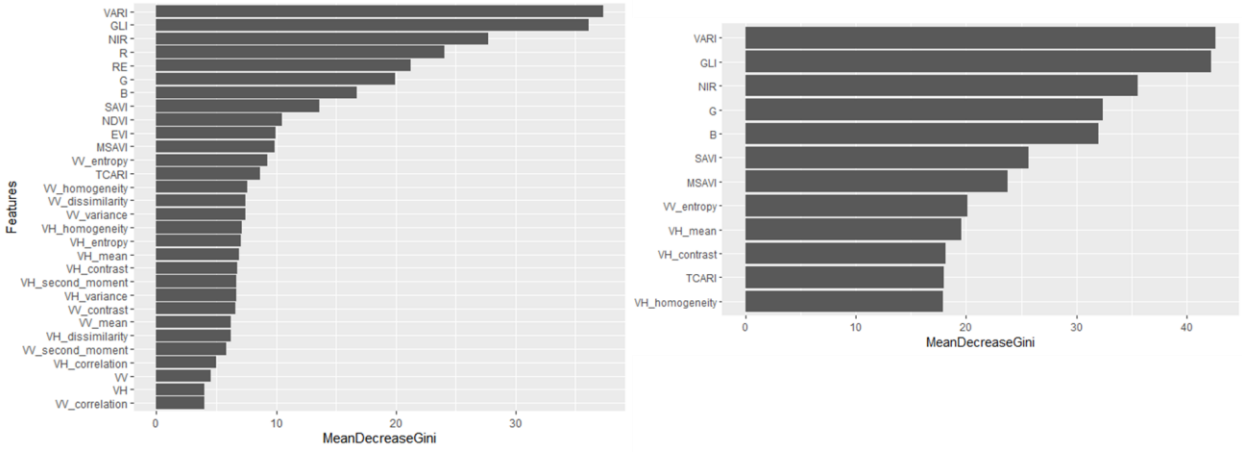

Figure 26: Feature importance (A) and variable selection (B) for the classification of AFS in the Sudanian region

Classification assessment

In the ROI, seven different AFS were identified, but only the three most common AFS were represented, and the rest was labelled as others. This include fallow and agricultural farm were the main the most common trees were gum Arabic trees (*Acacia senegalensis*), African grapes (*Lannea macrocarpa*), barwood (*Pterocarpus erinaceus*) and cider trees (*Sclerocarya birrea*). The classification suggestede an OA =0.89 (Kappa 0.87), and the confidence interval at 95% of the accuracy at 95% is between 0.84 and 0.94. From a producer's point of view, the results showed that the omission error is lower for the apple ring (*Acacia albida*) (PA=1, UA=0.85) follow by

others (PA = 0.97, UA= 0.86), the African locust bean (*Parkia biglobosa*) (PA= 0.83, UA = 0.85), and shea tree (*Vitellaria paradoxa*) (PA=0.97, UA=0.86). The AUC also showed similar results with the lowest value AUC=0.89 corresponding to shea trees. the balanced accuracy per feature class was higher for apple ring (0.97) and others (0.96) compared to the African locust bean (0.91) and shea trees (0.81). The area statistic showed that the ROI was dominated by shea tree (55.7%), African locust bean (28.1%), others (10.8%) and apple ring (5.3%) and the map indicated that the protected areas were dominated by AFS based on the African locust bean (Figure 27). At the plot level, evidence of classification error was mainly found in the shea trees, which was either classified as others (Figure 11-snippet 1), African locust bean (Figure 11-snippet 2) or apple ring (Figure 11-snippets 3 and 4).

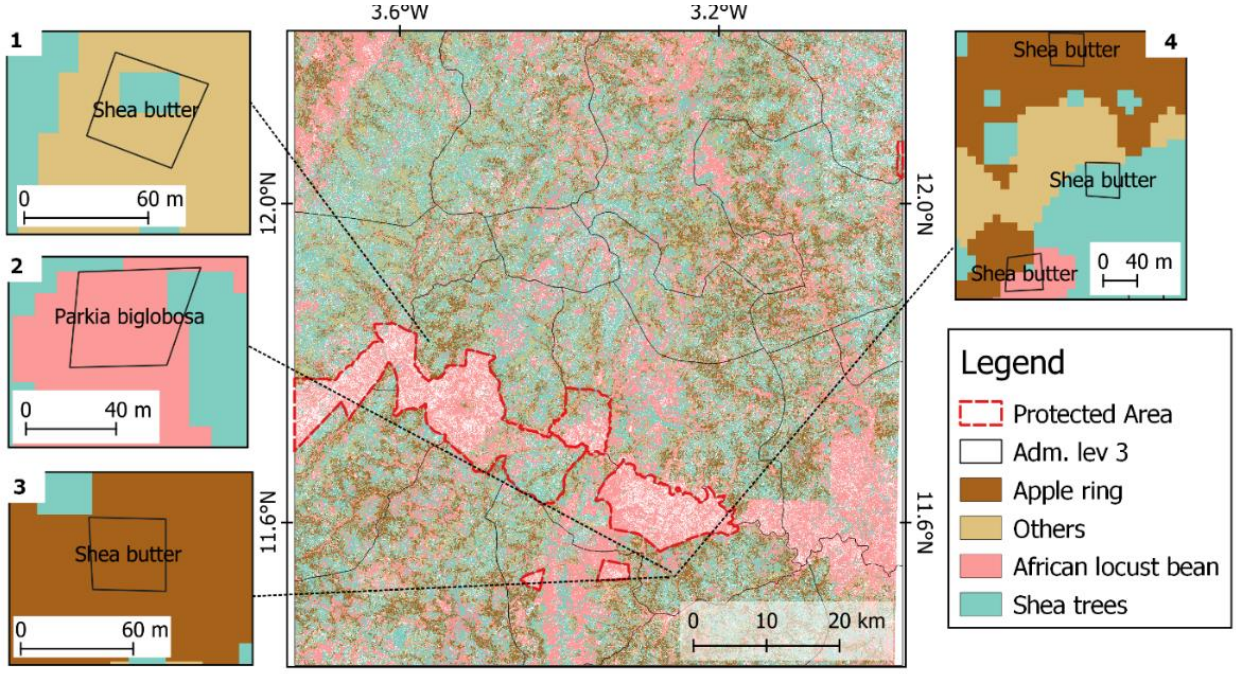

Figure 27: Classification of AFS in the Sudanian climate region of west Africa.

3.1.3.2 Spatial error assessment

The observation of the probability maps reveals that the protected area in the ROI is mainly covered by parkia AFS. The AFS are found in specific locations and there are some areas where there are absent. However, shea tree is evenly distributed across the region, except in the protected area (Figure 28).

Using the probability maps as input, an entropy map was generated, and different threshold values were considered to generate the error map. Figure 29 reveals that the overall entropy was high in the ROI. This is confirmed by the error maps where there was a homogenous reparation of mixed pixels across the ROI. However, in the protected area, the entropy was very low, which resulted in a low level of error pixels in that region.

The improved classification map showed a comparable pattern as the initial map. In the Sudanian region, the classification error was recorded predominantly in AFS farms based on shea tree. In the ROI, it was found that its spectral signature was comparable to other AFS such as fallow, but also Apple ring (Figure 30). The improvement of the classification was less effective in this region as shown in Figure 30-snippet 1. When the shea tree was surrounded by other crop types, the approach was unable to capture and remove mixed pixels. Also, it was also found that when the AFS was misclassified such as in the Figure 30-snippet 3, where shea tree was falsely classified as Apple ring, the approach was unable to deal efficiently with such error. The information loss per AFS resulting from the improvement of the classification showed that, using the field plots, the information within the AFS Apple ring and others was not lost. The percentage of pixel loss during the improvement was equal to zero. The highest information loss was found in The African locust bean (10.3%) and shea tree (4.8%).

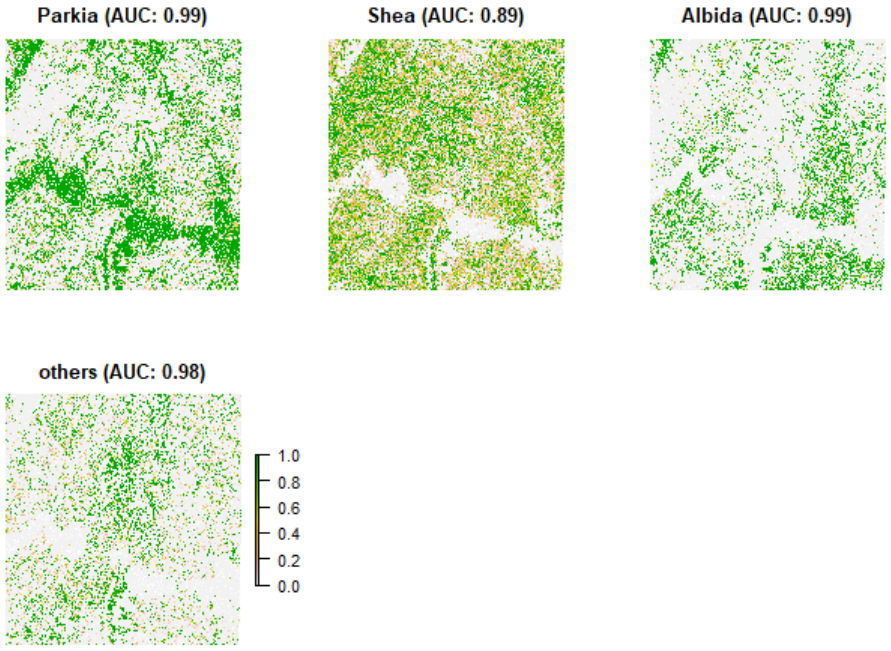

Figure 28: Probability maps of the AFS in the Sudanian region

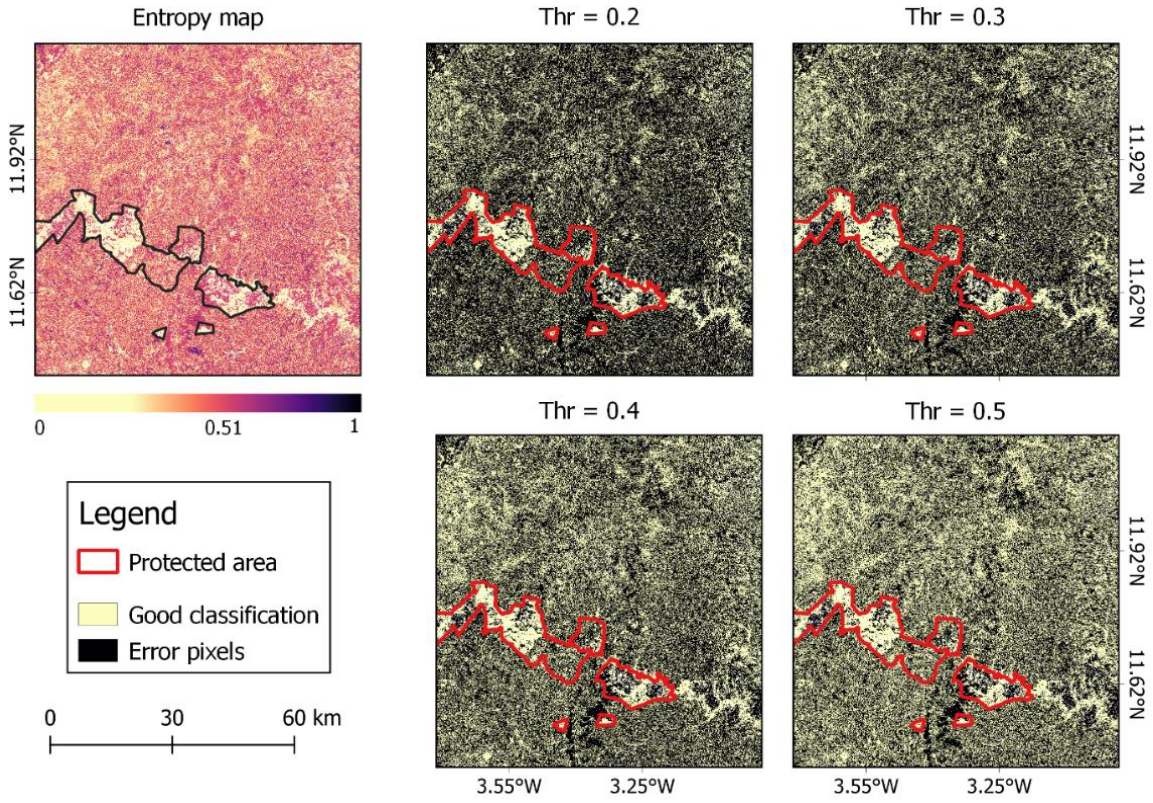

Figure 29: Entropy and error maps at different thresholds in the Sudanian region

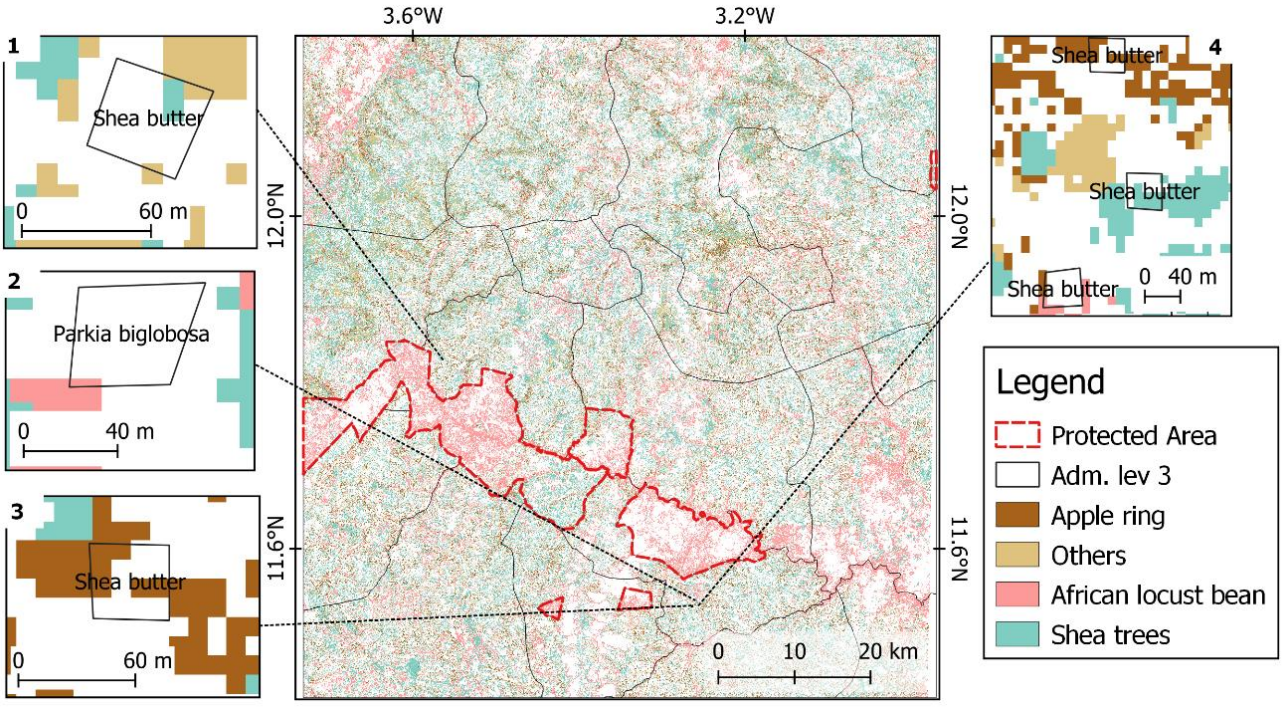

Figure 30: Improved AFS map in the Sudanian region

The area statistics showed that the region was dominated by shea butter, with about 350 km² using the field reference as threshold value for the entropy (Figure 31). It was also found that all the selected threshold values resulted in underestimating of the area for the AFS except for shea tree, where there was an overestimation of the area if the threshold value was greater than 0.3.

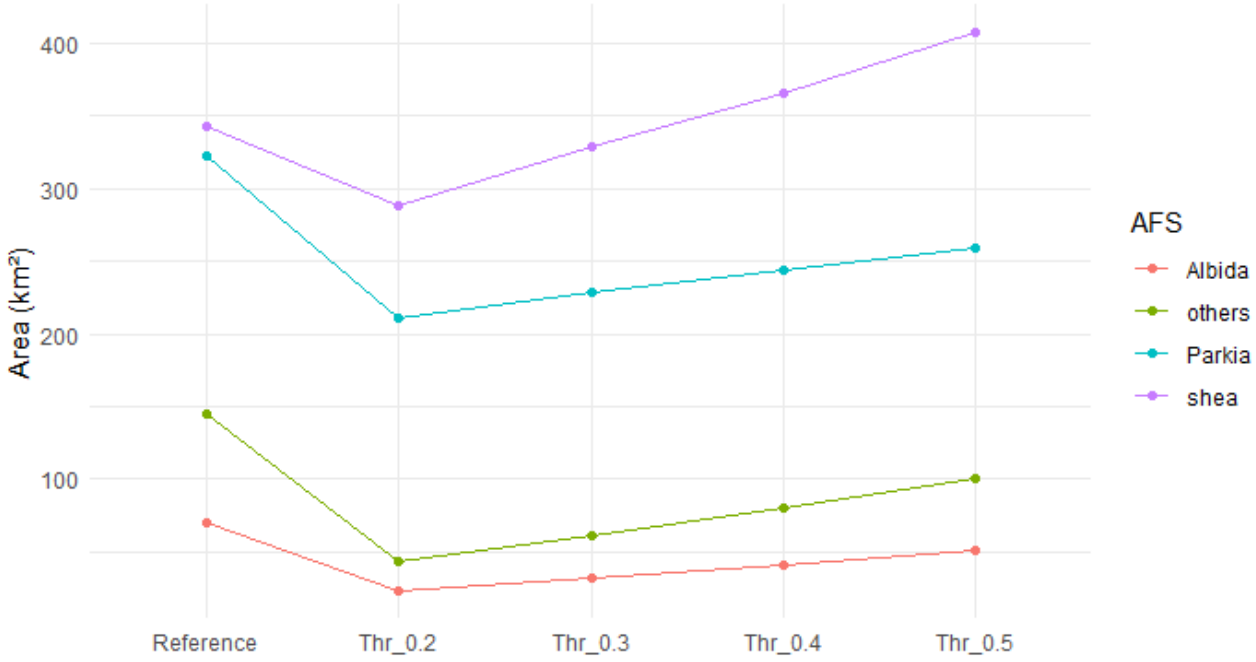

Figure 31: Area statistics for the main AFS in the Sudanian region

3.2 Geographically Weighted Regression

The generated error maps showing the spatial distribution of mixed pixels was considered in the estimation of the proportion of error in the different ROI. In ROI-1 corresponding to the Guineo-Congolian Region, about 50% of the estimated area was represented by mixed pixels considering the reference level. In the Guinean region (ROI-2), the error level on the classified map was estimated at 20% based on the reference entropy's threshold value. The Sudanian region (ROI-3) showed the highest level of mixed pixels with an estimated proportion around 56% (Figure 32). Across the different ROI, it appeared that an entropy threshold value of 0.4 gives an estimation of the error which was close to the reference value. Moreover, entropy threshold value below 0.4 tend to overestimate the proportion of mixed pixels while a larger value underestimate it.

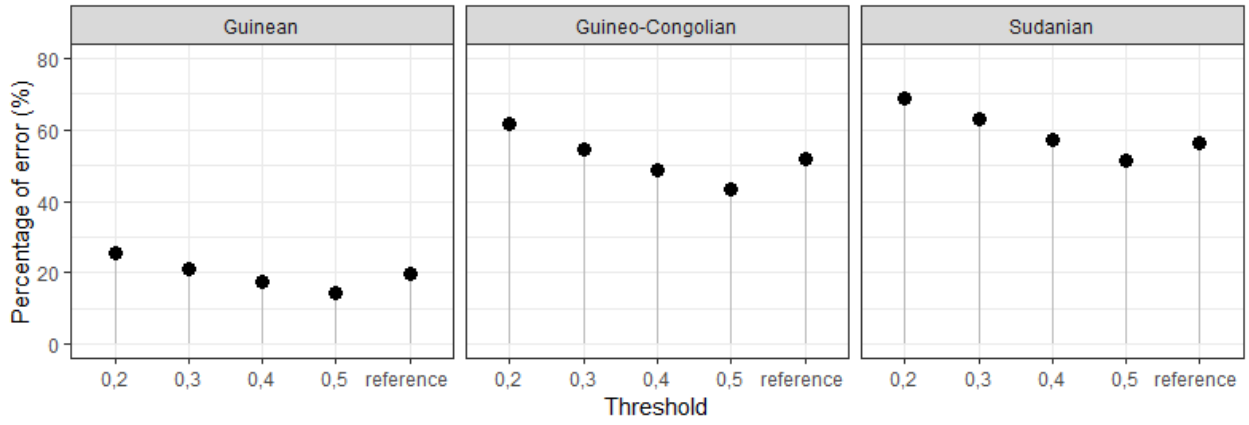

Figure 32: proportion of mixed pixels at different entropy threshold values

GWR was used to determine if the spatial distribution of mixed pixels across the classified map followed a spatial pattern. The summary of the GWR for each ROI at different threshold is presented in Table 8. The table shows that overall, there was a strong relationship between the predictors derived from Sentinel data and the corresponding error map, with an average R^2 value of 0.87, 0.85 and 0.77 for the Guineo-Congolian, Guinean and Sudanian region respectively. The assessment of the spatial correlation of the residuals from the logistic regression showed that it is not significant all the ROI, except for the Guineo-Congolian region, where a significant spatial correlation was reported for the entropy threshold value of 0.5. The implementation of the GWR model was found significant with a relatively low R^2 value of 0.31.

Based on the results derived from the GWR, there was evidence of spatial correlation of the classification error if the entropy threshold value of 0.5 was used. The analysis of the bandwidth of the predictors was applied to identify the predictors that were constant throughout ROI (global predictors) as well as the predictors that were varying within the ROI (local predictors) (Figure 33). It was found that four predictors including the intercept, namely: The Green Leaf Index (GLI), the Visible Atmospherically Resistant Index (VARI) and the mean GLCM of the VV polarization of S1. The seven others were local predictors based on the size of the bandwidth. This included Soil Adjusted Vegetation Index (SAVI), the mean GLCM texture of the VH polarization, the Transformed Chlorophyll Absorption in Reflectance Index (TCARI) and the Sentinel-2 bands blue (B), green (G), red (R), and red-edge (RE).

Table 8: summary of the GWR for the error assessment of AFS map

	Threshold	LR (R^2)	Number of features	Optimum number of neighbours	Moran I statistic (p-value)	GWR model (R^2)
Guineo-Congolian	0.2	0.87	16	4	0.25	
	0.3	0.82	19	4	0.12	
	0.4	0.78	19	2	0.10	
	0.5	0.76	18	6	0.09	0.31
	Reference	0.75	18	2	0.19	
Guinean	0.2	0.85	21	1	0.46	
	0.3	0.87	19	1	0.34	
	0.4	0.89	18	1	0.20	
	0.5	0.91	3	9	0.85	
	Reference	0.88	17	1	0.34	
Sudanian	0.2	0.77	20	3	0.17	
	0.3	0.75	18	1	0.30	
	0.4	0.72	17	1	0.34	
	0.5	0.68	15	3	0.45	
	Reference	0.72	17	1	0.25	

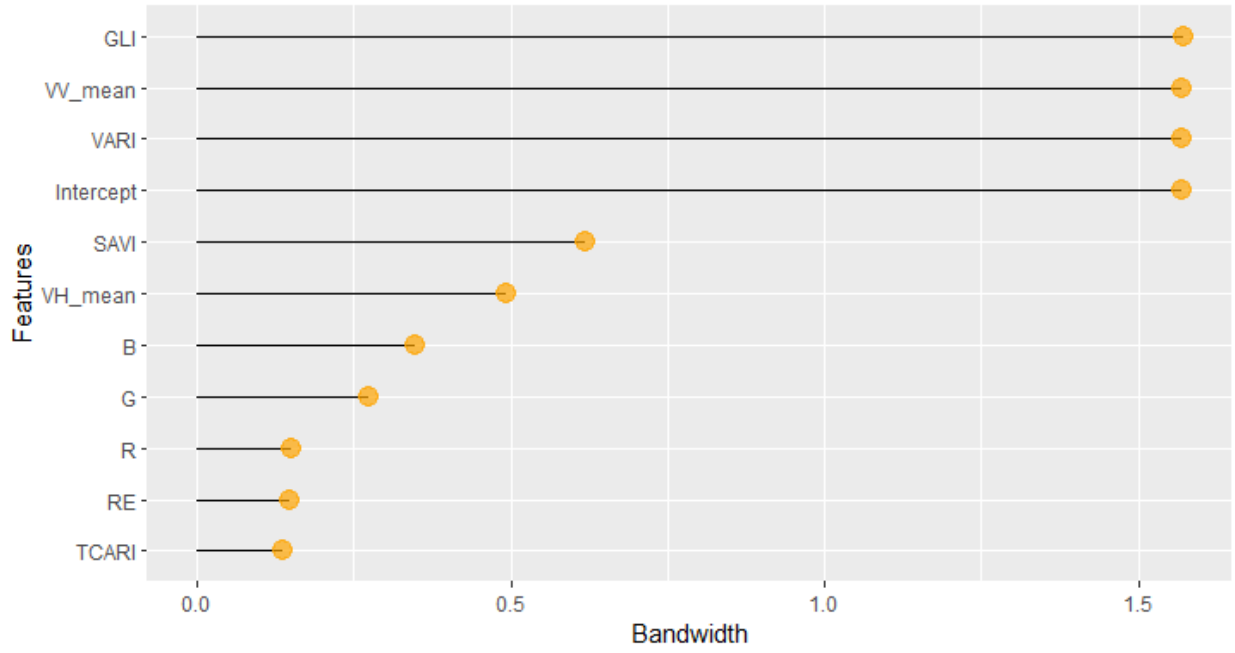

Figure 33: Bandwidth of the predictors for the error maps.

The GWR coefficient was retrieved and plotted to illustrate the spatial distribution of the change across the ROI (Figure 34). It appears that for predictors with smaller bandwidth up to four different regions could be identified. The first correspond to the extent of the TNP, followed by a small ring around it. Then smaller regions with coefficients in the same value ranges were identified in upper right corner of the ROI. For local predictors with larger bandwidth such as SAVI, it was found that about three regions could be identified as presented in the figure.

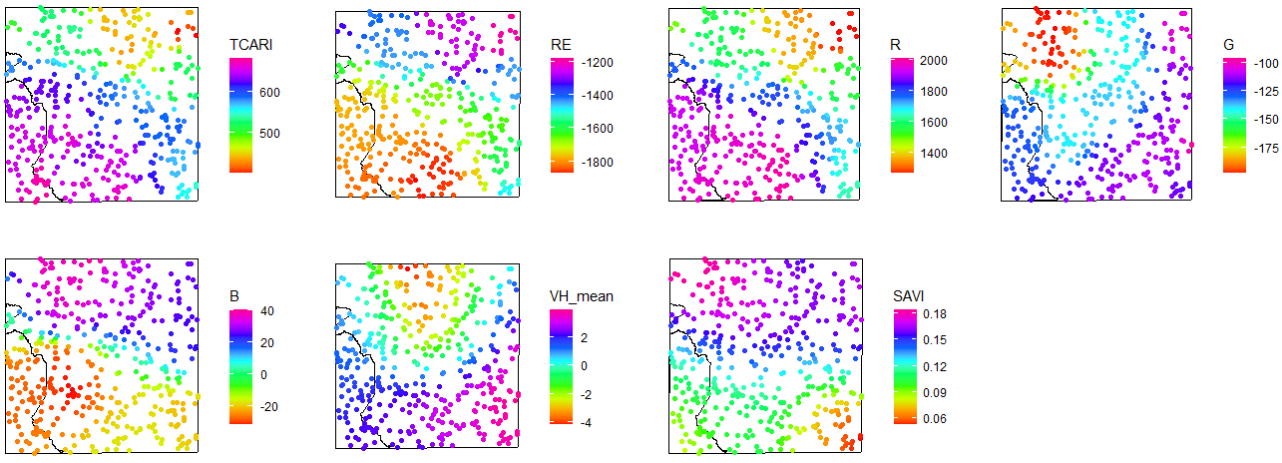

Figure 34: Spatial variation of the GWR coefficients for local predictors

Considering the global predictors (Figure 35), it was found that the range within the coefficient value was different compared to the local predictors. If the difference in value range within the local predictor with the smaller bandwidth was about 100 units, the difference within the range in global predictors was not more than 5 units. The overall value was constant across the ROI, with a variance of about 0.1 units, 0.5 units and 0.25 units for VARI, VV_mean and GLI respectively. Only the intercept showed variation corresponding to about 5 units, yet the spatial distribution of the coefficient did not show any pattern.

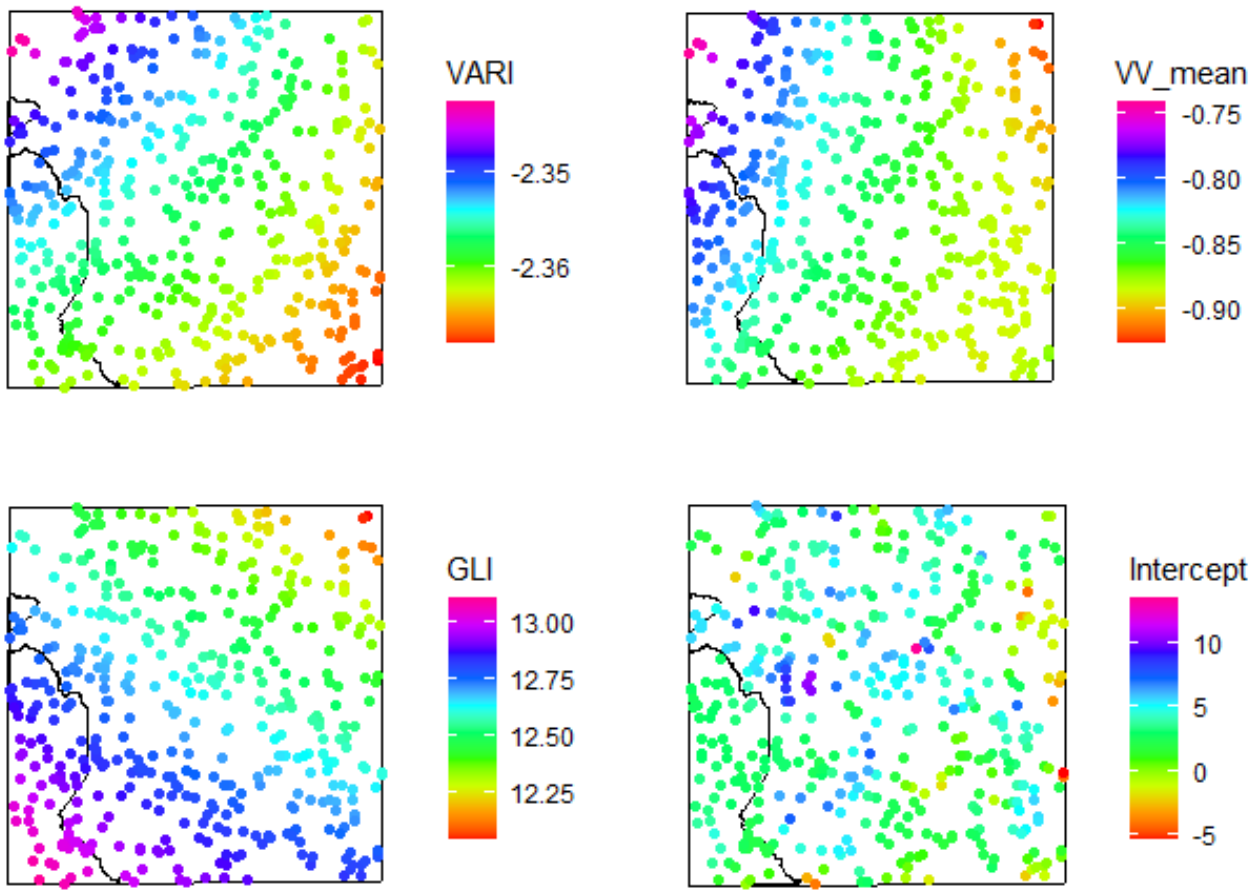

Figure 35: Spatial variation of the GWR coefficient for global predictors

3.3 Carbon stock in West Africa

Beyond the economic value of AFS and their contribution to the livelihood of local population, carbon modelling in AFS is crucial to assess the contribution of those systems to climate change. Since AFS was been reported as a viable solution to alleviate poverty and mitigate climate change, there is a need to provide a reliable remote sensing-based approach for carbon estimation in different AFS across west Africa. The aim was to compare the performance of different RS data sources and different machine learning algorithms to identify the best combination for carbon modelling in different climatic regions. Moreover, it was to compare the carbon stock level in different AFS across west Africa to identify the main predictors of biomass with the aim of making informed recommendations. The results from this section were published under the title "Estimation of aboveground biomass in agroforestry systems over three climatic regions in West Africa using Sentinel-1, Sentinel-2, ALOS and GEDI data" (Kanmegne Tamga, et al., 2022b). This section is organised in three main parts: (i) global modelling approach where different data were compared without consideration of the climatic regions; (ii) a modelling approach based on the comparison of different RS dataset in different climatic regions; (iii) the comparison of different machine learning algorithms and (iv) the comparison of the AGB level in different AFS across west Africa.

3.3.1 Global model for carbon estimation

The prediction performance of the aboveground carbon stocks using a single model -here referred to as global model- over the entire region of West Africa, was evaluated in a scatterplot between measured vs. predicted values for each of the AGB reference sources that was used as response variables namely AGB estimations derived from field measurements and AGB predictions from GEDI L4A. A trendline (in red) and a 1:1 ratio line (dotted) was added to the plot to assess the performance of the model (Figure 36).

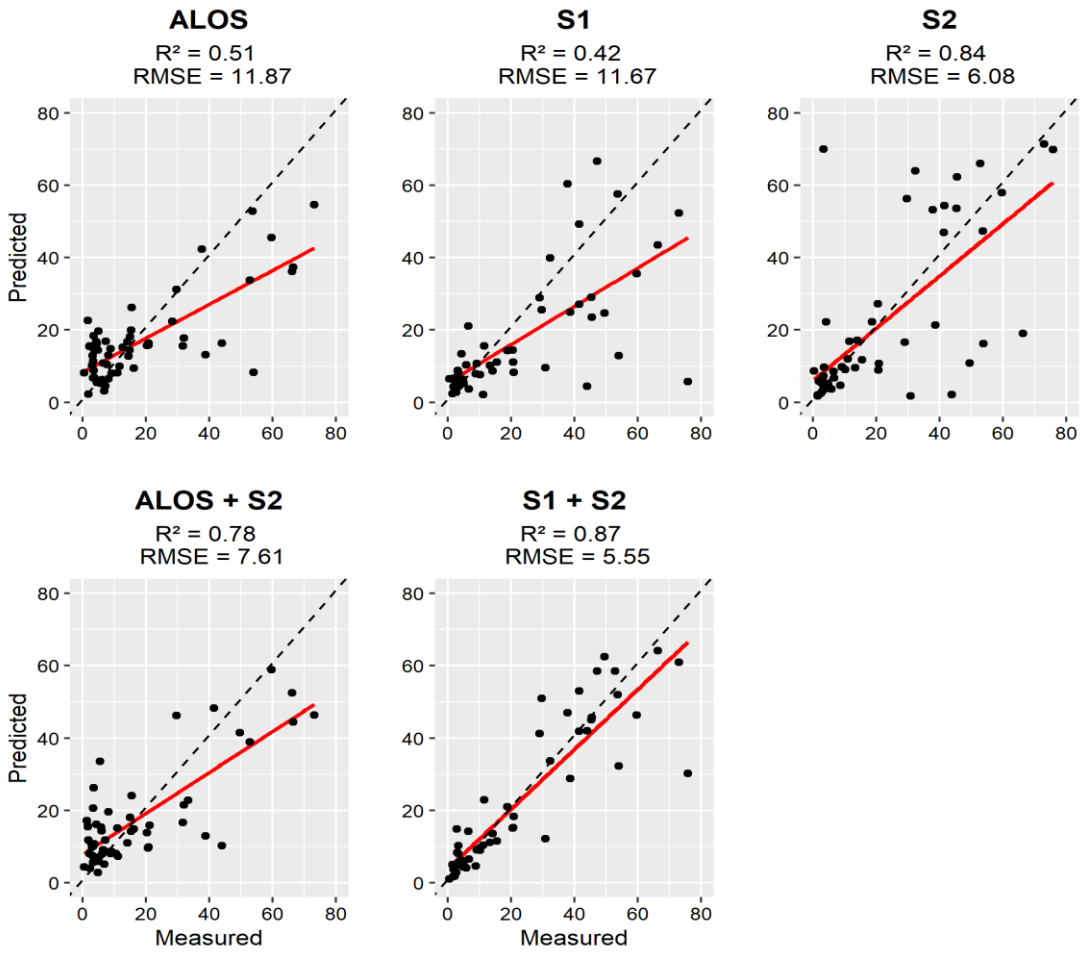

Figure 36: relation between measured and predicted AGB in West Africa using field measurements as reference data (Kanmegne Tamga et al., 2022b).

When considering AGB derived from field measurements as response variable, the results show that for single RS dataset, optical data derived from S2 were the most sensitive to AGB (R^2 = 0.84, RMSE = 6.08) compared to Radar data. For RADAR data, the error level reported by the RMSE was almost similar, but ALOS (R^2 = 0.51 RMSE = 11.87) was more sensitive to AGB than S1 (R^2 = 0.42, RMSE = 11.67). When optical and Radar data were combined, the best score was returned from the combination of S1 and S2 (S1 + S2) with R^2 = 0.87 and RMSE = 5.55, which was higher than the combination ALOS + S2 (R^2 =0.78, RSME = 7.61).

Global model using GEDI L4A

The AGB prediction of the GEDI L4A was used as response variable to train a global model for ASB estimation in West Africa (Figure 37). The results showed that the overall performance of

the prediction model was low, where S2 showed the highest score (R^2 = 0.13, RMSE = 75.16). for Radar data, a score of R^2 = 0.05, RMSE = 66.84 and R^2 = 0.03, RMSE = 67.55 was obtained for S1 and S2 respectively. based on the trendline, the model was underestimating the AGB level in the region when using GEDI L4A.

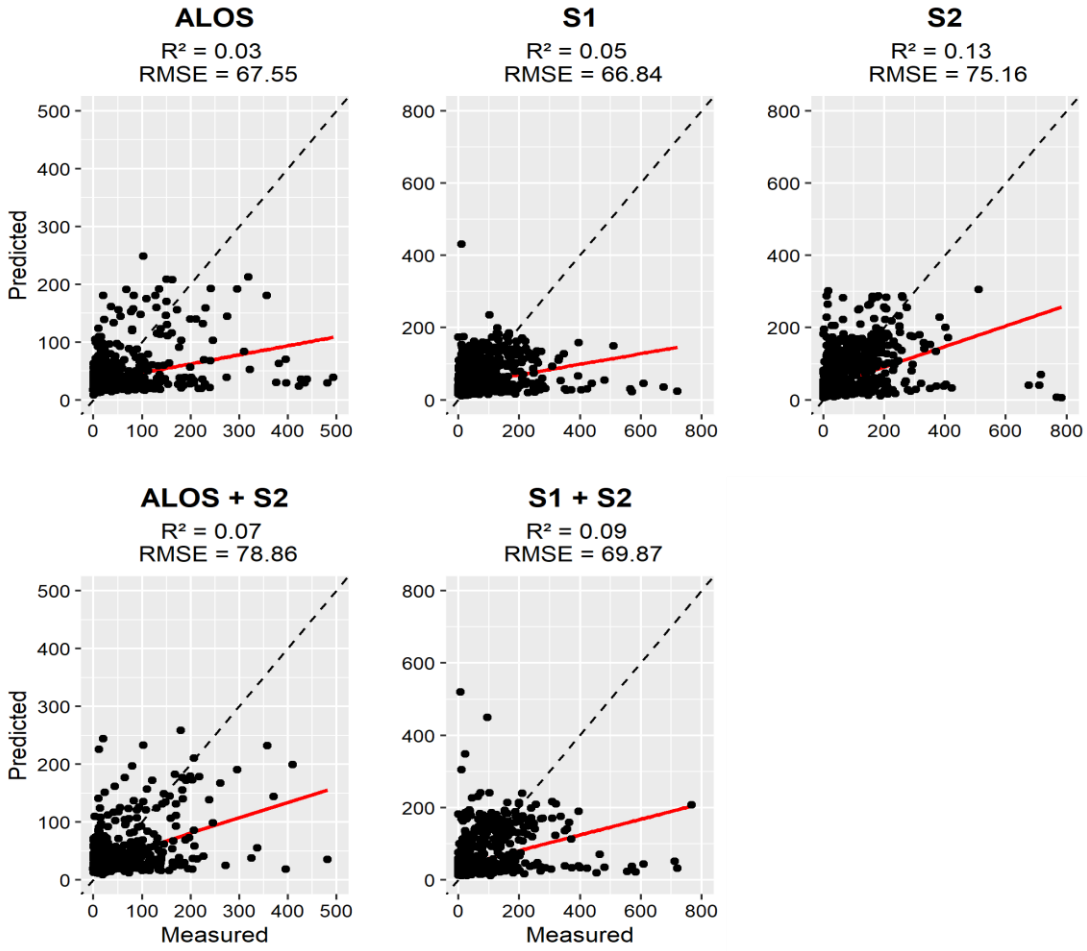

Figure 37: relation between measured and predicted AGB in West Africa using GEDI L4A as reference data (Kanmegne Tamga et al., 2022b)

3.3.2 AGB estimation in climatic regions

Guineo congolian

The next step in AGB modelling was to stratify the ROI by the climatic regions. AGB prediction models were then developed and compared between the existing climatic regions. Here also, both AGB reference data were considered (AGB from field measurements and GEDI L4A). In the southern part of Côte d'Ivoire which correspond to the Guineo-Congolian region, the main AFS

were represented by cocoa, rubber and palm oil plantations as well as agricultural farms. When using the AGB derived from field measurements as reference data, optical data from S2 returns the highest performance (R^2 = 0.9, RMSE = 4.12). For Radar data, the score obtained from ALOS data (R^2 = 0.54, RMSE = 10.58) was higher than the one from S1 (R^2 = 0.26, RMSE = 11.11). The highest score however was obtained when optical and radar data were combined (Figure 38). The combination that returned the highest score was S1 + S2 (R^2 = 0.91, RMSE = 3.82) which was higher than ALOS + S2 (R^2 = 0.86, RMSE = 5.64).

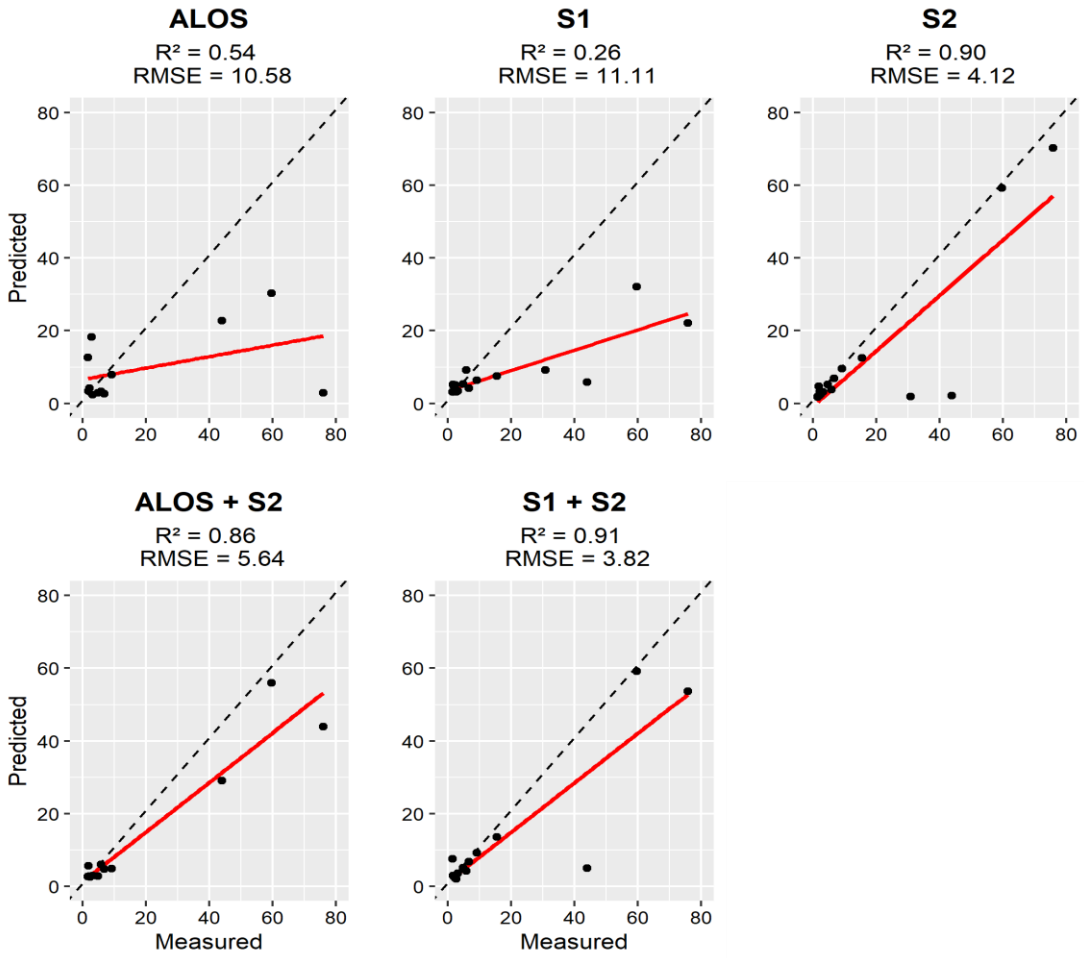

Figure 38: relation between measured and predicted AGB in the Guineo Congolian region using field measurements as reference data (Kanmegne Tamga et al., 2022b)

AGB prediction using GEDI L4A also returned interesting score for optical and radar data (Figure 39). The best performance was obtained with S2 (R^2 = 0.64, RMSE = 41.28) however, the error level was about 10 times higher compare to the score obtained with reference data derived from

the field. ALOS (R^2 = 0.61, RMSE = 34.16) was showing a better performance than the combination S1 +S2 (R^2 = 0.61, RMSE = 44.26). Even though both had the same R^2 value, ALOS has a lower prediction error. When combined with S2, the performance was reduced (R^2 = 0.54, RMSE = 36.9), and the score was lower than the single dataset ALOS and S2 respectively. The lowest score was obtained with the S1 dataset (R^2 = 0.36, RMSE = 56.39). It was also the dataset with the largest prediction error when using GEDI L4A.

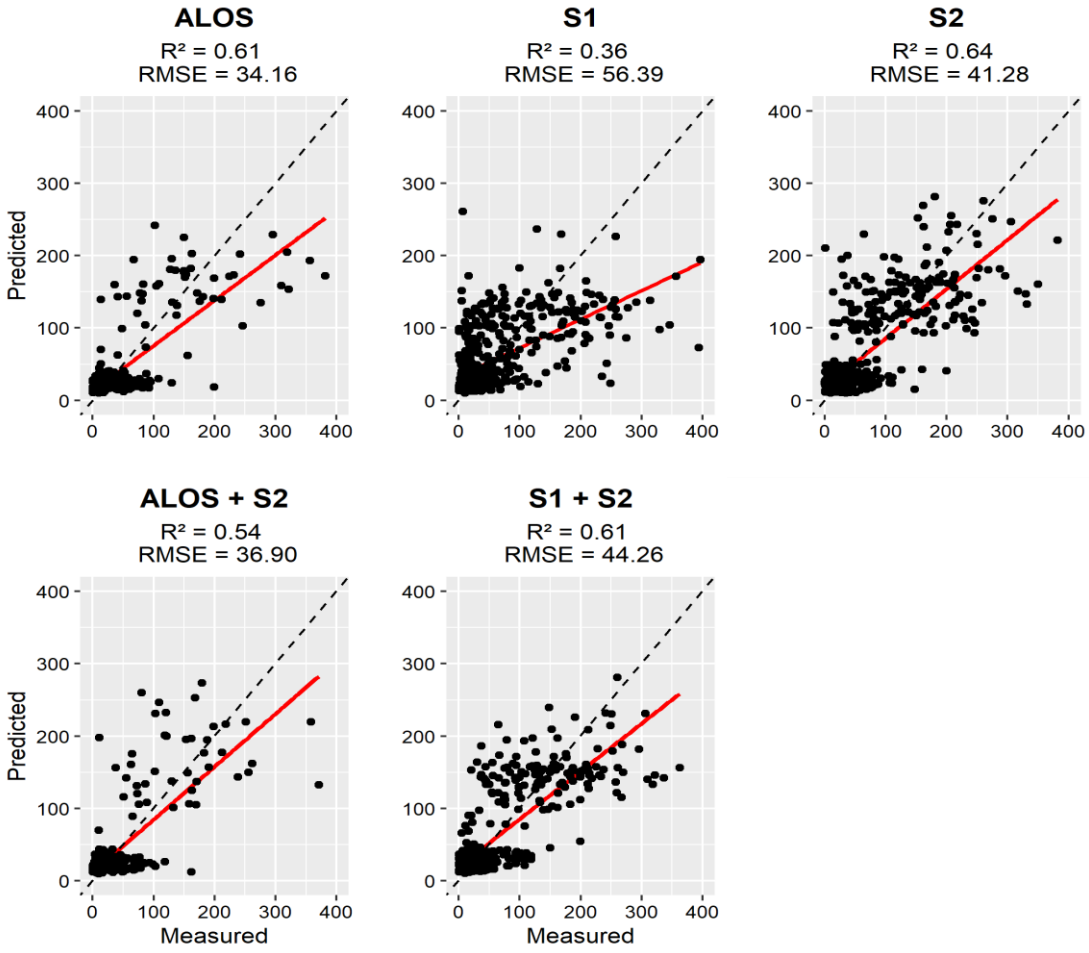

Figure 39: relation between measured and predicted AGB in the Guineo Congolian region using GEDI L4A as reference data (Kanmegne Tamga et al., 2022b)

Guinean

The Guinean region which corresponds to the northern part of Côte d'Ivoire was mainly dominated by cashew and mango plantations alongside with agricultural farms. The assessment of the AGB predictions using field measurement as reference data showed that when considering single

dataset, optical data from S2 provides the best score (R^2 = 0.72, RMSE = 9.64) which was lower compared to the Guineo-Congolian region (Figure 40). As far as radar data is concerned, S1 (R^2 = 0.6, RMSE = 11.91) showed a higher score compared to ALOS (R^2 = 0.39, RMSE = 13.23). it appeared that S1 was more sensitive to AGB in this region compared to the Guineo Congolian as the score was about 43% higher with about the same prediction error level. The highest score was obtained with S1 + S2 (R^2 = 0.82, RMSE = 8.45) while the combination ALOS + S2 (R^2 = 0.63, RMSE = 9.68) showed a score which is lower than S2. The trendlines showed that in their prediction, the models tend to overestimate AGB in locations with a low level of AGB, while they underestimated it in regions with high ABG level.

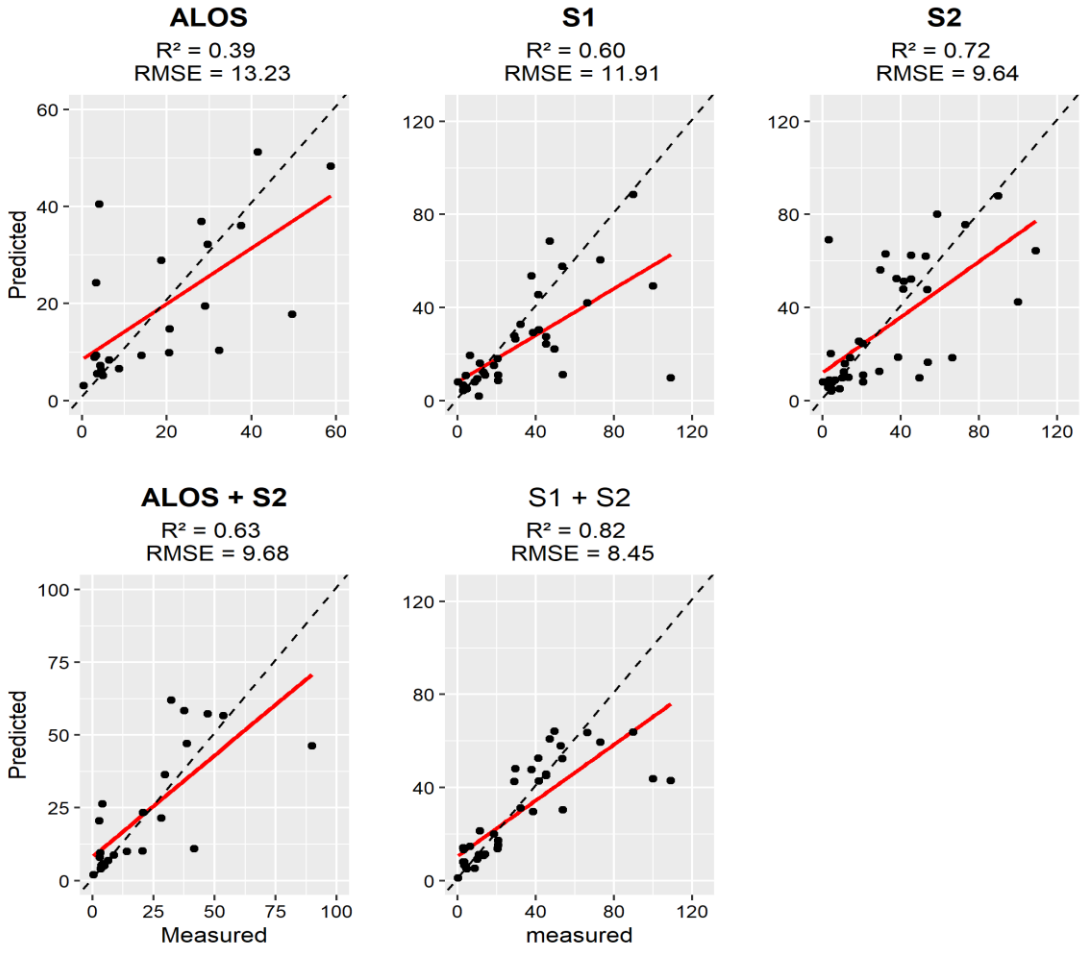

Figure 40: relation between measured and predicted AGB in the Guinean region using field measurements as reference data (Kanmegne Tamga et al., 2022b)

When trying to predict the AGB level in the Guinean region using GEDI L4A as reference data, the model was giving negative R^2 suggesting that the model was doing worse than guessing (Figure 41). Based on the level of the prediction error, the best score in this setting was obtain using S1 + S2 (RMSE = 45.98) followed by S2 (RMSE = 51.99). The worst score was returned by ALOS + S2 followed by ALOS (RMSE = 68.55).

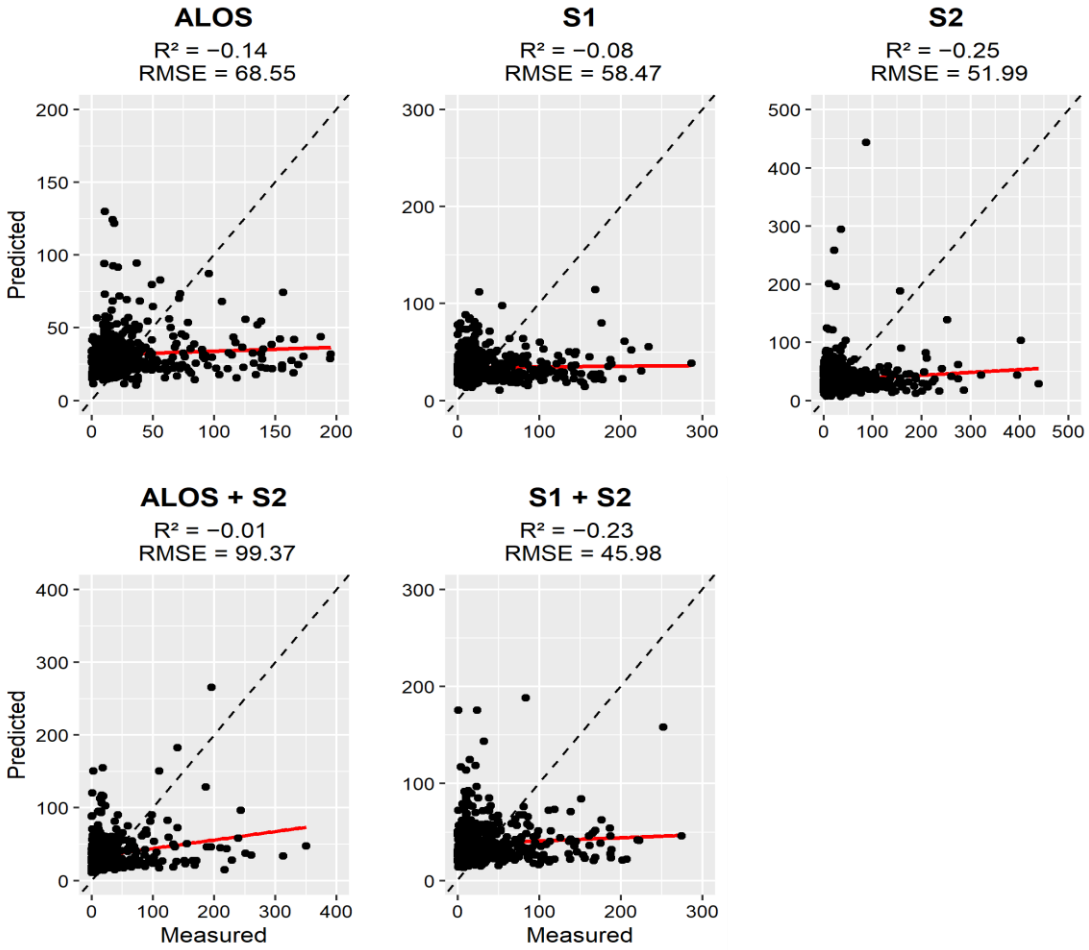

Figure 41: relation between measured and predicted AGB in the Guinean region using GEDI L4A as reference data. (Kanmegne Tamga et al., 2022b)

Sudanian

The sudanian region corresponded to the ROI located in Burkina Faso. In this location, diverse type of AFS were found, mainly in association with agricultural crops including cotton and sesame. The main AFS were represented by the African locust bean, apple ring and shea trees. The estimation of the AGB using reference data derived from field measurements showed that for

single RS dataset, the best score was obtained with S2 (R^2 = 0.84, RMSE =5.91) followed by ALOS (R^2 = 0.71, RMSE = 5.9) and S1 (R^2 = 0.55, RMSE = 10.21). when the data were combined, S1 + S2 is slightly higher than S2, with R^2 = 0.86 and RMSE = 5.3, while the combination ALOS + S2 (R^2 = 0.7, RMSE = 6.24) was worse than ALOS alone (Figure 42). Also, it was found that, when using ALOS data, the model overestimate AGB predictions for area with low biomass levels.

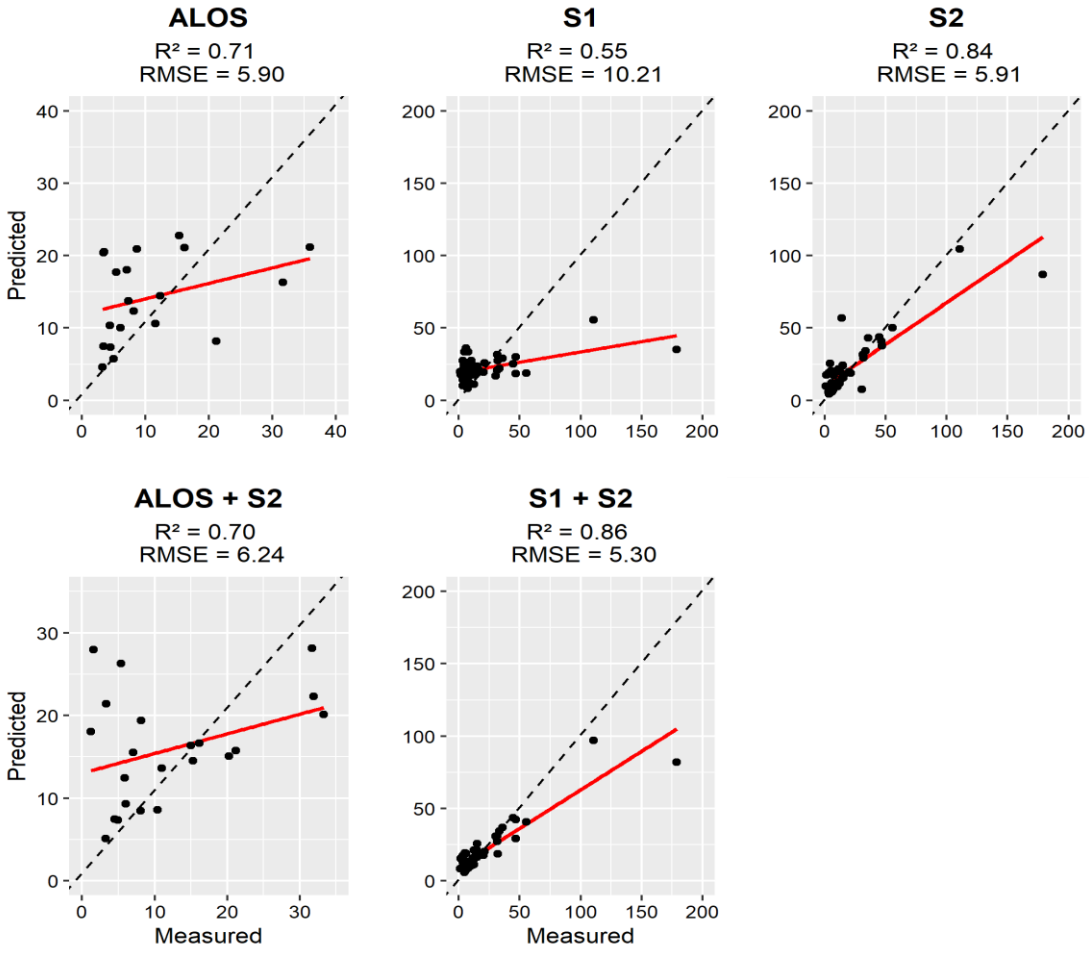

Figure 42: Relation between measured and predicted AGB in the sudanian region using field measurements as reference data (Kanmegne Tamga et al., 2022b)

The usability of AGB predictions from GEDI L4A for biomass modelling in the Sudanian region results in models which predictions were worse than guessing as shown by negative R^2 (Figure 43). The combination ALOS + S2 shows the lowest error level (RMSE = 80.17) which was 15.5

times higher than the predictions based on field measurements. In this scenario, S2 showed the worst performance with an RMSE = 109.13.

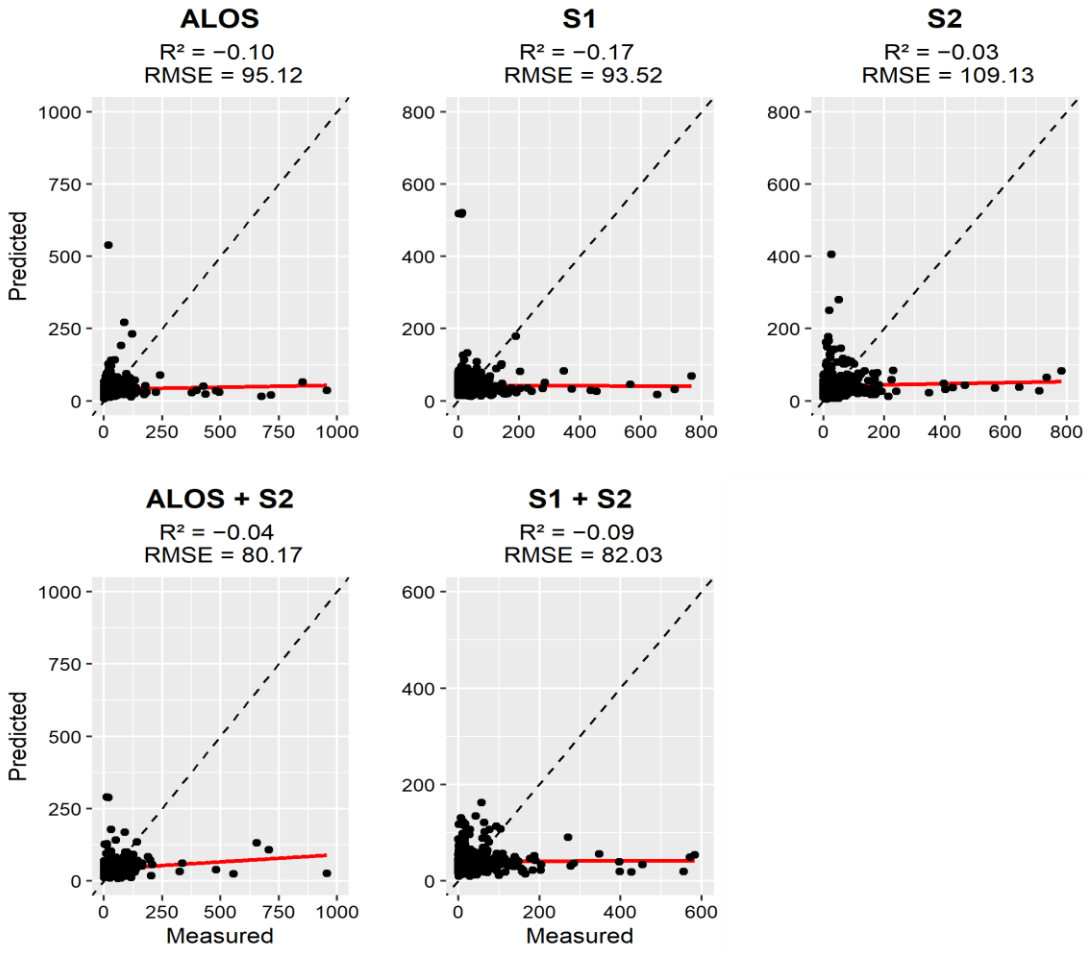

Figure 43: Relation between measured and predicted AGB in the sudanian region using GEDI L4A as reference data. (Kanmegne Tamga et al., 2022b).

3.3.3 Machine learning algorithms

Modelling the AGB in different climatic of West Africa could be heavily influenced by the machine algorithm used in the process. The performance of different machine learning algorithms (ML) were compared based using their coefficient of determination and error level using the different reference data. Based on their coefficient it appeared that for linear models namely linear, ridge Lasso and ElasticNet regression models, the prediction performance was almost similar for both reference data (Figure 44). It also appears that a higher R^2 was achieved when using the combination S1 + S2. However, for non-linear models, it was found that there is an important

difference between predictions based on field data and GEDI L4A. The predictions based on field measurements had a higher R^2 for RF, VSURF and SVM. The best model however was achieved using RF with S1 + S2 (R^2=0.91). When using GEDI L4A as reference, the accuracies were similar for S2, ALOS+S2 and S1+S2 (R^2=0.63). The same trend was observed when VSURF and SVM are used.

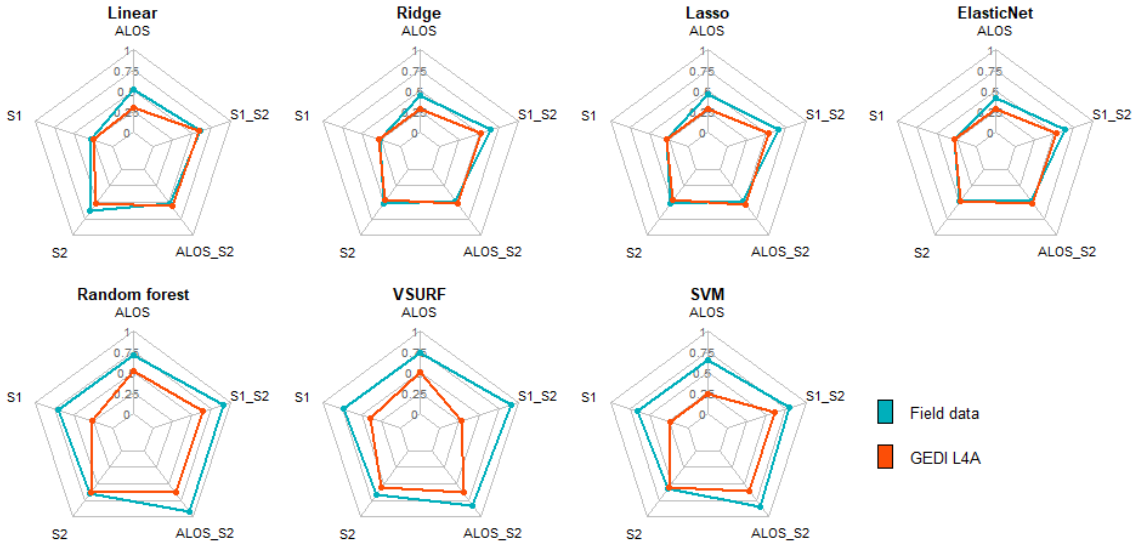

Figure 44: R^2 of ML algorithms for AGB predictions in West Africa (Kanmegne Tamga et al., 2022b)

The assessment of the RMSE showed that the prediction error was higher for prediction based on GEDI L4A (Figure 45). This error was recorded to be much higher for linear ML, except for the linear regression model which showed a prediction error comparable to RF for all the different datasets. The smallest RMSE value was obtained with RF when using field data and S1+S2 (RMSE=3.78), while the same combination returned an error level about 10 times higher (RMSE= 37.28) when evaluating against GEDI L4A data.

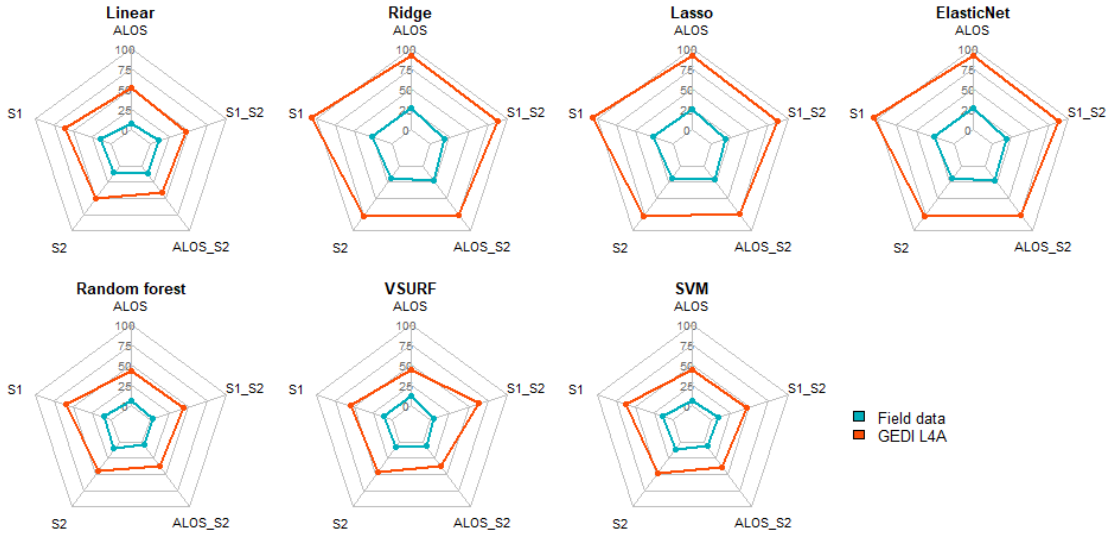

Figure 45: RMSE of ML algorithms for AGB predictions in West Africa (Kanmegne Tamga et al., 2022b)

3.4 Carbon maps and uncertainties

Guineo-Congolian.

The AGB map in Guineo-Congolian region was generated using RF and the combination S1 + S2 and the prediction error at each pixel was generated (Figure 46). The classification assessment showed a $R^2 = 0.91$ and RMSE =3.82, and the RMSE value was used as a threshold to define four classes of different level of prediction error; low and very low if the RMSE was lower than 1.91 and 0.95 respectively or high and very high if the pixel value was higher than one or two time. The interpretation of the carbon map revealed that higher biomass levels were observed in the region corresponding to the Taï national park. The sample plots presented in snippet-1 showed that the biomass level was higher in rubber plantations compared to cocoa farms. The prediction error was found to be high across the ROI. The region around the Taï national park showed a prediction error which was higher than the prediction from the model. At the sample level, the prediction error was higher in cocoa AFS compared to rubber and farm (Figure 46 snippet-2).

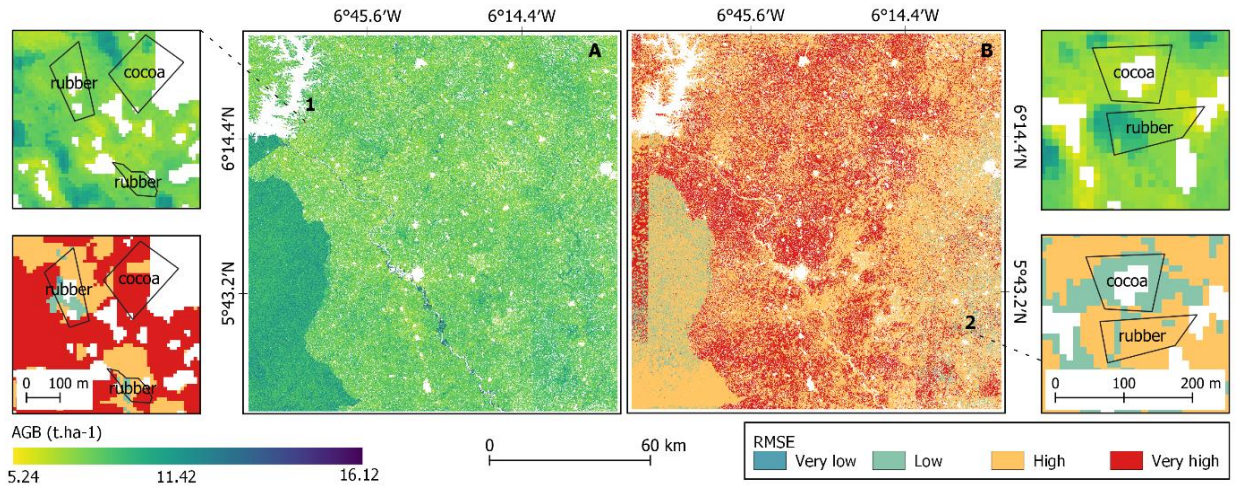

Figure 46: carbon map in the Guineo-Congolian region (A) and the uncertainty map (B). (Kanmegne Tamga et al., 2022b)

Guinean

The AGB level was found to be uniform across the ROI in the Guinean region (Figure 47). The observation at sample level showed that AGB in cashew plantations was slightly higher compared to mango.

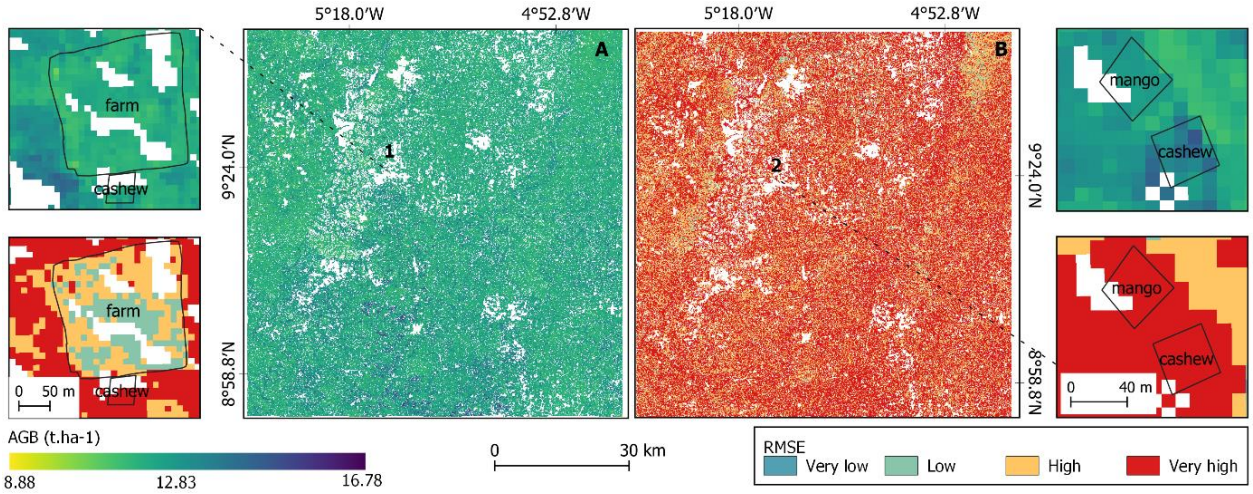

Figure 47: Carbon map in the Guinean region (north Côte d'Ivoire) (A) with the uncertainty map (B). (Kanmegne Tamga et al., 2022b)

The level of prediction error was very high across the area. In farms, there was heterogeneity in the spatial distribution of the prediction error, so that the prediction error was low in the middle of

the farm but increased around the boundaries of the plot (Figure 47, snippet-1). On the other hand, the prediction error was uniform for cashew and mango plantations with a very high level of error (Figure 47, snippet-2).

Sudanian

The AGB level of the ROI in the Sudanian region was uniform across the area, except from the protected area, where the AGB level was lower (Figure 48). The area is showing a very low prediction error except from certain spot where there are higher prediction errors. As an illustration, the Figure 48 snippet-1 shows the AGB and prediction error for a plot of the African locust bean (*Parkia biglobosa*). The AGB level as well as the associated prediction error was not evenly distribution within the plot. The predictor at certain areas were not as reliable as the prediction around it. Moreover, the Figure 48 snippet-2 shows that the error in AGB estimation varies from one plot to the other for shea based AFS.

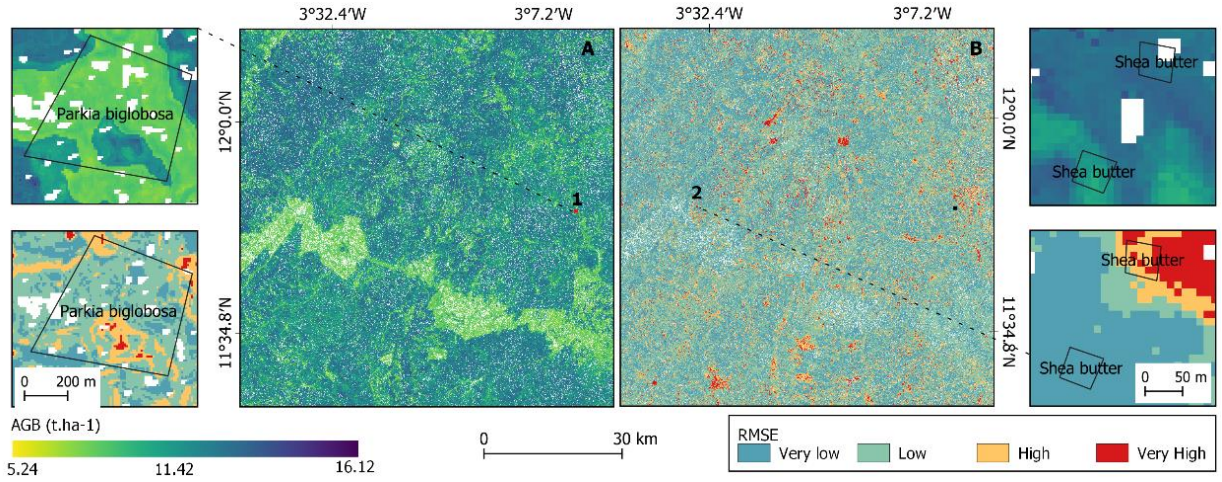

Figure 48: Carbon map in the Sudanian region (A) with the uncertainty map (B) (Kanmegne Tamga et al., 2022b)

3.4.1 Carbon stocks for each AFS in West Africa

The average AGB level was estimated for the different AFS in West Africa to create a reference to evaluate their contribution to climate change. Using the area statistics, the average AGB was determined in tonne per ha ($Mg.ha^{-1}$). Also, the carbon map was validated at plot level, and the accuracy for each AFS was reported (Table 9). In the Guineo-Congolian region, the higher AGB level was found in cocoa plantations (7.51 ± 0.6 $Mg.ha^{-1}$) followed by rubber (7.33 ± 0.3 $Mg.ha^{-1}$)

and farm (6.97 ± 0.4 Mg.ha^{-1}). The assessment of the prediction at pixel level showed that the AGB map was more accurate in farm (R^2 = 0.76, RMSE = 7.0) and cocoa farms (R^2 = 0.6, RMSE = 7.48) compared to rubber plantations (R^2 = 0.25, RMSE = 13.86).

In the Guinean region, the highest AGB level was found in cashew plantations (13.78 ± 0.9 Mg.ha^{-1}) followed by mango (12.82 ± 0.6 Mg.ha^{-1}) and farm (11.78 ± 0.2 Mg.ha^{-1}). The assessment of the AGB map showed that the best prediction accuracy was achieved in farm (R^2 =0.78, RMSE = 6.62) followed by mango (R^2 = 0.58, RMSE = 21.07). AGB estimation in cashew plantations was very low (R^2 =0.37, RMSE = 38.68) with a very high level of error.

The AFS in the sudanian region were associated with the highest level of AGB level in west Africa. The largest AGB stock was reported in AFS dominated by custard apple (82.11 Mg.ha^{-1}), African locust bean (43.97 ± 54.4) and apple ring AFS (23.24 ± 10.3 Mg.ha^{-1}). The shea tree which was one of the most popular AFS in the region was having an AGB level (15.05 ± Mg.ha^{-1}) which was higher than all the AFS in the Guineo-Congolian and Guinean region.

Table 9: Summary of AGB estimations of AFS in West Africa (Kanmegne Tamga et al., 2022b)

Climatic regions	AFS	Carbon (Mg ha^{-1})	R^2	RMSE	N plots
Guineo-Congolian	Farm	6.97 ± 0.4	0.76	7.00	62
	Cocoa	7.51 ± 0.6	0.6	7.48	30
	Rubber	7.33 ± 0.3	0.25	13.86	30
Guinean	Cashew	13.78 ± 0.9	0.37	38.68	21
	Mango	12.82 ± 0.6	0.58	21.07	22
	Farm	11.78 ± 0.2	0.78	6.62	23
Sudanian	Custard apple	82.11			1
	Shea tree	15.05 ± 7.3			11
	Apple-ring	23.24 ± 10.3			5
	Marula	6.59 ± 0.3			2
	African locust bean	43.97 ± 54.4			6

The assessment of the relationship between the AGB level, the biometric parameters (height and diameter) and the tree composition in each AFS revealed that the biometric parameters of the trees were more important than the composition of the AFS. In fact, the AGB was more sensitive to diameter (R^2 =0.45) and tree height (R^2 = 0.13) compared to tree density (R^2 =0.1) (Figure 49). Therefore, AFS with trees that have larger diameter and height tends to return large AGB levels

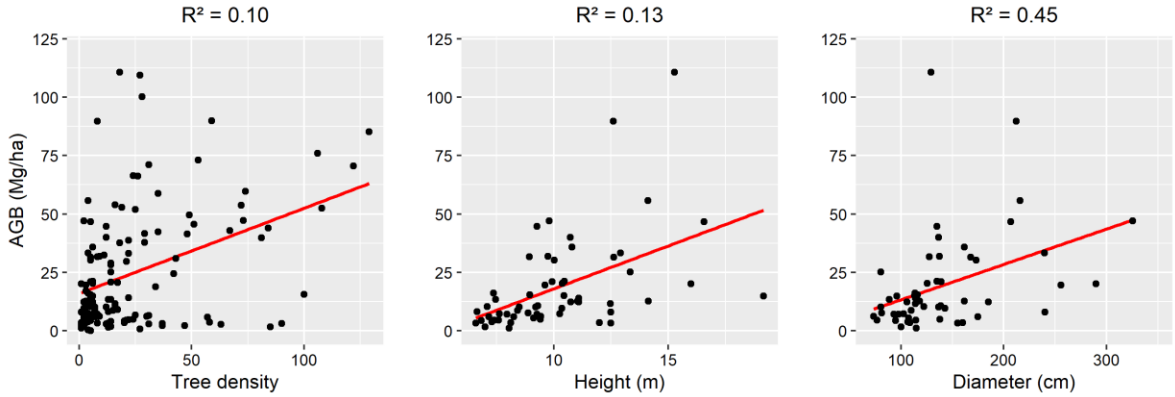

Figure 49: Relation between tree parameters and AGB of AFS in West Africa Map of carbon and RMSE in AFS (Kanmegne Tamga et al., 2022b).

The improved AFS maps were used to extract the spatial distribution of AGB level of the main AFS in each ROI. Rubber and cocoa plantations were identified as the dominant AFS in the Guineo-Congolian region, representing more than 75% of the land cover in the region. The AGB estimations in oil palm plantations were not presented because the development of the model did not include training samples from that AFS. The map shows that carbon stocks in cocoa plantations are evenly distributed across the ROI. However, the prediction error was lower in the municipalities of Guiberoua and Gagnoa, and higher in the southern part (Soubre, Sassandra and Gueyo) (Figure 50).

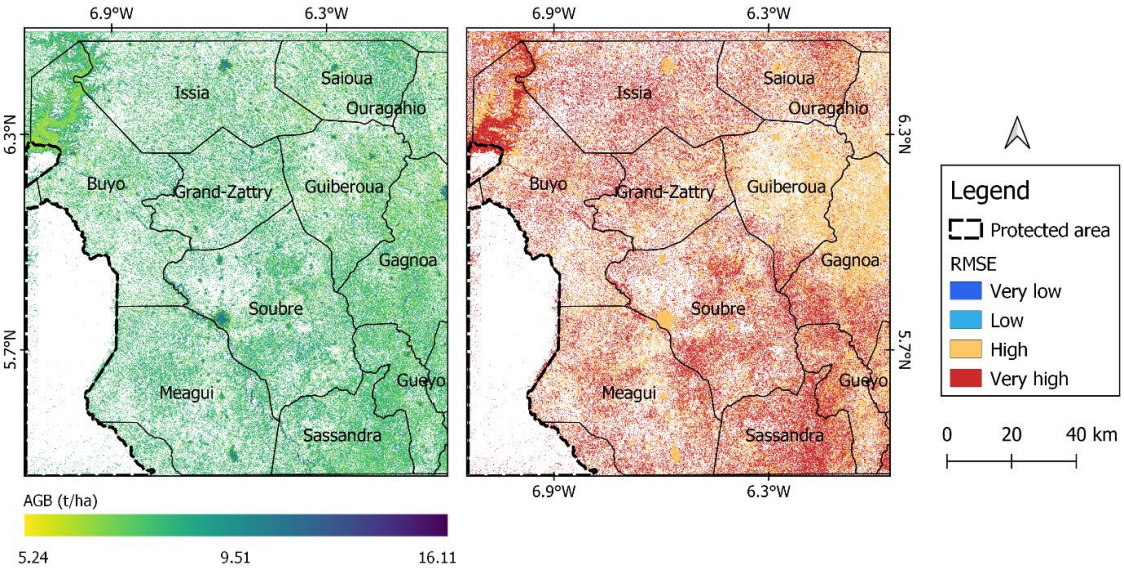

Figure 50: Spatial distribution of the AGB level of cocoa plantations in the Guineo-Congolian region.

In rubber plantations, the overall level of carbon stocks was lower compared to cocoa plantations and no specific municipality could be associated with a high level of rubber production. The map suggested no encroachment of cocoa plantations in the boundaries of the protected area, and the AGB prediction error was relatively high in the municipality of Sassandra. The spatial distribution of AGB level in farms is present in Figure 51.

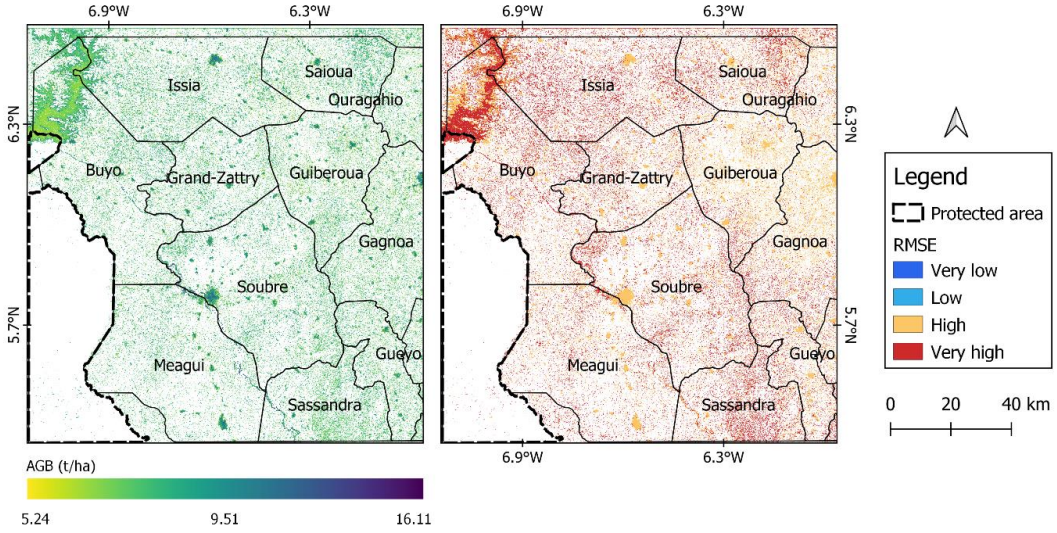

Figure 51: Spatial distribution of the AGB distribution of the AGB level of rubber plantations in the Guineo-Congolian region.

In the Guinean region, the main cash crops were represented by cashew and mango. As far as the carbon stocks distribution was concerned, cashew showed the highest level across the ROI, especially in the municipality of Tafiere (Figure 52). Cashew plantations with higher levels of AGB were identified in the eastern and western part of the municipality. The associated prediction error was found to be higher across the ROI, mainly in the central part of the municipality of Tafiere was showing higher uncertainties. In mango plantations, higher AGB levels are recorded in the municipalities of Sinematiali and Ferkessedougou. In the north-western part of Tafiere, the pattern of AGB level suggested that mango plantations are planted in the form of small, well-defined units (Figure 53).

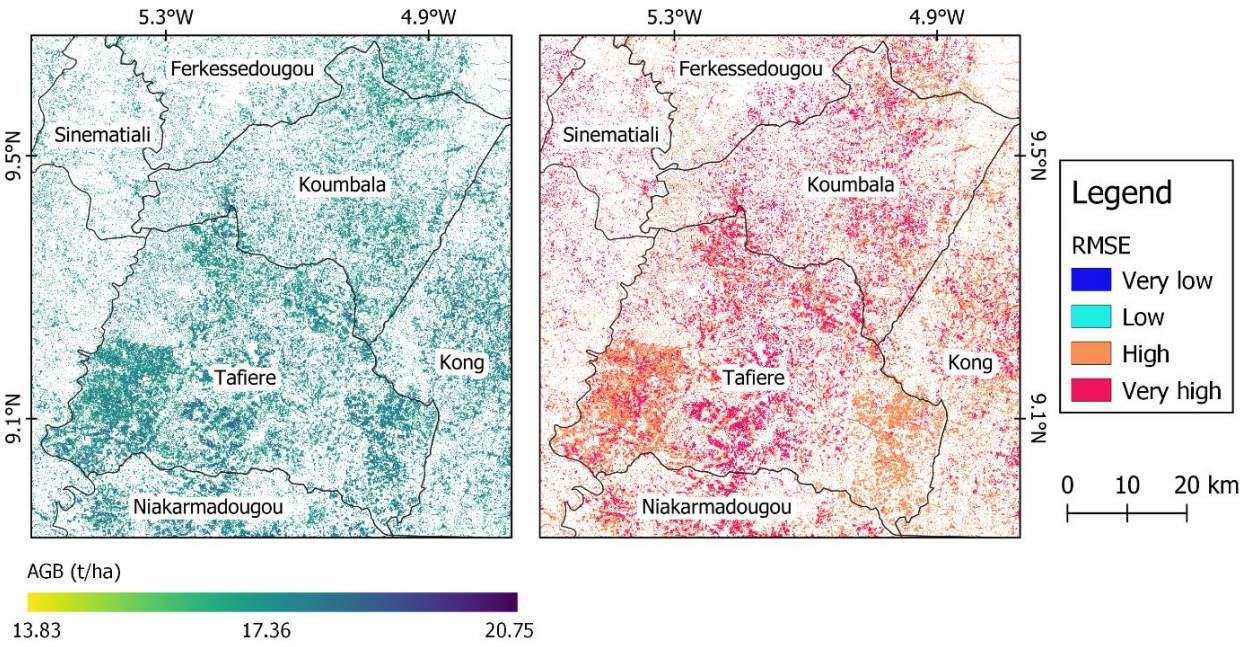

Figure 52: Spatial distribution of the AGB level of cashew plantations in the Guinea region

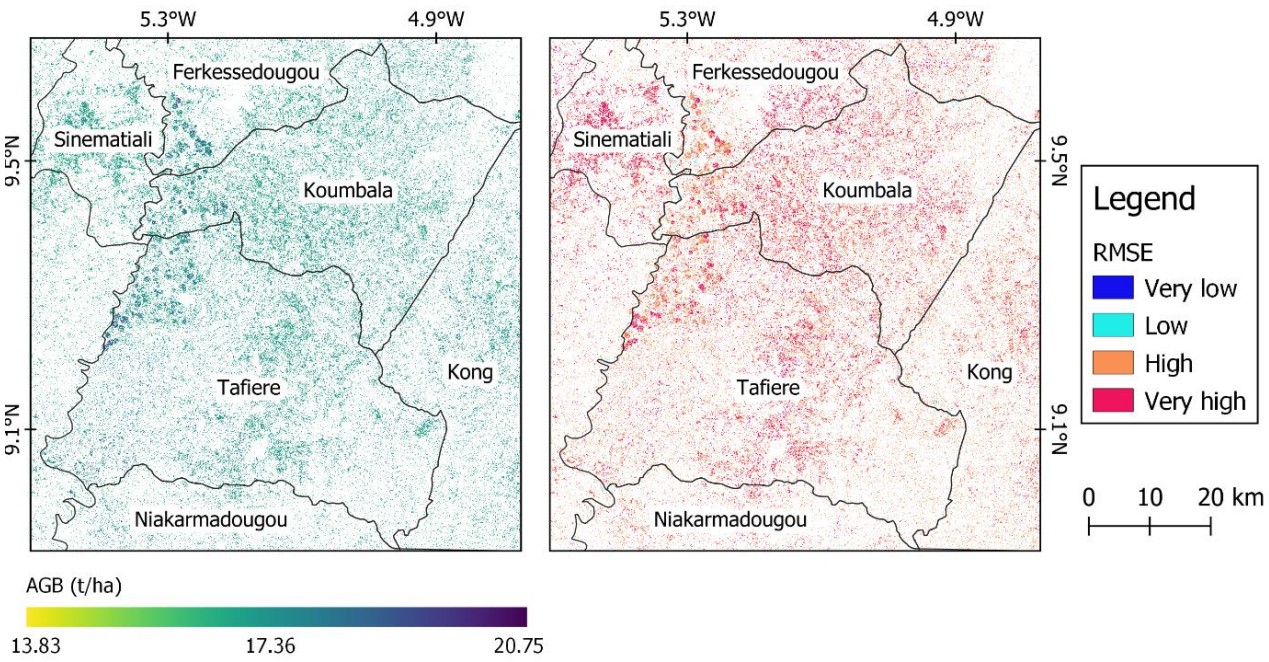

Figure 53: Spatial distribution of the AGB level of mango plantations in the Guinean region

3.4.2 Biodiversity assessment of AFS in West Africa

The biodiversity level was assessed in the AFS of West Africa using two ecological indices namely biodiversity and Simpson indices (Figure 54). The biodiversity index is the ratio between the number of species and the number of trees. The value ranges between 0 and 1 where 0 is associated with a poor biodiversity (monocropping for example) and 1 higher diversity. A higher biodiversity level was found in multipurpose trees on agricultural lands. In west Africa, the African locust bean AFS showed the highest biodiversity index (BI=0.84) followed by agricultural farms in the Guineo-Congolian region (BI=0.61). The AFS class referred to as others (BI= 0.55), shea trees (BI= 0.46) and apple ring (BI=0.37) which were found in the Sudanian region, showed a higher biodiversity compared to farms in the Guinean region (BI=0.32). Plantation crops which are mainly represented by mango (BI=0.08), cashew (0.07), cocoa (BI=0.05) and rubber (BI=0.03) were associated with the lowest biodiversity in West Africa.

The Simpson index was also used to assess the biodiversity in AFS. It considers the number of species as well as the relative abundance of each species. Based on this metric, it was found that farms in the Guineo-Congolian region (SI=0.57) showed a higher value compared to the African locust bean (SI=0.54). The Simpson index was also found to be higher in others (SI=0.49) and

farms of the Guinean region (SI=0.44) compared to shea trees (SI=0.23) and apple ring (SI=0.21). In plantation crops, the Simpson index values were the lowest in cashew (SI=0.12), mango (SI=0.1); cocoa (SI=0.08) and rubber (SI=0).

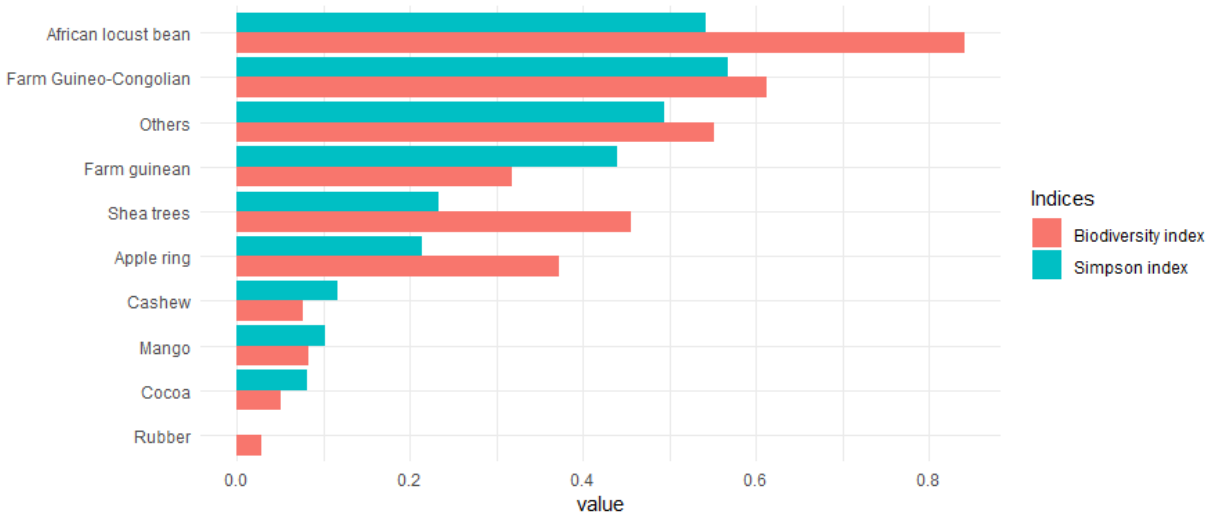

Figure 54: Biodiversity and Simpson indices of different AFS in West Africa

The relationship between the biodiversity indices and the estimated AGB was explored across the AFS in West Africa (Figure 55). It was found that the biodiversity index was showing a positive correlation with the AGB (R^2=0.57) while the relation between the AGB and the Simpson's index was weaker (R^2=0.31). However, the relation between biodiversity indices and AGB was not significant in AFS at a significance threshold of 5%, suggesting that the AGB level was not determined or influenced by the level of biodiversity.

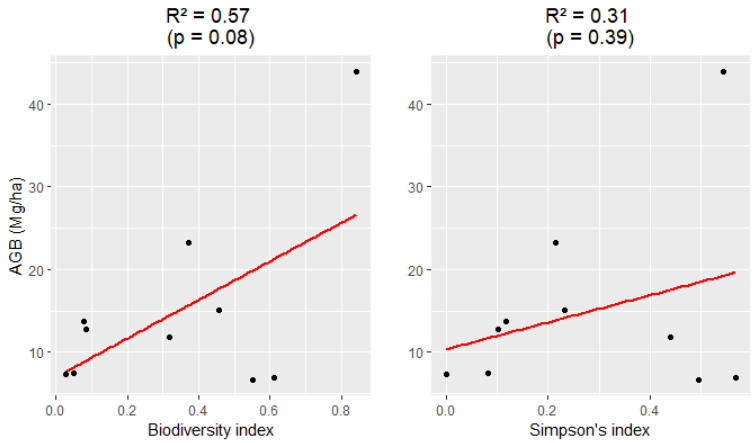

Figure 55: Relation between the biodiversity indices and the AGB level of AFS in West Africa

3.5 Carbon stock dynamic within AFS in West Africa

The assessment of carbon stock dynamic of AFS in west Africa was based on the comparison of yearly AGB estimations to the average AGB maps and the corresponding standard deviation map in each climatic region between 2017 and 2021. The average and variance maps corresponding to the above-mentioned period are presented in Figure 56. The maps show that the overall AGB level is higher in the Sudanian, and Guinean compared to the Guineo-Congolian region, and the SD was lowest in the Guinean region.

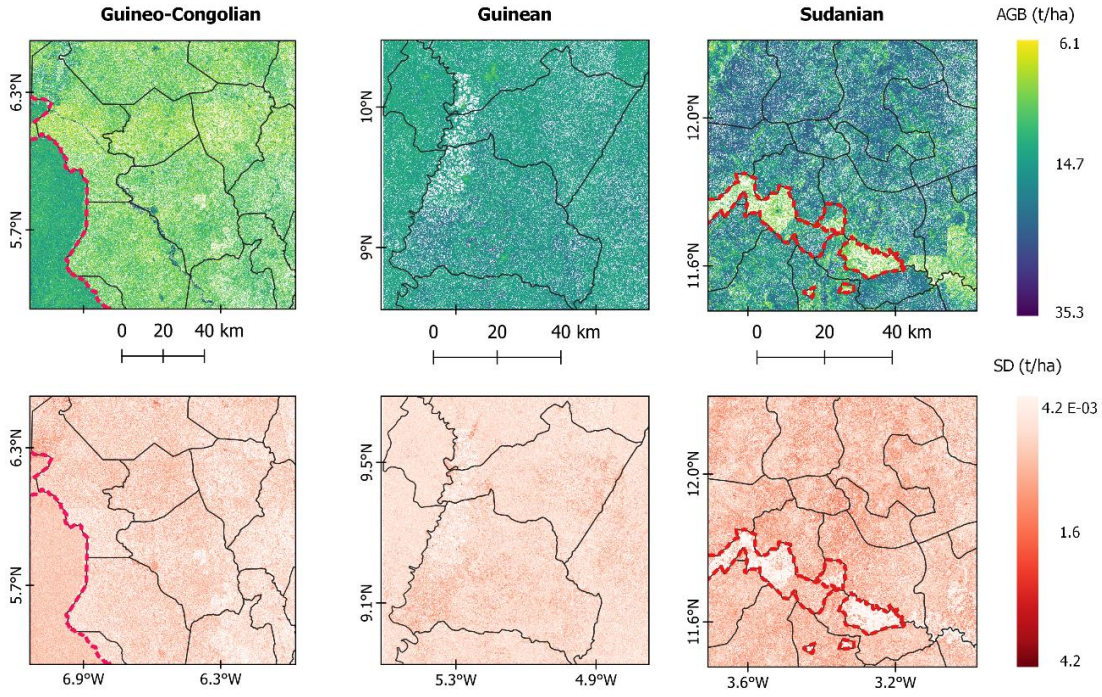

Figure 56: Average AGB level and the corresponding standard deviation maps between 2017 and 2021.

3.5.1 The Guineo-Congolian region

The difference between the AGB level at a given year and the average AGB level was used to detect anomalies, which referred to location where the AGB level was different from the long-term trend. SD was used as threshold to determine if the differences were significant, and the locations were labelled as carbon source if the anomalies suggested a loss of biomass or carbon sink for increase in AGB. Figure 57 shows the carbon dynamic of a cocoa and rubber field plots. In cocoa plantations, it was found that the dynamic of the standing biomass was higher, with an increase of carbon sinks between 2017 to 2019, a significant AGB loss in 2020 followed by an

increase in AGB in 2021. In rubber plantations on the other hand, it was found that the proportion of carbon sinks were increasing consistently from 2017 to 2021.

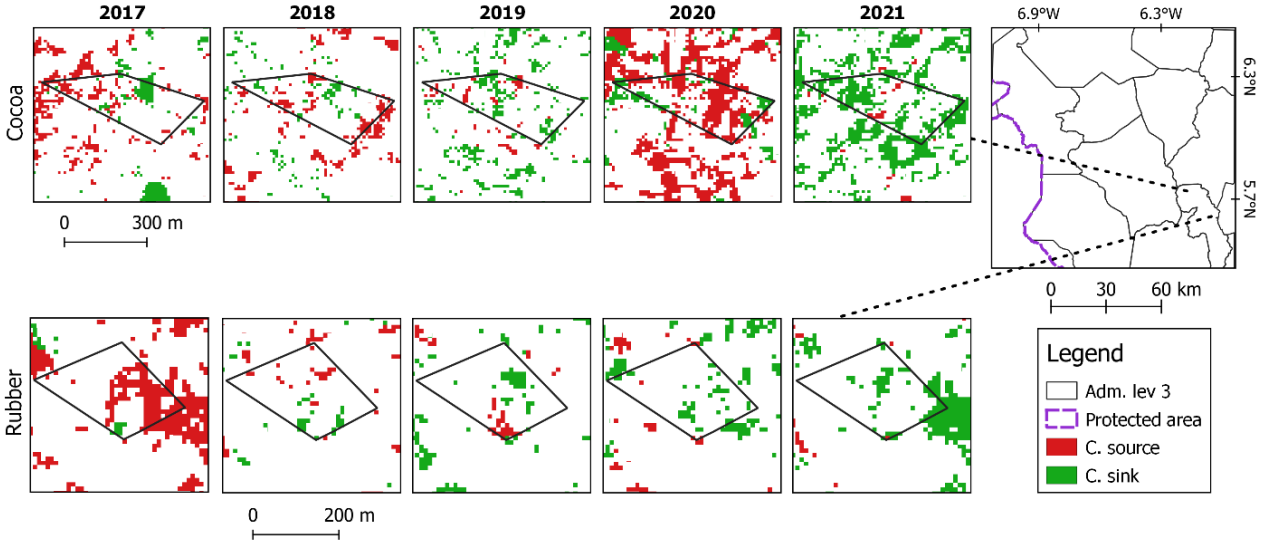

Figure 57: Dynamic of carbon stocks of crop plantations in the Guineo-Congolian region

The dynamic of carbon in the entire ROI is summarized in Figure 58. The map suggests that AFS were mainly behaving as carbon sources between the year 2017 and 2018. However, from year 2019, the overall AGB level started to increase, as illustrated by the increase of carbon sinks across the ROI.

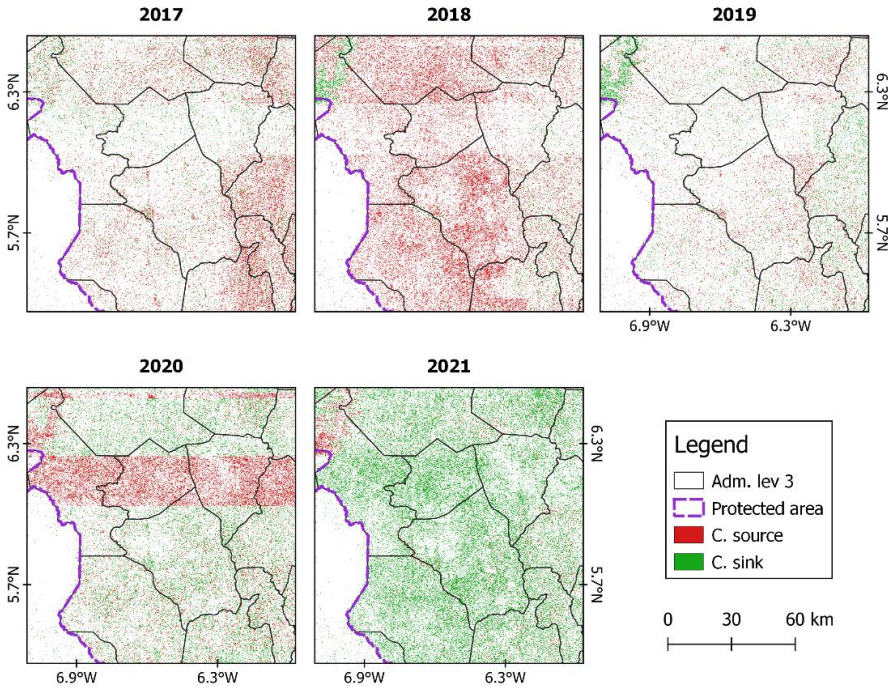

Figure 58: spatial distribution of the carbon pools and carbon sinks in the Guineo-Congolian region

The area statistics showed a decrease of the proportion of carbon sinks, going from 36.5% to 3.5% between 2017 and 2018. This decrease is followed by an increase of proportion of carbon sinks going from 44.9% in 2019 up to 85% in 2021 (Figure 59).

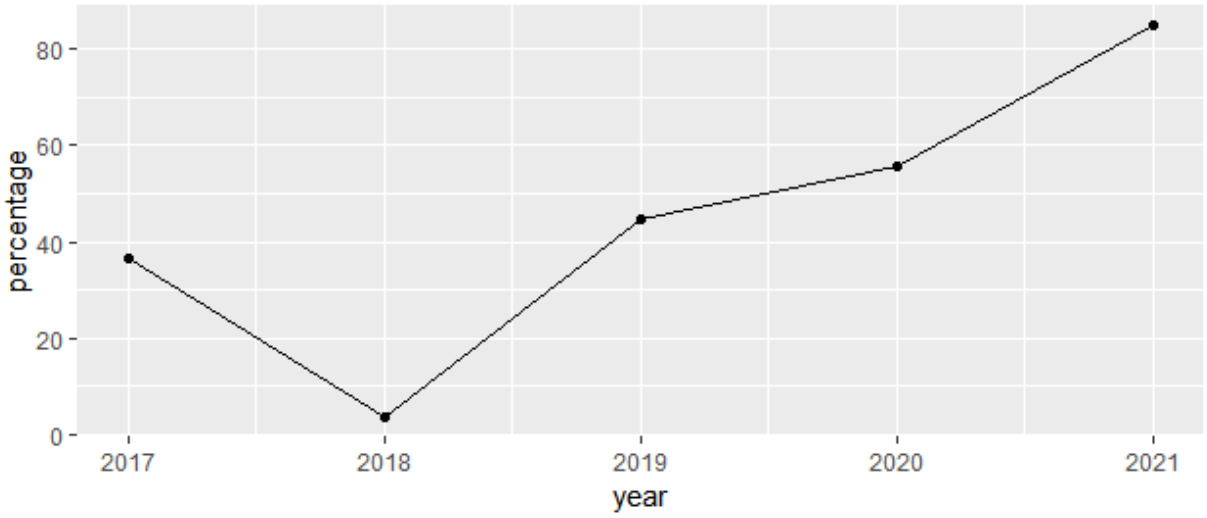

Figure 59: Dynamic of the proportion of carbon sinks in the Guineo-Congolian region

3.5.2 The Guinean region

In the Guinean region, the carbon stock dynamics observed in farm, cashew and mango plantations are presented in Figure 60. It was found that in farms (the line on the top), the carbon stock level was varying, showing a decrease of carbon sinks from 2017 to 2018 and from 2020 to 2021, while a large increase of AGB was captured between 2019 and 2020. In cashew and mango plantations, the trend suggested no change in the carbon level. In fact, the carbon level in 2017 barely decreased across the year, except for a significant loss of carbon in cashew plantations in 2019.

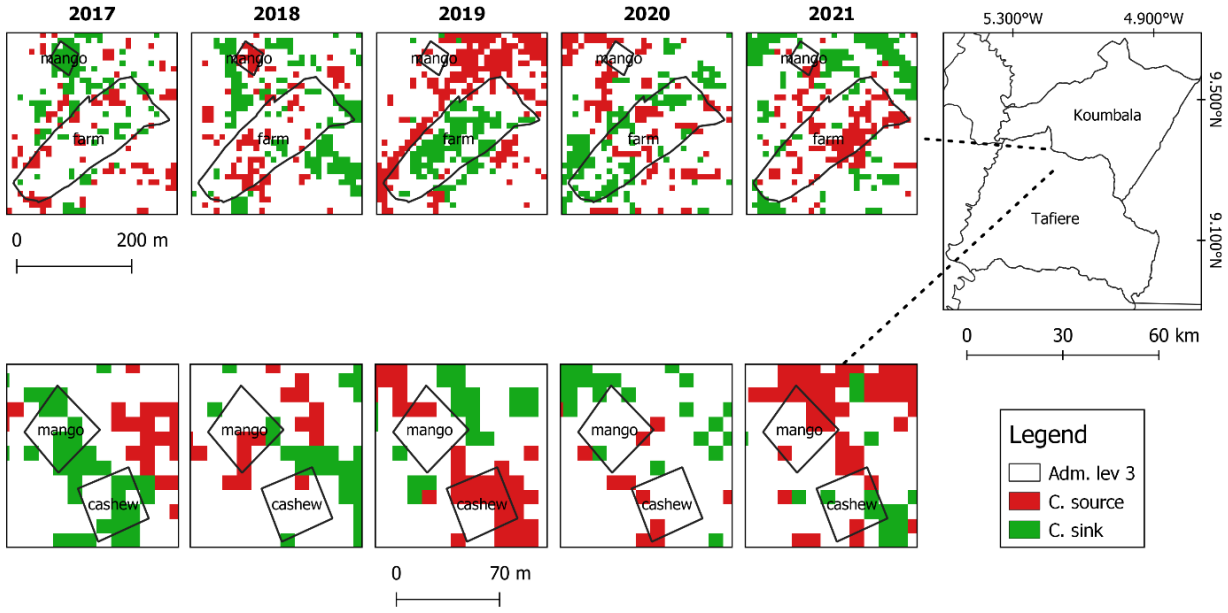

Figure 60: Dynamic of carbon stocks of some AFS in the Guinean region

The spatial distribution of carbon sinks and carbon sources in the ROI is presented in Figure 61. It was found that from 2017, the carbon level decreased until 2019. The year 2020, the carbon level had increased, as presented by the increase of carbon sinks. In 2021, there was a decrease in carbon sink, suggesting a lower AGB level compared to the long-term trend.

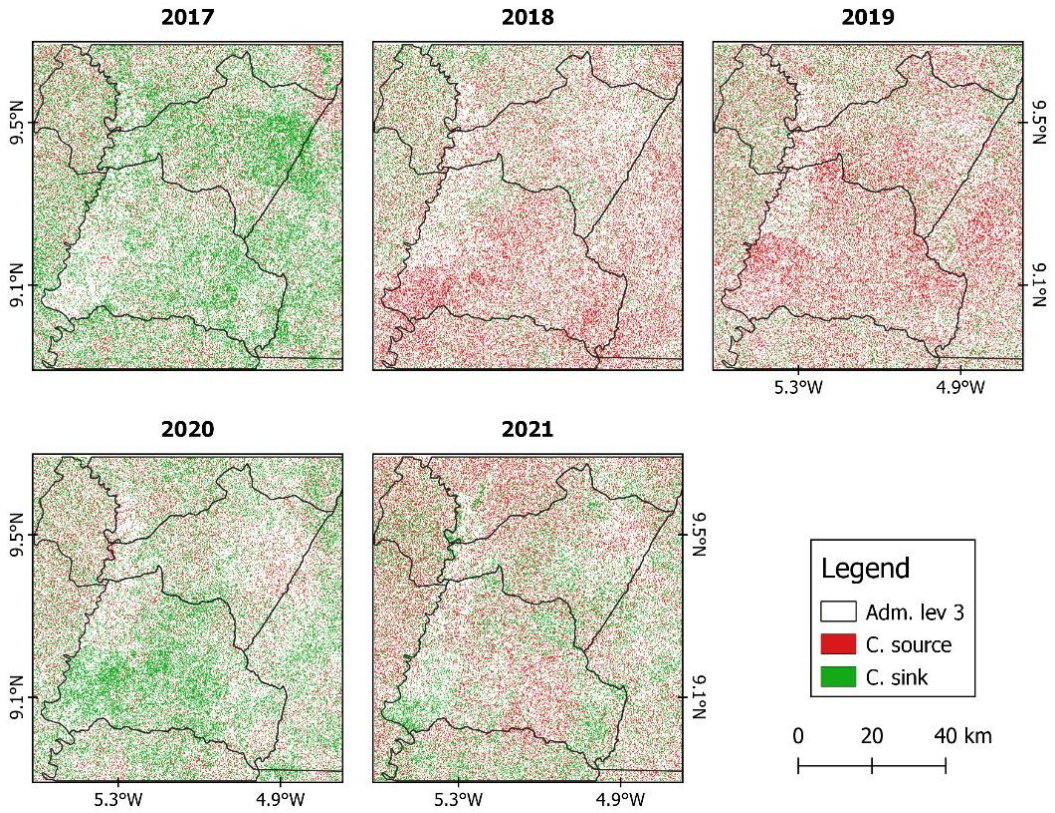

Figure 61: spatial distribution of the carbon pools and carbon sinks in the Guinean region of west Africa

The area statistics suggested a decrease of the proportion of carbon sinks over the period of observation, with 74.4% in 2017 to 49.5% in 2021 (Figure 62). It was also found that the proportion of carbon sinks was very low for the years 2018 (30.6%) and 2019 (29.6%). In 2020, the proportion of carbon sinks increased up to 69.2%.

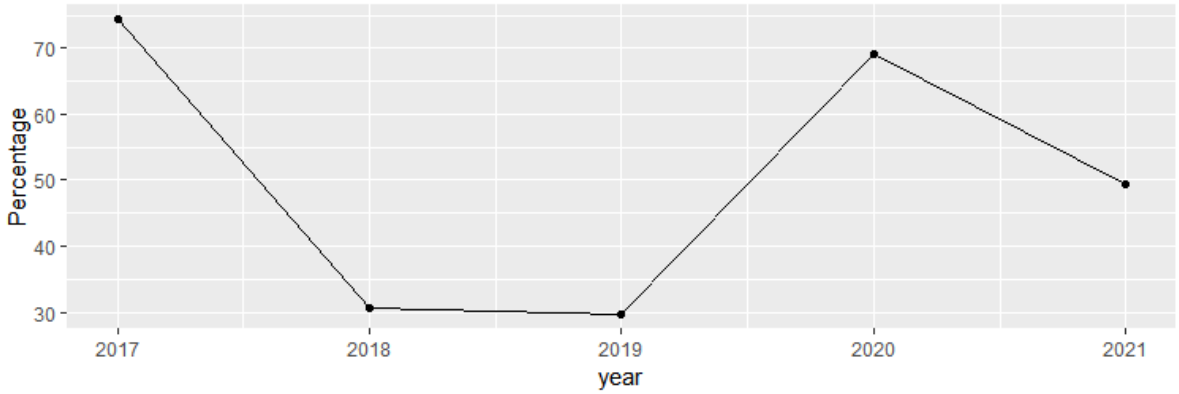

Figure 62: Dynamic of the proportion of carbon sinks in the Guinean region

3.5.3 The sudanian region

In the Sudanian region, the carbon stock dynamic was observed for the African locust bean and the shea trees (Figure 63). It was found that for both AFS, the AGB level was very low in 2017 compared to the average AGB level. For the African locust bean, the AGB level was found to be constant over time, while shea trees showed an increase in carbon sinks suggesting the increases in the AGB level.

When considering the entire ROI, the year 2017 was characterised by an overall lower AGB level compared to the average AGB level (Figure 64). In the year 2018, there was an increase in the proportion of carbon sinks mainly in the northern part, while the AGB level in the south remained low. In 2019, the overall level of AGB increased, showing an important change in the southern part of the ROI and within the boundaries of the protected areas. In 2020, A decrease in the AGB level was detected, mainly in the southern part of the ROI. In 2021, the overall AGB level increased, mainly in the southern part of the ROI and within the protected area.

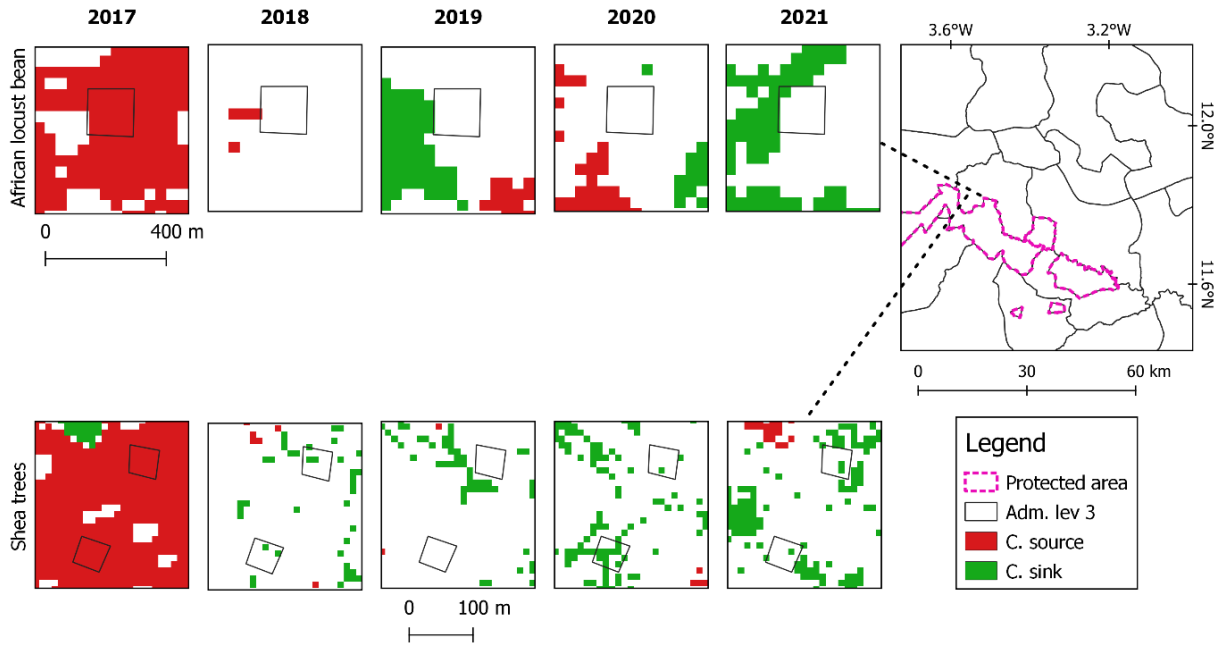

Figure 63: Dynamic of carbon stocks of some AFS in the sudanian region

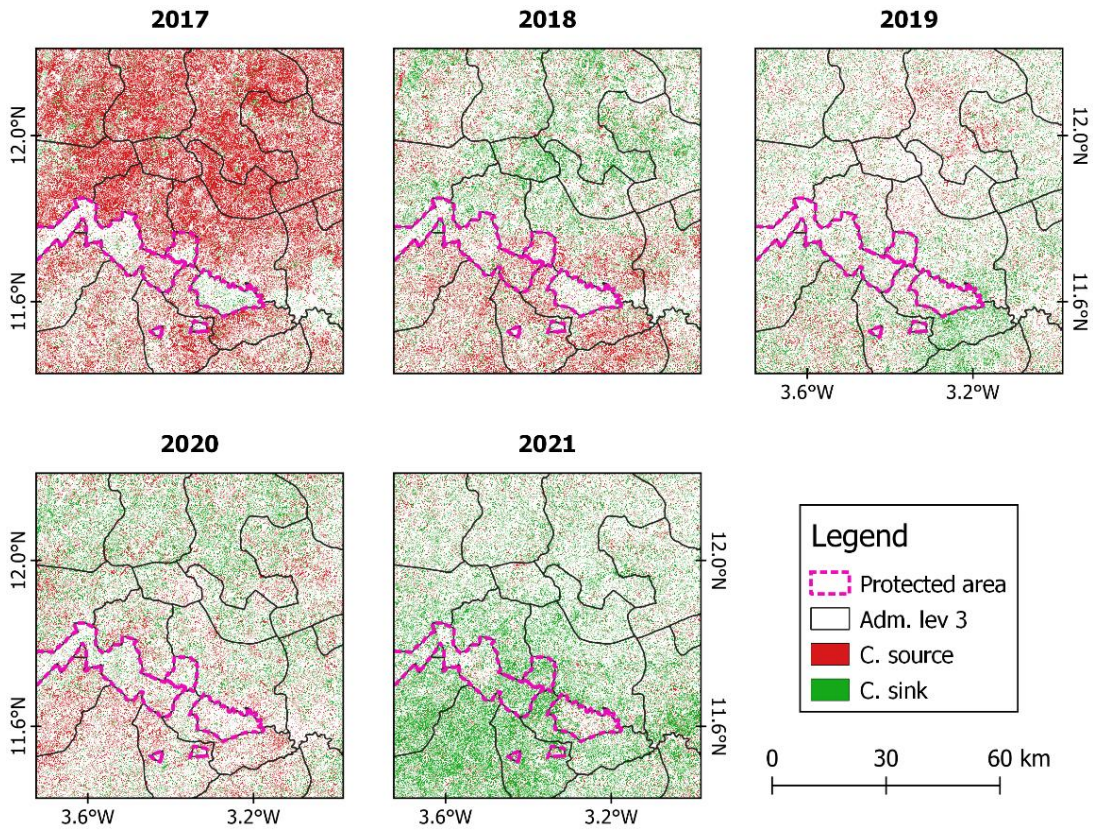

Figure 64: Spatial distribution of carbon pools and carbon sinks in the Sudanian region of West Africa

The area statistics of the proportion of carbon sink in the sudanian region showed an increase during the temporal window used for the analysis, going from 18.5% in 2017 to 82.3% in 2021. From 2017 to 2019, the area of carbon sinks increased linearly and reached 61.3% in 2017. It was also found that in the year 2020, the proportion of carbon sinks decreased to 51.3% (Figure 65).

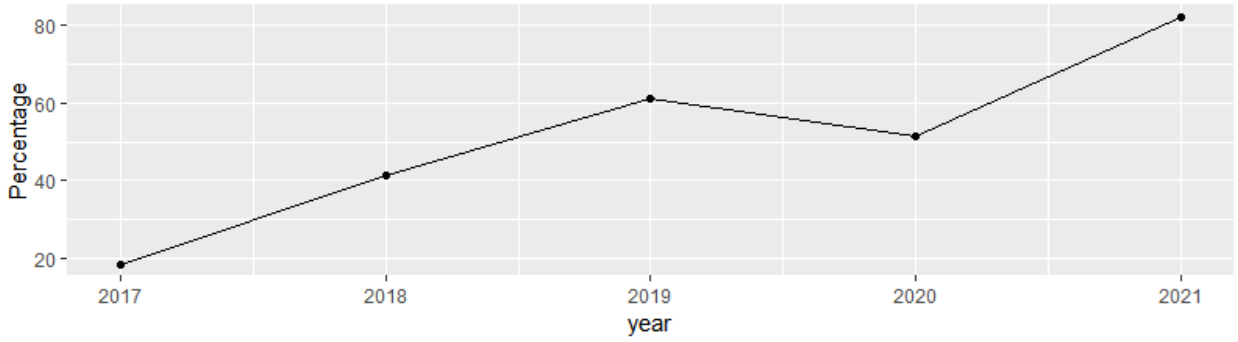

Figure 65: Dynamic of the proportion of carbon sinks in the Sudanian region

3.6 Proportion of the carbon sinks in each AFS

The improved classification map of the AFS in each climatic region was used to extract the area statistic of the carbon sink between 2017 and 2021 (Figure 66). The proportion of carbon sink corresponds to the proportion associated to each AFS for the entire ROI. The largest proportion of carbon sinks was found within the AFS in the Guinean region. In the year 2017, the largest proportion of sinks was found in agricultural farms (42.4%) followed by cashew (18.4%) and mango (13.2%). Then in 2018, cashew showed the highest proportion of carbon sink, where 57% of the increase in AGB was found in cashew plantations. In 2019, the proportion of cashew sinks decreased to reach 4.7%. In 2020 and 2021, the largest proportion of sinks in the AFS was found in farms, followed by cashew and mango plantations. In the Guineo-Congolian region, it was found that the largest proportion of Sink was found in cocoa plantations, when rubber plantations and farms were showing similar values. In 2017, the proportion of sinks in cocoa plantations was estimated at 13.1% of the ROI, compared to 8.2% and 8.4% for farm and rubber plantations respectively. From 2019 to 2021, the proportion of sinks in cocoa plantations increased from 15.6% to 29.7% suggesting either an increase in the AGB level within existing plantations or an increase of the area of cocoa plantations in the ROI. Comparatively, an increase from 10.2% to 19.1% was recorded for rubber plantations. In the sudanian region, the dynamics of the proportion of carbon sinks in the AFS moved similarly, with values that were similar. In 2017, the proportion of carbon sinks between AFS varied between 2.7% and 3.4%. It was found that this proportion has increased over time to reach 12.7 to 13.6% in 2021. No AFS was found more important than the others, rather they showed the same pattern over time.

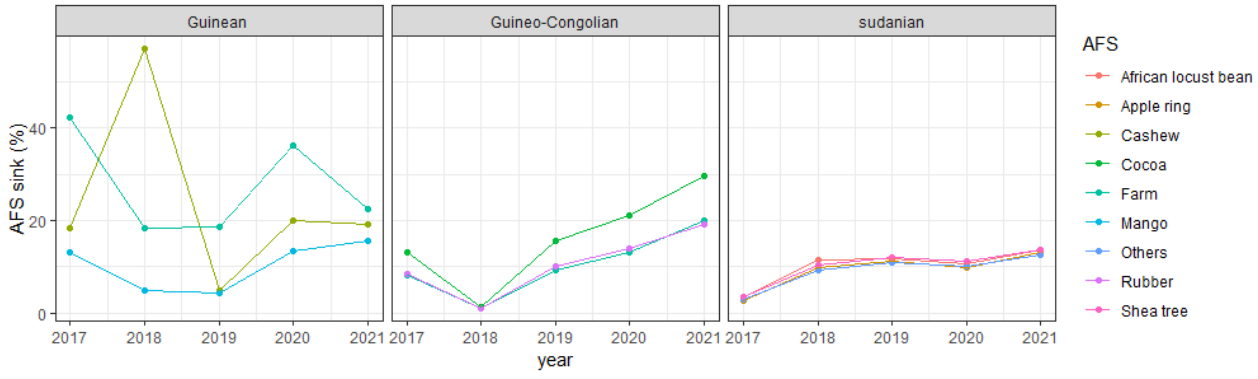

Figure 66: Dynamic of the proportion of carbon sinks of the AFS in different climatic region of West Africa

Chapter 4

Discussion

4.1 Agroforestry systems

The occurrence and the spatial distribution of the main agroforestry systems (AFS) in West Africa depends on several factors including economic and sociocultural. However, the major determinant of the adoption of an AFS in a region are the environmental conditions including soil and climatic properties. In West Africa, the humid climatic conditions associated with the Guineo-Congolian region is favourable for cash crop plantations such as cocoa farming, rubber plantation, and oil palm. In the ROI, the AFS was mainly dominated by rubber (38.9%) and cocoa (36.4%), but also oil palm (10.8%). The investigation on the field revealed that those AFS are often established on previous fallow and/or secondary forests for an extensive period (30 years in average). The main reason is economic as cocoa farming provides sufficient income for about 33% of farmer in the region (Boeckx et al., 2020). Cocoa beans production is a major commodity in Cote d'Ivoire and represent about 5% of the revenues from exports. The country is the world largest cocoa beans producer with over two million tons in 2020 (Shahbandeh, 2021). Cocoa farming is also the main driver of deforestation , responsible of the loss of more than 80% of the forest cover in Cote d'Ivoire between 1961 and 2000 (Sabas et al., 2020), with consequences such as encroachment in protected areas, habitat degradation, loss of biodiversity, soil degradation and climate change. Yet sustainable intensification of cocoa production could be a solution for poverty alleviation and climate change as the demand for cocoa is projected to expand by 7.3% in 2025 mainly due to rapid growing of chocolate industries in emerging economies (Boeckx et al., 2020; GVR, 2019; Nair et al., 2010).

In drier and hotter conditions, AFS are mainly represented by either cashew and mango plantations in the Guinean region, where the precipitation level guarantees sufficient water for the crops, or by multipurpose trees on agricultural land. The area statistics revealed that the ROI was mainly represented by farms (71.4%), and the cash crops represented only 15.2% and 13.4% for mango and cashew respectively. For local farmers, cashews and mango represent the main source of income. Because they are highly perishable, mangoes are sold to local industries or to local market. Cashew on the other hand are dried and stored to be sold later on to meet family needs. Like the Guinean region, farm was the main AFS in the Sudanian region, mainly dedicated to agricultural cash crops such as cotton and sesame, associated with fruit trees. Trees are maintained on farms mainly for the derived non-timber products (fruits, edible leaves, fodder, and medicine). The

region is dominated by shea trees (55.7%) which is one of the most important crops in West Africa, primarily because it is included in the diet of the farmer, but also because of the high demand on the international market. In fact, the market was valued at 655.2 million dollars in 2020, and the demand is estimated to reach 2.4 billion by 2030 (Anil & Roshan, 2021; Dagnogo et al., 2021; Wadudu et al., 2016).

Agricultural farms and cash crops plantations are managed differently in West Africa, yet the spatial distribution of trees within similar AFS is comparable across the region. For instance, an average tree density of 20 trees/ha was observed in farms across West Africa, and the main crops were mainly determined by the climatic conditions and the diet of the farmers. Moreover, the production system in farms is extensive, relying mainly on crop rotation as nutrient management practice (Acevedo-Siaca & Goldsmith, 2020). For cash crop plantation on the other hand, the production system is semi-intensive especially in cocoa plantations with the use of pesticides to protect the cocoa trees against common disease including brown cocoa pod rot, cocoa stem canker or brown root rot among others. However, cocoa production is threatened by the swollen shoot, an endemic pathology in West Africa which is caused by the cocoa swollen shoot virus, and which is responsible for cocoa tree mortality with important consequences on cocoa yields (Adopo et al., 2022). The economic loss due to the decrease of the yield is one of the major triggers for cocoa expansion, leading to deforestation in the region (Ruf et al., 2014).

4.2 Satellite-based classification of AFS

Guineo-Congolian

Forest loss is a major issue as far as climate change is concerned; therefore, an accurate mapping of AFS is crucial for monitoring deforestation in West Africa. In the Guineo-Congolian region, cocoa farming is acknowledged as the main driver of deforestation, threatening the integrity of protected area like the Taï national park. When using open-source data from the sentinel mission, it was found that a combination of ten input variables including vegetation indices and some texture parameters (GLCM mean) returns an overall accuracy of 89%, with a confidence interval at 95%. between 86 and 92% at 95%. Looking at the detection of the main cash crops, the error of omission was higher for cocoa (11%) compared to rubber and palm oil (8%), and cocoa also showed the highest error of commission (16%). The detection of cocoa farms derived from this AFS classification is more accurate than the cocoa detection map proposed by Abu et al. (2021) in

the same region, using the same RS-data. This could result from the fact that Abu et al. (2021) carried a classification at national level, focussing only on cocoa farm in Cote d'Ivoire and Ghana. A second point could be related to the fact that the current study considered multiple classes, which therefore reduce the level of misclassification error, as it was demonstrated that multi-class is more efficient than single-class (Madden et al., 2005). Moreover, the balanced accuracy associated with cocoa farms is superior to the accuracy presented by Numbisi et al. (2019) in the delineation of cocoa agroforests in Cameroon, central Africa. This could be explained by the fact that the challenges of cocoa mapping are different in Central and west Africa. In central Africa, the higher forest tree density in cocoa plantations makes it difficult to separate cocoa farm from secondary forest (Yemefack, 2005). Higher balanced accuracies were reported for rubber and oil palm plantations probably because they are monocrop plantations where trees are established at regular intervals, which is not the case for agricultural farms and cocoa plantations in which no spatial arrangement is observed.

The assessment of the classification map showed that there is evidence of classification errors mainly in cocoa plots, which are falsely classified either as rubber or oil palm. An important point to keep in mind is that based on the variable selection procedure prior to the classification, it was found that optical data and the derived vegetation indices were significantly more important that SAR data for AFS mapping. This could mean that cocoa, rubber and oil palm return similar spectral signature at 10 m resolution, making difficult to properly delineate them. Similar findings were reported in the literature, presenting the difficulty to delineate cocoa farm from rubber plantations in west Africa, mainly because cocoa are grown full sun, showing there the same structure as rubber plantations (Minang et al., 2014). Furthermore, the probability maps of the feature class showed that at pixel level, the confusion is higher between cocoa and rubber compared to cocoa and oil palm.

Guinean

The classification map of cashew and mango plantations in the Guinean region was much precise compared to the AFS map in the Guineo-Congolian. The assessment of the returned and overall accuracy of 91% with a confidence interval between 86 and 95%. The classification accuracy of cashew and mango were found to be comparable (0.94 and 0.96 respectively) as suggested by the area under the curve (AUC). However, it was harder to accurately detect agricultural farms (AUC=

0.86). this could be due to the spatial arrangement of cashew and mango which are monocrop, and where trees are established using regular intervals. In west Africa few information related to cashew farming is available, meanwhile cashew plantation area is expanding. In Benin for instance, it was found that cashew plantation area almost doubled from 2015 to 2021, where over 55% of new plantations are established within protected areas (Yin et al., 2023). Some studies also reported the difficulty to differentiate cashew plantations from other woody landcover. In India, it was found that cashew the combination of optical and SAR data was more suitable for the delineation of cashew plantation (Rege et al., 2022). A different conclusion was achieved in west Africa, as the variable selection revealed that out of the eight most important variables, only one variable derived from SAR data was significant. This could be due to the fact that in the Guinean region, cashew plantations are not established around forests, therefore, the vegetation indices derived from optical data are sufficient for their delineation. In the region, it was observed that boundaries between mango and cashew plantations were difficult to be set, resulting therefore in classification error at the edges of cashew farms. This observation is confirmed by the assessment of the probability maps of each AFS; showing a low proportion of overlapping pixels. The problem could be caused by the spatial resolution of the input data, which could be solved by using RS data with higher resolution like planet data (spatial resolution 2.4 m).

Sudanian

The sudanian region is a particular region in west Africa, because of the typology of their AFS. In fact, in other climatic region, AFS are defined around a cash crop that is mainly a tree (cocoa, rubber, cashew etc.), giving to associated AFS a high economic value. In this region on the contrary, the main cash crops such as cotton or sesame are not managed together with trees. Trees are primarily found in agricultural farms where they contribute to the livelihood of farmers at a lower level (diet or as medicine). In this setting, trees are allowed to grow larger and bigger making such systems distinguishable from monocrop farms using remote sensing. The variable selection showed that a balanced combination of optical and SAR data was required for AFS mapping in the ROI. Contrary to the other regions, four GLCM texture parameters for the VH polarization of S1 was significant for the classification of the AFS. This could be due to the fact that S1 is more sensitive to higher biomass level as we will see in the following section. An overall accuracy of 89% was achieved. Because of the large number of AFS in the region, the three most common AFS were considered namely apple ring (*Acacia albida*), African locust bean (*Parkia biglobosa*)

and shea trees (*Vitellaria paradoxa*) were considered while the rest was labeled as others. AFS based on apple ring trees were the most accurately detected with an accuracy of 97% followed by others 96%. The African locust bean which is the dominant tree in protected areas showed and accuracy of 91%. However, shea trees, the main AFS in the region, was associated with the lowest accuracy on the map (89%). This is explained by the fact that since all the AFS are agricultural farms, they are shea trees in almost every AFS because its fruit is a major component in the local diet. On the map, shea trees are associated with other AFS including apple ring, locust bean and fallows. Moreover, the probability maps showed overlapping of shea trees mainly with apple ring and others. Despite the economic importance of shea, research have shown that under climate change, its spatial distribution will decrease as a response to extension of arid condition under different climatic projections in west Africa (Chabi et al., 1970; Dimobe et al., 2020). Therefore, RS could support restoration activities and the monitoring of AFS extension in the sudanian region.

4.3 Spatial assessment of the classification error

The assessment of the classification is a part of the classification workflow require to evaluate the strength of the relation between the classified map and the image on the ground. Generally, it uses a confusion matrix where feature classes on the map are compared with the landcover at different point. From this matrix, the overall accuracy of them model and other metrics are calculated. One limitation associated to the above-mentioned method is that is does not provide any spatial information about the error. For the estimation of the classification error at pixel level, the probability of prediction was used to assess the level of heterogeneity. The Shannon entropy was proposed as a methodological approach to quantify the classification error on the map. It is one of the most popular methods which uses the prediction strength (class probability) as a proxy for measuring uncertainty (Dehghan & Ghassemian, 2007; Loosvelt et al., 2012). Other methods such ignorance uncertainty, α-quadratic entropy and maximum probability which have been successfully used in remote sensing to detect regions of confusion on the map are mainly applicable for subpixel (fuzzy) classification (Giacco et al., 2010; Stehman, 1997). The entropy map was classified using thresholds of purity which separate good pixels from error (mixed pixels). This approach has two related shortcomings: firstly, good pixels are not pure pixels as they still have integrated level of impurity and could be misclassified pixels. Also, accurately classified pixels could be labelled as error. This is particularly true in complex landscape such as AFS where

the spatial and spectral resolution of open-source data remain too coarse to appropriately capture the difference between different AFS (Filella, 2018). Therefore, the approach will not perfectly capture the uncertainties on the map. However, as the threshold is derived from field measurements, the resulting error maps will significantly reduce the confusion between the AFS in the ROI. This approach was used to assess the classification error in different climatic region of west Africa.

The classification error was found to be larger in the Sudanian and Guineo-Congolian regions compared to the Guinean region. The fact that the AFS (cashew and mango) in the Guinean region are planted in a regular manner result in a very low classification error in the area. However, for irregular plantations or AFS with mixed trees, the classification error is higher at moderate resolution (10 m). The threshold derived from the field plots was varying from one AFS to the others, ranging for example from 0.35 to 0.49 in the Sudanian region. The estimation of areas using the entropy threshold value from the field plots (reference threshold) suggested that the error represented 56.1% of the total area in the Sudanian region, and 54.6% and 19.9 % in the Guineo-Congolian and Guinean region respectively. Acknowledging that field measurements are difficult to get, different threshold was evaluated, and it was found that the optimum threshold value was found to be between 0.3 and 0.4 in the Guinean and Guineo-Congolian region, while a threshold value between 0.4 and 0.5 was optimum in the Sudanian region. It was found that lower values overestimated the classification error while higher values underestimated the error. The spatial autocorrelation was assessed in the error maps using GWR. Evidence of spatial autocorrelation in the error would suggest the predictors' coefficients for the classification error are not constant but vary across the map (local predictor with a small bandwidth). This situation was observed in the Guineo-Congolian region when a threshold of 0.5 was used to generate the error map. Because the error at this threshold is underestimated, the GWR showed evidence of spatial correlation of the classification error. On the contrary, no spatial autocorrelation suggests that the predictors' coefficients of the error are constant across the map (Comber et al., 2020). It was found that the classification error was stationary for the optimum threshold, and no spatial autocorrelation was detected in the classification error. The approach used to improve the classification was to remove mixed (error) pixels from the classified map. During the process, it was noticed that well classified pixels was removed. This effect referred to as information loss, was higher in mango (33.9%), oil palm (30.8%), rubber (23.7%), cashew (21.9%) compared to the African locust bean, cocoa (4.9%)

and shea trees (4.8%). For relevant AFS such as cocoa plantations and shea trees which have a larger ecological and economic impacts, the approach scored a loss of less than 5% of the original classification. This could be therefore integrated in the classification workflow for monitoring those AFS by reducing the error and conserving 95% of the class information.

4.4 Protected areas

Another interesting aspect related to mapping AFS in west Africa is their relation and interaction with protected areas. In fact; agriculture is acknowledged as the main driver of deforestation in West Africa, mainly AFS. As a matter of fact, cocoa farming is the leading cause of deforestation in the Guineo-Congolian and cashew in the Guinean region (Rege et al., 2022; Sabas et al., 2020; Yin et al., 2023). According to recent studies, it was found that cocoa farming has encroached into protected areas. Abu et al. (2021) showed that 18.2% of protected areas in the region (about 5649 ha) were converted into cocoa plantations in 2019. Acknowledging the contribution of cocoa farming to deforestation, the governments in west Africa especially of Côte d'Ivoire and Ghana and the world's leading cocoa and chocolate compagnies agreed to end deforestation and promote forest restoration and protection in cocoa supply chain. Under this initiative also known as cocoa and forest initiative, 28 million trees were planted for the purpose of forest regeneration in Côte d'Ivoire, resulting in about 9 448 ha of degraded forest that was restored (Von Maillot, 2020). In the same report, it is recorded that cocoa and chocolate companies distributed 11.3 million non-cocoa trees for the development of agroforestry in the region to promote sustainable cocoa farming. Effort on landscape restoration is a good point as far as climate change is concerned, but it also improves the economic life of the farmers, since income is one of the major drivers behind the pressure of deforestation. Monitoring the supply chain for cocoa farm is therefore the most important aspect especially in the light of the new EU deforestation supply chain that guaranty premium price for cocoa beans harvested on deforestation-free farms. Nowadays, the cocoa farming in west Africa have reached a 72% traceability in their direct supply chains.

The AOI of the Guineo-Congolian covers the northern portion of the TNP. The approach used for the detection of encroachments consisted of allowing the algorithm to classify the protected area into different AFS, with the idea that encroachments would be associated with a very low classification error. As expected, the error assessment revealed that the entire region was entirely constituted of mixed pixels regardless of the threshold values. After the map has been improved

by removing error pixels, evidence encroachments were detected in the TNP. However, when considering the average size of cocoa plantation (about 2ha), those detections within the boundaries of the park where not significant. This result was supported by the management reports of the TNP which claimed no human activities within the boundaries of the park (Bitty et al., 2015; GIZ, 2020; Riezebos et al., 1994). Moreover, in situ verification during field campaigns confirmed the information presented in the management reports. Therefore, the AFS encroachments detected within the TNP could be attributed to the shortcomings of the approach or could be artefacts related to the fact that a composite image was used as input data.

In the Sudanian region, it was observed that protected areas are mainly covered by African locust bean trees. It is one of the most important multipurpose agroforestry trees in Sahelian region because of its commercial and consumption value, and it is the most appreciated indigenous species across ethnic and gender groups (Fischer et al., 2020). In the region of interest, the protected area was converted into AFS, mainly the African locust bean because of the socioeconomic benefits. As previously acknowledged in different part of West Africa, agriculture is the major threat both for parklands and protected area. It is reported in the literature than the management of AFS in the region depends on the social status of the farmer, where migrant farmer is less likely to install and manage AFS. It was also found that AFS near protected areas had more stable structural parameters, higher species richness and natural regeneration rate compared to AFS far from protected area (Zoungrana et al., 2023). AFS are therefore more likely to be preserved compared to natural woodlands which is often perceived as available land for agriculture.

4.5 Carbon stocks in west Africa

In carbon studies, carbon stocks are derived from the estimation of the biomass using a conversion factor of 0.5, where half of the measured biomass correspond to pure carbon stock. This is particularly applicable in natural forest ecosystems however, in AFS because of the tree species and the land management among other reasons, the conversion is often lower than 0.5 and varies from one AFS to the other (Nair & Nair, 2014). The study uses the biomass as an indication of carbon stocks in different AFS, but only the standing biomass (AGB) was considered. In fact it is well known that the larger portion of carbon in an AFS is stored in the soil, and some studies reported that the soil organic carbon was four time higher than the standing biomass in certain AFS (Thangata & Hildebrand, 2012). In this research, the carbon pool to be investigated was determined

by the tools and methods. In fact, RS data was the main data source used throughout this research and has its inherent limitations such as the unavailability of opensource data accurate soil mapping. Therefore, only the AGB was considered, which is the most important layer in the carbon cycle which allows the conversion of atmospheric carbon (CO_2) into biomass and soil carbon.

Impact of climate on carbon stocks

The importance of climatic stratification was assessed by comparing the results of carbon estimation in West Africa before and after applying a climatic stratification. It was found that the stratification of the study area into different climatic zones was crucial for biomass estimation in west Africa. In fact, regional or national studies tends to overlook the effect of climatic conditions which have a significant impact on the estimated AGB level in AFS (Balima et al., 2021). The analysis revealed that the prediction error was reduced by 31.2% and 4.5% for the Guineo-Congolian and Sudanian region respectively, but was increased by 52.3% in the Guinean when field measurement was used as reference data. The estimations based on GEDI L4A showed that the prediction error was reduced by 36.6% and 34.8% in the Guineo-Congolian and Guinean region respectively but was increased in the Sudanian region by 17.4%. In most cases, it was found that regardless of the reference data used stratification resulted in a more accurate estimation of the AGB, with different level of uncertainties at each region.

Remote sensing and reference data

Optical and SAR data were used as predictors of AGB while field measurements and GEDI L4A predictions were considered as reference data. S2 data was found to be more sensitive to biomass compared to SAR data for all climatic regions and for all reference data. Similar results were reported in AFS and forest where vegetation indices derived from S2 were better explanatory variables of the variance in AGB (Chang & Shoshany, 2016; Nuthammachot et al., 2020, Forkuor et al., 2020). Also, S1 showed a better performance in the Guinean and Sudanian region compared to ALOS based on the prediction error and the accuracy of prediction (R^2). In the Guineo-Congolian region, it was observed that ALOS performed better than S1. When combined, it was found that S1 + S2 gave the highest prediction score and the lowest prediction error in all the climatic region and for all reference data. This was in line with the literature that suggested that

the combination of optical and SAR data result in higher accuracies both for landcover classification and for biomass estimation (David et al., 2022; Nuthammachot et al., 2020).

The GEDI L4A product provides prediction of the AGB that could be used as reference data. it was found that in the Guineo-Congolian region, an accuracy of 64% was achieved with S2 data. this prediction is relatively low compared to when field measurement is considered. The prediction error is reduced by 90% going from 41.28 to 4.12 and the prediction accuracy increased from 64% to 90%. In the other climatic regions, the biomass predictions suggested that when using the predictions were worse than guessing. GEDI L4A are therefore not usable in those regions. When using the GEDI L4A product, the prediction error was found 8.94 times higher than the error level derived from field measurements. This could be explained by the fact that AGB predictions in the GEDI L4A product were generated using models that were calibrated with forest tree data. As a matter of fact, in ecosystems with high tree density such as forests, the AGB predictions from the GEDI L4A product were more accurate (Duncanson et al., 2022; Leite et al., 2022). In addition to the remote sensing variables, another important parameter in biomass modelling is the selection of the best allometric model for the conversion of field measurement into biomass. For this conversion, the pan-tropical allometric equation proposed by Chave et al. (2014) was not used, rather a mixed-species model which was developed locally was considered (Aabeyir et al., 2020). To validate their allometric model, Aabeyir et al. (2020) compared the predictions derived from both allometric equations which was found to be equivalent, and therefore could be used following the GPG of IPCC. Moreover, the model showed a higher mean value for AGB predictions in West Africa compared to the one from Chave et al. (2014), and all the species that were used to develop that model was found in AFS across West Africa.

AGB estimations in West Africa

The AGB estimations in AFS showed that, in cocoa plantations, the AGB level was 12 times lower than the average AGB in cocoa agroforestry (Asigbaase et al., 2021; Ballesteros-Possú et al., 2022). Low levels of biomass were found in Côte d'Ivoire because cocoa is grown in pure stands, also known as full sun cocoa, where all the shade trees are removed. Full sun cocoa gives a higher productivity per hectare compared to agroforests, allowing the farmers to have two harvest per year (Tondoh et al., 2015). In similar studies, cocoa trees were associated with forest trees, which explain the observed higher AGB level. This pointed out that for a sustainable cocoa production

system, more trees should be added to existing cocoa plantations (Tondoh et al., 2015). Companion trees (tree components in an AFS) also played an important role in the AGB level of a system. In the Sudanian region, the average AGB level in the AFS was 4.7 times higher than in cocoa plantations, even though cocoa plantations have 10 times more trees. It was found that the diameter (R^2 = 0.45) and the height (R^2=0.13) of the trees were more important to the level of AGB than tree density (R^2 = 0.1). The same conclusion was found in the Sudanian region, diameter and height was reported to describe 69% and 28% of the carbon variation respectively in different AFS in Burkina Faso. The association of forest trees such as the white silk-cotton tree (*Ceiba Pentandra*) or kola tree (*Kola accuminata*) could improve the carbon level in cocoa plantations (Zomer et al., 2022). Concerning the prediction accuracies of AGB in AFS, rubber and cocoa plantations in the Guineo-Congolian region, and cashew and mango in the Guinea region were found to have low accuracies at the plot level. A plausible reason could be related to the sampling scheme, as the sample size was not sufficient to capture the diversity between those classes. Increasing the sample size has been reported as a way to reduce the prediction error in AGB estimation (Araza et al., 2022; Zomer et al., 2022). However, a larger sample size does not guarantee a lower prediction error, as it was demonstrated that the similarity in the spectral response in AFS resulted in higher error, especially when open-source remote sensing is used (Filella, 2018; Kanmegne Tamga et al., 2022). The spatial assessment of the prediction of AGB should be associated with the Carbon map, to report the area where the estimation could be affected by error associated with the methodological approach. Such transparency is required by the GPG of the IPCC and is crucial for carbon estimation to be considered in the MRV process.

4.6 Biodiversity in AFS

Biodiversity is an important element for the assessment of the health as well as the sustainability of a given ecosystem. It refers the variability among living organisms, including genetic and structural difference between individual and within and between species. As far as climate change is concerned, biodiversity strengthens the resilience of natural systems towards extreme events such as droughts, storms or wildfires (AparnaRathore & Yogesh, 2013). In general, LULUCF leads to a decrease of the biodiversity mainly because it is intimately associated with deforestation. Moreover, the production system of cash crops, which is a major production system in West Africa (palm oil, cocoa, rubber, cashew and mango) is mainly a monoculture. Yet, the sustainability of

AFS depends significantly on the biodiversity. It was reported that the sustainable cocoa farming requires among other element a variety of tree species combined with cocoa trees. In this consideration, cocoa agroforestry is more sustainable than full sun cocoa, but also less productive. There is therefore a trade-off between biodiversity (sustainability) and profitability.

In west Africa, there was a need to analyse the biodiversity in each AFS and investigate their relation to carbon sequestration. Biodiversity in this case was restricted to tree species because of their ability for carbon sequestration. The biodiversity and the Simpson's indices were considered as proxies to assess the biomass level in different AFS. As expected, crop plantations which are mainly monocultures are associated with the lowest biodiversity. In West Africa, rubber and palm oil plantations are pure monoculture. Before their establishment, all the vegetation is removed for the trees to grow freely. It is only in cocoa and cashew plantations that trees are purposely maintained on farm for other services, therefore increasing the biodiversity. The literature reported that biodiversity could be improved by the adoption of agroforestry rubber plantations, which were found to provide modest biodiversity benefits compared to monoculture without compromising the yield (Warren-Thomas et al., 2020). The main benefits included butterfly, bird and reptile richness which increased with the height of herbaceous vegetation. In rubber plantations, herbaceous plants are intentionally removed to limit the risk of encountering dangerous reptiles, because the farmers do not use appropriate personal protection equipment such as rubber shoes. On the other hand, cocoa, cashew, and mango plantations have similar levels of biodiversity with about 2-4 species/ha. Even though cocoa production is the main driver of biodiversity loss in West Africa, it is also regarded as environmentally preferable to any other land use system, primarily for its potential to conserve forest trees, birds, ants and other lifeforms (Asare, 2006). In Côte d'Ivoire, the cocoa production system which is full-sun cocoa instead of cocoa agroforests, doesn't allow the presence of trees, instead shade is momentarily provided in the early stage by banana trees. The biodiversity level is higher in multipurpose trees on agricultural land, with a richness level ranging from about 2 species/ha in shea butter plantations up to 5 species/ha in fallows in the Sudanian region. At first, it seems that the higher the biodiversity in an AFS the higher the AGB level. But, even if the relationship between AGB and biodiversity shows a positive correlation between the two variables, this relation is not significant in AFS of West Africa, suggesting that shifting the resilience and sustainability of a system does not result in an improvement of the carbon sequestration capacities. The findings of this research demonstrate that AGB level is related

to the size of trees (diameter and height) even if it is a single tree species. These findings are supported by the existing literature on natural forest, where it was found that increase in the AGB level resulted in the decrease of the biodiversity due to the competition for sunlight (Pesola et al., 2017). Also, the relation between AGB and biodiversity is reported to be dynamic, and it was found that it is strong in the early stage of the tree development, but weak later on, as a result of positive selection (Lasky et al., 2014).

It is clear that the biodiversity level does not account for carbon sequestration; yet, it has an important contribution in improving the resilience of cocoa farming. In fact, the cocoa swollen shoot virus disease is the major threat for cocoa productivity in west Africa. At the moment, there is no available treatment and the only solution is to cut down trees that are visibly infected. Very few studies have investigated the contribution of biodiversity to the resilience of cocoa farms. Yet, it is reported that while resistance breeding and mild strain cross-protection may reduce the swollen shoot disease by 30 percent, diversification measures including shading (agroforestry) and barrier cropping could reduce the infection between 40 to 85 percent (Andres et al., 2017). Further research showed that AFS with a tree shade around 50% (between 14 and 17 trees/ ha) in cocoa plantations is the optimal configuration to balance between the symptom severity of the swollen shoot disease and the reduced cocoa yield until disease trees are replaced by more resistant trees (Andres et al., 2018). Moreover, it is reported that high exposition to sunlight, which is the main characteristic of full sun cocoa, is one of the major factors responsible of the severity the swollen shoot disease. Increasing and maintaining the biodiversity in AFS is important to enhance the resilience of plantations but also increases the productivity of by products as it is the case in cashew plantations. Bees are one of the most common managed animals in cashew plantations because they are attracted to the flowers of the trees allowing apiculture which is practiced by about 79% of the cashew farmers in Cote d'Ivoire. The product from this side activity represents and additional source of income, and a valuable source of nutrients to supplement the diet and traditional pharmacopoeia.

4.7 Carbon dynamics in AFS

Another interesting aspect in modelling carbon sequestration in AFS is to understand carbon flows and dynamics across the systems. Understanding carbon dynamics informs on the contribution of AFS to climate change as it helps identifying those that behave as carbon sources (emitter of carbon

in the atmosphere) or carbon sinks (remover of carbon from the atmosphere). A good point to keep in mind is that AFS are not natural ecosystems, rather a particular type of man-made land use where natural trees are allowed to develop (to fulfill a specific function). In that sense, the dynamic of carbon stocks within such setting is very much limited to from one year to the other and could rapidly change from woodlands to bare soil if a cashew farm is converted into agricultural land for cotton production for example (less like to happen but possible). This being said, this section is exploring the potential of remote sensing to capture the trend in biomass dynamic under "normal" management conditions and give an impression on the optimal AFS to consider to tackle climate change.

The approach used is a well-known approach which is often used in climatology and yield modelling in agriculture under the name anomaly detection. Anomaly detection is a processing approach in remote sensing with the purpose of identifying pixels whose spectrum are significantly different form the surrounding. In the case of a time series it helps identifying pixels with "abnormal" values, that is away from the general trend (often the mean). It is a very efficient process, but the results are affected by noise and therefore require specific technics using algorithm such as local Reed-Xiaoli (LRX) (Lindner et al., 2023). For this research the approach was based on comparing the pixel value with the mean value of the same location over the considered period of time (2017 to 2021). The standard deviation was used as a threshold value to minimize the noise from one year to the other. Using this approach locations with a biomass level higher than the mean value were considered as sinks for that year, while locations with lower biomass level were reported as carbon sources. In the literature, a robust assessment of carbon/biomass dynamic is a more complex process which should include factors related to biomass gain and loss including tree growth, accrue biomass over time, tree mortality, disturbances and tree recovery among others (Wulder et al., 2020). Therefore, depending on the factor to monitor, the optimum time frame should be selected between 8 years in studies interested in biomass recovery, up to 33 years for long term studies (Lasky et al., 2014; Pesola et al., 2017; Wulder et al., 2020). These requirements were mainly implemented on studies in natural forest environment, with limited anthropogenic interventions. AFS in the contrary have a different lifespan, going from a year to a maximum of around 25 years for crop plantations. Therefore, for most AFS, five years is a sufficient time-frame window to capture the trends of carbon flux, since AFS are dynamic system by themselves compared to natural forests.

Talking about the AFS, cocoa and rubber in the Guineo-Congolian region, cashew and mango in the Guinean region as well as all of the AFS in the Guinean region were considered. Cocoa plantations are larger carbon sinks compared to rubber plantations. However, there is a lot more dynamics in cocoa plantations while the biomass in rubber plantations remain constant, increasing consistently across time. This could be explained by the fact that management practices in rubber plantations does not included practices such as pruning, removing/adding trees which is the case in cocoa farm. In fact, cocoa trees are often pruned to improve the production or for regeneration. Also because of the swollen shoot disease, certain trees are often removed and replaced. The proportion of carbon sinks in the Guineo-Congolian is increasing overtime time. This could be improved by the introduction of larger trees in cocoa plantations which will result in a lower annual fluctuation of carbon stocks. In Cashew and mango plantations, the biomass level tends to be constant over time. This could be explained by the fact that when the trees reached maturity, the biomass is maintained. Also, the management practices do not include stimulation biomass growth. In fact, biomass has to remain low and constant as it is reported that there is a negative relationship between biomass and fruit production: the higher the biomass level, the lower the fruit production (Rosati et al., 2018). However, AFS referred to as tree on farm (farm), there is an increase of biomass over time suggesting that farms in the Guinean region are better sinks compared to mango and cashew farms. The overall region appears as a carbon source in west Africa, where the biomass decreases over time. The conversion of forest and other wooded land into cashew and mango plantations is responsible of larger amount of carbon emission in the atmosphere. The argument of cashew and mango plantations as a solution for climate change is not valid, considering the report of their carbon stock dynamic.

In the sudanian region, AFS based on shea trees and African locust bean were considered because they are the most abundant form of land management in the region. It was found that most of the region was having a very low level of biomass in early 2017. The proportion of carbon sinks in the region have increased significantly for both AFS, but with larger proportions for the African locust bean. Sinks in AFS based on shea trees increase in smaller size, revealing patterns of smallholder farming, while African locust bean's AFS sinks cover larger area. This could be the result of a national program or a kind of organisation activities. This assumption agrees with the spatial distribution of the AFS in the region, where African locust bean is the main tree encountered in protected areas. According to the centre of International Forestry research, The African locust

bean is more than just a tree as it is part of the local diet, provide additional household income, provide fodder for the cattle and improve soil fertility. Looking at the evolution of carbon sinks in the sudanian region, it appears that biomass in the region increases over time across the AFS, allowing those systems to sequestrate more CO_2. Based on the results that were obtained in the sudanian region, it seems clear that reforestation program should consider the integration of indigenous forest tree species due to their socio-economic benefits in addition to the environmental aspect.

Chapter 5

Conclusions and Recommendations

Carbon sequestration modelling is an important thematic in the context of climate change because it provides quantitative evidence of the contribution of anthropic activities to global warming. Based on the deforestation rate, West Africa is significantly contributing to carbon emission, and is one of the regions in Africa where the impact of climate change is expected to be more severe. The main driver of deforestation in the region is agricultural extension, primarily the conversion of forested land into agroforestry systems (AFS) for cash crop production including cocoa, rubber and cashew among others. An AFS is a land management practices where the interaction between forest trees and crops are managed on the same land unit. Some of those systems include crop plantations (cocoa, rubber and cashew) and tree on farms. Because of the importance of the tree component in the system, AFS is acknowledged as a viable solution for climate mitigation based on their potential for carbon sequestration. However, a workable approach for the AFS mapping using open source remote sensing (RS) data is still missing, resulting in classified map with a higher level of classification error. Also, existing methodologies for carbon estimation derived from forestry are not applicable in AFS as they need to be adapted. Therefore, the carbon stock level and the potential of carbon sequestration of the different AFS in West Africa is unknown. The aim of this research was to propose an integrated methodological approach for modelling carbon sequestration of different AFS across the climatic regions of West Africa using remote sensing. This goal was organized around three objectives: (i) provide an accurate map of the different AFS in west by modelling the spatial distribution of the classification error; (ii) estimate the carbon stock of AFS in different climatic regions across west Africa using remote sensing and (iii) assess the carbon dynamic in AFS by evaluating the spatial distribution of carbon sources and carbon sinks within AFS in west Africa. This research is a significant contribution to the development of a valid scientific methodology for the estimation of carbon sequestration in AFS, which is the main land use in west Africa, to evaluate their contribution to climate change and support their integration into national emission reduction programmes and emission reduction program such as REDD+.

Mapping AFS in west Africa

AFS plays an important economic and sociocultural role in the livelihood of farmers across the different climatic region of west Africa. In Cote d'Ivoire, they are mainly represented by rubber and cocoa plantations in the southern part (Guineo-Congolian region), which are often established

on previous secondary forest for an average period of 30 years, while in the northern part of the country (Guinean region), cashew and mango plantations represent together about 30% of the AFS, the main AFS being trees on agricultural farm. In Burkina Faso, the main AFS was found to be shea trees, whose fruits are an important component in the local diet and an additional source of income. As far as the classification is concerned, an overall accuracy of 89% was obtained both in the Guineo-Congolian and Sudanian region and 91 % was reported in the Guinean region. In the Guineo-Congolian region, the highest classification error was reported in cocoa plantations, misclassified as rubber or oil palm plantations using 10 m resolution RS data. In the sudanian region on the other hand, the highest level of classification error was reported for Shea trees AFS which showed a higher confusion towards apple ring (*Acacia albida*) and African locust bean (*Parkia biglobosa*). The spatial assessment of the classification error revealed that the Shannon entropy was found between 0.35 and 0.49. About 55% of the ROI in the Guineo-Congolian and Guinean region, was associated with classification error. The Geographically Weighted Regression (GWR) showed no spatial autocorrelation in the classification error. However, when using a very small threshold (0.2 in this study), there was an overestimation of the classification error leading to the detection of spatial autocorrelation in the Guineo-Congolian region. By removing pixels with a high classification error (mixed pixels), the information loss in the main AFS was around 5%.

Carbon stocks in AFS

The combination of optical and SAR data from the Sentinel mission was found to be more sensitive to the biomass level across different AFS in West Africa. Moreover, the prediction error was reduced about 30% when carbon estimation was carried after a stratification into different climatic regions. Field measurements was identified as the best source of reference data for the carbon estimation in AFS, even though an accuracy of 64% was obtained in the Guineo-Congolian region using GEDI L4A product as reference data. But, the prediction error was about 9 times higher than predictions based on field measurements. The estimation revealed that cocoa plantations have the largest carbon stock in the Guineo-Congolian region with 7.51 ± 0.6 Mg / ha (R^2 =0.91). In the Guinean region cashew showed 13.78 ± 0.9 Mg / ha (R^2 = 0.82), But the largest carbon stocks were found in the sudanian region with an average of 34.2 ± 18 Mg / ha (R^2 = 0.86). It was found that the biometric parameters of the tree component in an AFS (diameter and height) were the most

important factor, describing about 70% of the carbon variation. The biodiversity in AFS showed no significant relationship with carbon stocks. However, played a significant role in the resilience of crop plantations as it could reduce the infection to up to 85% for the swollen shoot cocoa disease in west Africa.

Carbon dynamics in AFS

Cocoa, rubber in the Guineo-Congolian region, cashew and mango in the Guinean region and all the AFS in the Sudanian region showed interesting performance as carbon sinks. First in the Guinean region, cocoa plantations are larger carbon sinks compared to rubber plantations. However, the carbon dynamic is higher in cocoa plantations with large decrease in biomass level between year due to management practices. The trend in carbon stocks showed that the proportion of carbon sinks is increasing in the region, suggesting that AFS are storing more carbon over time. In Cashew and mango plantations in the Guinean region, the carbon level tends to stagnate as biomass is inversely related to fruit production. The trend in the Guinean region showed that the biomass level in AFS is decreasing overtime, suggesting that cashew and mango are not good carbon sinks, rather behave as carbon source. In the sudanian region, Shea trees and African locust bean are the major carbon sinks. Even though both increased over time, it was observed that African locust bean grew faster than shea trees. The overall trend in the region showed that more carbon is stored in the Sudanian region over time.

Paths for improvement

Modelling carbon sequestration of AFS in West Africa using open-source RS data is challenging. However, the proposed methodology was able to produce accurate and reliable results. Some of the issue that needs to be addressed are related to:

a) The resolution of the RS data. Agroforestry systems are complex landcover because of their composition. As such, the accurate delineation of field boundaries is a constant issue due to the phenomenon of mixed pixels which is by far the most important challenge in AFS mapping. The spatial and spectral resolutions offered by open-source data including the Sentinel mission remain insufficient to ensure a very high output quality and the end of the process. For this reason, VHR data is often considered in research and project. There is a need for open-source data with higher spatial and spectral accuracies to reduce the level

of classification especially if the final map is to be used for the evaluation of mechanism such as REDD+ to support supply chain analysis in the framework of the EU deforestation law for instance.

b) The classification processes. This is an important part of the workflow where the errors could be reduced. Future studies could use more field data which could be collected with direct method during field campaign or indirectly using VHR data at a subpixel resolution. Detailed field information combined with more powerful machine learning techniques including deep learning could significantly reduce the prediction error on the final classification. Also, for biomass measurement, high resolution SAR data could be used in addition to field measurement to get accurate estimations of biomass especially in AFS with low tree density.

c) The classification error assessment routine. From the analysis it was found that even though the classification was corrected to a certain extent, the final map was still containing some classification error. Error assessment routines other than the Shannon entropy need to be explore to identify the most appropriate approach for AFS.

d) Biomass to carbon conversion factor. A usable conversion factor of biomass to carbon is still missing. For this reason, the carbon was presented in term of biomass to avoid conversion error. Studies should be carried on trees in AFS to establish the existing relation between biomass and carbon content. Useful studies have already improved the allometric equations, and the research should be pushed more into that direction.

e) Long term study of carbon in AFS. As far as carbon sequestration is concerned, there is a need for long term study to understand the life cycle of the main AFS in West Africa, with the aim of capturing the development (growth and production) of all the component in the AFS in order to create and/or used more accurate carbon model such as the CO2FIX model, which gives not only the carbon stocks, but also the carbon sequestration expressed in terms of Mg / ha / year.

Recommendations

The findings of this research demonstrated that AFS in west Africa have a real potential for carbon sequestration on the one hand, and on the other remote sensing data could be used to quantify and monitor the carbon stock levels of AFS in different climatic regions. The proposed methodology

could be used as good practice guidance as it allowed a realistic estimation combined with the quantification of the error associated with the approach. To improve the performance of carbon sequestration in West Africa, it is necessary to

- Increase the density of forest trees in AFS. As it was demonstrated in this document, diameter and height are the most important parameters to influence the biomass level of AFS. In cocoa plantations, there is a need to move from full sun cocoa farming back to cocoa agroforests. Projects such as the Vision for Change (V4C) led by the World Agroforestry center (ICRAF) in west Africa should be multiplied, because cocoa is the AFS in west Africa with the largest potential for carbon sequestration. Forest trees with high values (socioeconomic or cultural) should be introduced in cocoa farms, while industries around derivatives from those trees (gum or fruits) should be promoted to ensure diversification in household income and prevent further deforestation.
- Increase biodiversity in cocoa plantations. In addition to improving carbon biomass, introducing forest trees in AFS will also increase the biodiversity. Biodiversity is a major aspect for the resilience of cocoa plantations. In cote d'Ivoire, cocoa farms are destroyed because of the swollen shoot disease with severe economic consequences. In addition to resistant cocoa tree varieties, it was demonstrated that a higher biodiversity level in cocoa plantations could be a more economical solution. Therefore, efforts should be put in place to provide adequate trees and promote good practices among local farmers.
- Limit cashew and mango production. The results revealed that cashew and mango production are not a good solution as far as climate change is concerned, as they are behaving more as carbon source than carbon sinks. Over time, the biomass level in cashew plantations showed a decreased, releasing more carbon in the atmosphere. This is explained by the wood density of those trees which is significantly lower than those of forest trees. As a solution, research should be oriented toward the impact of introducing forest trees into cashew and mango plantations, while existing forest should be protected.

A good implementation of these recommendations could improve carbon sequestration level in AFS, increasing therefore their contribution to national emission reduction efforts, making them eligible for financial compensation under REDD+ mechanism.

Appendices

Appendix 1: Sources and materials

The methodology of this research project was based on field data collection and the use of satellite data. The field campaign was carried in the framework of the WASCAL-DE-Coop in collaboration with the research institute including ICRAF/CIFOR in Côte d'Ivoire and WASCAL in Burkina Faso as presented in the following table. The satellite data used are open access and freely accessible online, and the data processing was based on existing methodologies available in the literature.

Institution	Contribution	Contact
German Federal Ministry of Education and Research (BMBF)	via the project carrier at the German Aerospace Agency (DLR)Support through the WASCAL-DE-Coop Project (KFZ: 01LG1808A)	Dr. Michael Thiel (Project leader) michael.thiel@uni-wuerzburg.de
World Agroforestry (ICRAF/CIFOR) Abidjan-Côte d'Ivoire	Support for field data collection by providing field assistants.	Dr Jules Bayala (Supervisor) j.bayala@cgiar.org
West African Science Service centre on Climate Change and Adapted Land Use (WASCAL)	Support for field data collection by providing field assistants	Dr. Michael Thiel michael.thiel@uni-wuerzburg.de
Department of remote sensing, Institute of Geology and Geography, University of Würzburg	provide a working place including field equipment for data collection (GPS, altimeter and measuring tape)	
Graduate School of Science and Technology (GSST)	Provide mentors to carry out the research projects. They help in the conceptualization, the development of the methodology and the review of the publication and the dissertation	Prof. Dr. Tobias Ullmann Tobias.ullmann@uni-wuerzburg.de

Appendix 2: List of publications

1. Kanmegne Tamga, D., Latifi, H., Ullmann, T., Baumhauer, R., Thiel, M., & Bayala, J. (2022). Modelling the spatial distribution of the classification error of remote sensing data in cocoa agroforestry systems. *Agroforestry Systems*. https://doi.org/10.1007/s10457-022-00791-2

2. Kanmegne Tamga, D., Latifi, H., Ullmann, T., Baumhauer, R., Bayala, J., & Thiel, M. (2022). Estimation of aboveground biomass in agroforestry systems over three climatic regions in west Africa using Sentinel-1, Sentinel-2, ALOS, and GEDI data. *Sensors 2023, Vol. 23, Page 349*, *23*(1), 349. https://doi.org/10.3390/S23010349

Appendix 3: Credit author statement:

The table presents the contribution to all the publications listed in Appendix 2.

Terms	Definition	Author's name
Conceptualization	Ideas; formulation or evolution of overarching research goals and aims	Kanmegne Tamga D. Ullmann T. Latifi H. Thiel M.
Methodology	Development or design of methodology, creation of models	Kanmegne Tamga D. Ullmann T. Latifi H.
Software	Programming, implementation of the computer codes and supporting algorithms	Kanmegne Tamga D.
Validation	Verification, whether as a part of the activity or separate, of the overall replication/reproducibility of results	Kanmegne Tamga Ullmann T. Latifi H.
Formal analysis	Application of statistical, mathematical, computational or other formal techniques to analyze or synthesize study data	Kanmegne Tamga D.
Investigation	Conducting a research and investigation process, specifically performing the experiments, or data/evidence collection	Kanmegne Tamga D.
Resources	Provision of study materials, reagents, materials, computation resources or other analysis tools	Thiel M. Bayala J.
Data curation	Management activities to annotate (produce metadata), scrub data and maintain research data (including software code, where it is necessary for interpreting the data itself) for initial use and later reuse	Kanmegne Tamga D.

Writing – Original draft	Preparation, creation and/or presentation of the published work, specifically writing the initial draft (including substantive translation)	Kanmegne Tamga D.
Writing – Review & editing	Preparation, creation and/or presentation of the published work by those from the original research group, specifically critical review, commentary or revision – including pre-or post-publication stages	Kanmegne Tamga D. Baumhauer R. Ullmann T. Latifi H. Bayala J. Thiel M.
visualization	Preparation, creation and/or presentation of the published work, specifically visualization/data presentation	Kanmegne Tamga D.
Supervision	Oversight and leadership responsibility for the research activity planning and execution, including mentorship external to the core team	Baumhauer R. Ullmann T. Latifi H. Thiel M.
Project administration	Management and coordination responsibility for the research activity planning and execution	Thiel M. Bayala J.
Funding acquisition	Acquisition of the financial support for the project leading to this publication	Thiel M.
Overall contribution of the candidate (%)	90 %	

Appendix 4: Statement on reused materials

Some results presented in this dissertation have been peer reviewed and published in international scientific journals in partial fulfillment of the requirements of the GSST. The content of the publications and the corresponding sections in the dissertation is presented in the table below. The text from the paper was not reproduced *ad verbatum* in the dissertation, and some figures were resused as specified in the table. All the co-authors (Ullmann T., Latifi H., Bayala J. and Thiel M.) have been consulted and gave their approval for reusing the published results in the thesis. Concerning the copyright and licensing, it is stated on the website of both journals that: "*copyright is retained by the authors. Articles are licensed under and open Access Creative Commons CCG BY 4.0 license (…). In addition, the article may be reused and quoted provided that the orignal publised version is cited*".

Title of the article	Content of the publication	Reference in the thesis
Modelling the spatial distribution of the classification error of remote sensing data in cocoa agroforestry systems	The aim of the paper was to propose a workflow to detect misclassified pixels in the mapping complex landscapes such as the cocoa agroforestry systems (AFS) in south of Côte d'Ivoire. The topic covered by this article corresponds to a subset of the first objective of the dissertation.	The materials and methods are presented in chapter 2, in sections: 2.1, 2.2.1 and 2.3: (description of the study area) 2.5.1 (field data collection) 2.7.1.1; 2.7.2 and 2.7.3 (remote sensing data) 2.8.2 (data processing) The published results are found in chapter 3, partly found in section: 3.1.1 (mapping) 3.2 (error assessment and Improving the classification)
	Illustrations: <u>Figures</u>: (1) study area, (2) classification, (3) error map and (4) improved classification <u>Tables</u>: (1) GLCM texture parameters and (2) Vegetation indices formulae <u>Pictures</u>: No pictures	<u>Figures</u>: No figure from the publication was resused. <u>Tables</u>: the table was adapted and correspond to table 7 and table 6 in the dissertation respectively. <u>Pictures</u>: No picture.

	Formulae: Equations: (1) Shannon entropy and (2) GWR	The equation was reused in the dissertation, and correspond to equation 2 and -3 respectively.
Estimation of aboveground biomass in agroforestry systems over three climatic regions in West Africa using Sentinel-1, Sentinel-2, ALOS and GEDI data	The aim of the paper was to evaluate the performance of different satellite data for the estimation of the the aboveground biomass in west Africa and to compare the biomass density of different AFS and climatic regions of west Africa. The topic covered by this article corresponds to the second objective presented in this dissertation	The materials and methods are presented in chapter 2, in sections: 2.1, 2.2 and 2.3 (description of the study area) 2.4 (description of the agroforestry systems 2.5 (field data collection) 2.6 (remote sensing data) 2.8.3 (data processing)
		The published results are found in chapter 3, partly found in sections 3.3 (assessment of data sources and machine learning algorithms) 3.4.1 (uncertainties assessment and mapping) 3.4.1 (comparison of aboveground biomass across AFS)
	Illustrations Figures: (1) study area, (5-8) scatterplots of the predictions, (9 and 10) performance of machine learning algorithms, (11-13) uncertaincies	Figures: the figure of the study area was not used in the dissertation. The other figures were adapted and reused. The are found in the dissertation as figure 36-43 (scatterplots of predictions), figure 44 and

	mapping of biomass predictions, (14) relation between biomass and tree parameters. Tables: (1) description of AFS, (2) vegetation indices and (3) GLCM texture parameters formulae, (4) summary of the biomass estimations in different AFS. Pictures: (2 and 3) illustration of AFS, (4) illustration of field data measurement.	45 (performance of machine learning algorithms), figure 46-48 (uncertainties mapping of biomass predictions). Tables: All the tables were resused. They correspond to table 4 (description of AFS), table 6 (vegetation indices), table 7 (texture parameters) and table 9 (summary of biomass estimations) Pictures: all the pictures were reused in the dissertation, and correspond to picture 6 and 7 (illustration of AFS) and picture 9 (illustration of field data collection)
	Formulae: Equations: (1) allometric equation, (2) RMSE formula, (3) R^2 formula	The equations were reused in the dissertation, and correspond to equation 1 (allometric equation), equation 4 (RMSE and R^2 formulae)

References

(CILSS), C. inter-états de L. conte la S. dans le S. (2016). *Landscapes of West Africa: a window on a changing world*. https://eros.usgs.gov/westafrica/sites/default/files/ebook-English/index.html#p=3

Aabeyir, R., Adu-Bredu, S., Agyare, W. A., & Weir, M. J. C. (2020). Allometric models for estimating aboveground biomass in the tropical woodlands of Ghana, West Africa. *Glob Chang Biol*, *20*, 3177–3190. https://doi.org/10.1186/s40663-020-00250-3

Abdullah, M. M., Al-Ali, Z. M., & Srinivasan, S. (2021). The use of UAV-based remote sensing to estimate biomass and carbon stock for native desert shrubs. *MethodsX*, *8*. https://doi.org/10.1016/J.MEX.2021.101399

Abu, I. O., Szantoi, Z., Brink, A., Robuchon, M., & Thiel, M. (2021). Detecting cocoa plantations in Côte d'Ivoire and Ghana and their implications on protected areas. *Ecological Indicators*, *129*. https://doi.org/10.1016/J.ECOLIND.2021.107863

Acevedo-Siaca, L., & Goldsmith, P. D. (2020). Soy-maize crop rotations in sub-Saharan Africa: A literature review. *International Journal of Agronomy*, *2020*. https://doi.org/10.1155/2020/8833872

Adopo, W. A., Adolphe, M. G., Tiehi, N., Koffi, C., Kouakou, K., & Ballo, Z. (2022). Impact of Swollen Shoot Disease on the Livelihoods of Smallholder Cocoa farmers in Côte d'Ivoire. *European Scientific Journal, ESJ*, *11*, 258–258. https://doi.org/10.19044/esipreprint.11.2022.p258

Aguilar, R., Zurita-Milla, R., Izquierdo-Verdiguier, E., & de By, R. A. (2018). A cloud-based multi-temporal ensemble classifier to map smallholder farming systems. *Remote Sensing*, *10*(5). https://doi.org/10.3390/rs10050729

Ali, F., Zamir, A., Khan, I., Khalil, A. U., Umrani, A. M., & Ahmed, S. (2022). Comparative analysis of carbon stocks in different agro-forestry systems of district Mardan. *International Scholars Journals*, 10. www.internationalscholarsjournals.com

Anderson, K., Hancock, S., Disney, M., & Gaston, K. J. (2016). Is waveform worth it? A

comparison of LiDAR approaches for vegetation and landscape characterization. *Remote Sensing in Ecology and Conservation*, *2*(1), 5–15. https://doi.org/10.1002/rse2.8

Andres, C., Blaser, W. J., Dzahini-Obiatey, H. K., Ameyaw, G. A., Domfeh, O. K., Awiagah, M. A., Gattinger, A., Schneider, M., Offei, S. K., & Six, J. (2018). Agroforestry systems can mitigate the severity of cocoa swollen shoot virus disease. *Agriculture, Ecosystems & Environment*, *252*, 83–92. https://doi.org/10.1016/J.AGEE.2017.09.031

Andres, C., Gattinger, A., Dzahini-Obiatey, H. K., Blaser, W. J., Offei, S. K., & Six, J. (2017). Combatting Cocoa Swollen Shoot Virus Disease: What do we know? *Crop Protection*, *98*, 76–84. https://doi.org/10.1016/J.CROPRO.2017.03.010

Anil, K., & Roshan, D. (2021). *Shea Butter Market Size ,Share | Industry analysis 2030*. https://www.alliedmarketresearch.com/shea-butter-market-A13671

Araza, A., de Bruin, S., Herold, M., Quegan, S., Labriere, N., Rodriguez-Veiga, P., Avitabile, V., Santoro, M., Mitchard, E. T. A., Ryan, C. M., Phillips, O. L., Willcock, S., Verbeeck, H., Carreiras, J., Hein, L., Schelhaas, M. J., Pacheco-Pascagaza, A. M., da Conceição Bispo, P., Laurin, G. V., … Lucas, R. (2022). A comprehensive framework for assessing the accuracy and uncertainty of global above-ground biomass maps. *Remote Sensing of Environment*, *272*. https://doi.org/10.1016/J.RSE.2022.112917

ArcGIS. (2005). *How Spatial Autocorrelation (Global Moran's I) works—ArcGIS Pro | Documentation*. https://pro.arcgis.com/en/pro-app/latest/tool-reference/spatial-statistics/h-how-spatial-autocorrelation-moran-s-i-spatial-st.htm

Asare, R. (2006). *A review on cocoa agroforestry as a means for biodiversity conservation. Paper presented at world cocoa foundation partnership conference*. 13. https://www.researchgate.net/publication/313079119_A_review_on_cocoa_agroforestry_as_a_means_for_biodiversity_conservation_Paper_presented_at_world_cocoa_foundation_partnership_conference

Ashiagbor, G., Forkuo, E. K., Asante, W. A., Acheampong, E., Quaye-Ballard, J. A., Boamah, P., Mohammed, Y., & Foli, E. (2020). Pixel-based and object-oriented approaches in segregating cocoa from forest in the Juabeso-Bia landscape of Ghana. *Remote Sensing Applications:*

Society and Environment, *19*, 100349. https://doi.org/10.1016/J.RSASE.2020.100349

Asigbaase, M., Dawoe, E., Lomax, B. H., & Sjogersten, S. (2021). Biomass and carbon stocks of organic and conventional cocoa agroforests, Ghana. *Agriculture, Ecosystems & Environment*, *306*, 107192. https://doi.org/10.1016/J.AGEE.2020.107192

Atangana, A., Khasa, D., Chang, S., & Degrande, A. (2014). *Tropical Agroforestry*.

Balima, L. H., Kouamé, F. N. G., Bayen, P., Ganamé, M., Nacoulma, B. M. I., Thiombiano, A., & Soro, D. (2021). Influence of climate and forest attributes on aboveground carbon storage in Burkina Faso, West Africa. *Environmental Challenges*, *4*, 100123. https://doi.org/10.1016/J.ENVC.2021.100123

Ballesteros-Possú, W., Valencia, J. C., & Navia-Estrada, J. F. (2022). Assessment of a Cocoa-Based Agroforestry System in the Southwest of Colombia. *Sustainability*, *14*(15), 9447. https://doi.org/10.3390/su14159447

Bauer-Marschallinger, B., Cao, S., Navacchi, C., Freeman, V., Reuss, F., Geudtner, D., Rommen, B., Vega, F. C., Snoeij, P., Attema, E., & Reimer, C. (2021). *The Sentinel-1 Global Backscatter Model (S1GBM) - Mapping Earth's Land Surface with C-Band Microwaves*. TU Wien. https://researchdata.tuwien.ac.at/records/n2d1v-gqb91

Bitty, A. E., Gonedele, S. B., Koffi Bene, J. C., Kouass, P. Q., & Mcgraw, W. S. (2015). Tropical Conservation Science | ISSN 1940-0829 | Tropicalconservationscience.org Cite this paper as. *Mongabay.Com Open Access Journal-Tropical Conservation Science*, *8*(1), 95–113. http://creativecommons.org/licenses/by/3.0/us/.The:95-113.Availableonline:www.tropicalconservationscience.org

Boeckx, P., Bauters, M., & Dewettinck, K. (2020). Poverty and climate change challenges for sustainable intensification of cocoa systems. *Current Opinion in Environmental Sustainability*, *47*, 106–111. https://doi.org/10.1016/J.COSUST.2020.10.012

Bopp, L., Bowler, C., Guidi, L., Karsenti, É., & De Vargas, C. (2002). *ocean-climate.org A MAJOR ROLE FOR THE OCEAN IN THE EVOLUTION OF ATMOSPHERIC CO 2 The Ocean: a Carbon Pump*.

Bousbih, S., Zribi, M., Hajj, M. El, Baghdadi, N., Lili-Chabaane, Z., Gao, Q., & Fanise, P. (2018). Soil moisture and irrigation mapping in a semi-arid region, based on the synergetic use of Sentinel-1 and Sentinel-2 data. *Remote Sensing*, *10*(12). https://doi.org/10.3390/rs10121953

Brahma, B., Nath, A. J., Deb, C., Sileshi, G. W., Sahoo, U. K., & Kumar Das, A. (2021). A critical review of forest biomass estimation equations in India. *Trees, Forests and People*, *5*, 100098. https://doi.org/10.1016/J.TFP.2021.100098

Breiman, L. (2001). Random forests. *Machine Learning*, *45*(1), 5–32. https://doi.org/10.1023/A:1010933404324

Brunsdon, C., Fotheringham, A. S., & Charlton, M. E. (1996). Geographically Weighted Regression: A Method for Exploring Spatial Nonstationarity. *Geographical Analysis*, *28*(4), 281–298. https://doi.org/10.1111/J.1538-4632.1996.TB00936.X

Busquet, M., Bosma, N., & Hummels, H. (2021). A multidimensional perspective on child labor in the value chain: The case of the cocoa value chain in West Africa. *World Development*, *146*, 105601. https://doi.org/10.1016/J.WORLDDEV.2021.105601

Carsan, Orwa, S., Harwood, C., Kindt, C., Stroebel, R., Neufeldt, A., & Jamnadass, R. (2012). *African Wood Density Database*. World Agroforestry Centre, Nairobi. http://apps.worldagroforestry.org/treesnmarkets/wood/index.php#

Chabi, J. F., Gnanglè, F. O., Bello, C. P., Yabi, O. D., Ahoton, I., & Saïdou, L. (1970). Modelling the Current and Future Spatial Distribution Area of Shea Tree (Vittelaria paradoxa C. F. Gaertn) in the Context of Climate Change in Benin. *American Journal of Climate Change*, *10*, 263–281. https://doi.org/10.4236/ajcc.2021.103012

Chang, J., & Shoshany, M. (2016). Mediterranean shrublands biomass estimation using Sentinel-1 and Sentinel-2. *International Geoscience and Remote Sensing Symposium (IGARSS)*, *2016-Novem*(July), 5300–5303. https://doi.org/10.1109/IGARSS.2016.7730380

Chave, J., Réjou-Méchain, M., Búrquez, A., Chidumayo, E., Colgan, M. S., Delitti, W. B. C., Duque, A., Eid, T., Fearnside, P. M., Goodman, R. C., Henry, M., Martínez-Yrízar, A., Mugasha, W. A., Muller-Landau, H. C., Mencuccini, M., Nelson, B. W., Ngomanda, A.,

Nogueira, E. M., Ortiz-Malavassi, E., … Vieilledent, G. (2014a). Improved allometric models to estimate the aboveground biomass of tropical trees. *Global Change Biology*, *20*(10), 3177–3190. https://doi.org/10.1111/GCB.12629

Chave, J., Réjou-Méchain, M., Búrquez, A., Chidumayo, E., Colgan, M. S., Delitti, W. B. C., Duque, A., Eid, T., Fearnside, P. M., Goodman, R. C., Henry, M., Martínez-Yrízar, A., Mugasha, W. A., Muller-Landau, H. C., Mencuccini, M., Nelson, B. W., Ngomanda, A., Nogueira, E. M., Ortiz-Malavassi, E., … Vieilledent, G. (2014b). Improved allometric models to estimate the aboveground biomass of tropical trees. *Global Change Biology*, *20*(10), 3177–3190. https://doi.org/10.1111/gcb.12629

Collins, J. M., & Walsh, K. (2017). Hurricanes and Climate Change. *Hurricanes and Climate Change*, *3*, 1–255. https://doi.org/10.1007/978-3-319-47594-3

Comber, A., Brunsdon, C., Charlton, M., Dong, G., Harris, R., Lu, B., Lü, Y., Murakami, D., Nakaya, T., Wang, Y., & Harris, P. (2020). *The GWR route map: a guide to the informed application of Geographically Weighted Regression*. 1–34. http://arxiv.org/abs/2004.06070

Copernicus. (2022). *User Guides - Sentinel-1 SAR - Acquisition Modes - Sentinel Online - Sentinel Online*. https://sentinels.copernicus.eu/web/sentinel/user-guides/sentinel-1-sar/acquisition-modes

Coulibaly, J. Y., Chiputwa, B., Nakelse, T., & Kundhlande, G. (2017). Adoption of agroforestry and the impact on household food security among farmers in Malawi. In *Agricultural Systems* (Vol. 155, pp. 52–69). Elsevier Ltd. https://doi.org/10.1016/j.agsy.2017.03.017

Covey, K. R., Orefice, J., & Lee, X. (2012). The Physiological Ecology of Carbon Science in Forest Stands. In *Managing Forest Carbon in a Changing Climate* (pp. 31–49). Springer Netherlands. https://doi.org/10.1007/978-94-007-2232-3_3

da Costa, M. B. T., Silva, C. A., Broadbent, E. N., Leite, R. V., Mohan, M., Liesenberg, V., Stoddart, J., do Amaral, C. H., de Almeida, D. R. A., da Silva, A. L., Lucas, L. R., Cordeiro, V. A., Rex, F., Hirsch, A., Marcatti, G. E., Cardil, A., de Mendonça, B. A. F., Hamamura, C., Corte, A. P. D., … Klauberg, C. (2021). Beyond trees: Mapping total aboveground biomass density in the Brazilian savanna using high-density UAV-lidar data. *Forest Ecology and*

Management, *491*, 119155. https://doi.org/10.1016/J.FORECO.2021.119155

Dagnogo, F., Fofana, L., Konaté, D., Ousmane, T., Coulibaly, S. S., Dagnogo, F., Fofana, L., Konaté, D., Ousmane, T., & Coulibaly, S. S. (2021). Socio-Economic Impact of Shea Butter Production on the Living Conditions of Producers in the Regions of Poro and Tchologo (Northern Côte d'Ivoire). *Open Journal of Social Sciences*, *9*(11), 149–158. https://doi.org/10.4236/JSS.2021.911012

Damianidis, C., Santiago-Freijanes, J. J., den Herder, M., Burgess, P., Mosquera-Losada, M. R., Graves, A., Papadopoulos, A., Pisanelli, A., Camilli, F., Rois-Díaz, M., Kay, S., Palma, J. H. N., & Pantera, A. (2021). Agroforestry as a sustainable land use option to reduce wildfires risk in European Mediterranean areas. *Agroforestry Systems*, *95*(5), 919–929. https://doi.org/10.1007/S10457-020-00482-W/FIGURES/1

David, R. M., Rosser, N. J., & Donoghue, D. N. M. (2022). Improving above ground biomass estimates of Southern Africa dryland forests by combining Sentinel-1 SAR and Sentinel-2 multispectral imagery. *Remote Sensing of Environment*, *282*, 113232. https://doi.org/10.1016/J.RSE.2022.113232

Dehghan, H., & Ghassemian, H. (2007). Measurement of uncertainty by the entropy: application to the classification of MSS data. *Http://Dx.Doi.Org/10.1080/01431160600647225*, *27*(18), 4005–4014. https://doi.org/10.1080/01431160600647225

Dimobe, K., Ouédraogo, A., Ouédraogo, K., Goetze, D., Stein, K., Schmidt, M., Ivette Nacoulma, B. M., Gnoumou, A., Traoré, L., Porembski, S., & Thiombiano, A. (2020). Climate change reduces the distribution area of the shea tree (Vitellaria paradoxa C.F. Gaertn.) in Burkina Faso. *Journal of Arid Environments*, *181*, 104237. https://doi.org/10.1016/J.JARIDENV.2020.104237

Dubayah, R., Blair, J. B., Goetz, S., Fatoyinbo, L., Hansen, M., Healey, S., Hofton, M., Hurtt, G., Kellner, J., Luthcke, S., Armston, J., Tang, H., Duncanson, L., Hancock, S., Jantz, P., Marselis, S., Patterson, P. L., Qi, W., & Silva, C. (2020). The Global Ecosystem Dynamics Investigation: High-resolution laser ranging of the Earth's forests and topography. *Science of Remote Sensing*, *1*, 100002. https://doi.org/10.1016/J.SRS.2020.100002

Duncanson, L., Kellner, J. R., Armston, J., Dubayah, R., Minor, D. M., Hancock, S., Healey, S. P., Patterson, P. L., Saarela, S., Marselis, S., Silva, C. E., Bruening, J., Goetz, S. J., Tang, H., Hofton, M., Blair, B., Luthcke, S., Fatoyinbo, L., Abernethy, K., … Zgraggen, C. (2022). Aboveground biomass density models for NASA's Global Ecosystem Dynamics Investigation (GEDI) lidar mission. *Remote Sensing of Environment*, *270*, 112845. https://doi.org/10.1016/J.RSE.2021.112845

Duncanson, L., Neuenschwander, A., Hancock, S., Thomas, N., Fatoyinbo, T., Simard, M., Silva, C. A., Armston, J., Luthcke, S. B., Hofton, M., Kellner, J. R., & Dubayah, R. (2020). Biomass estimation from simulated GEDI, ICESat-2 and NISAR across environmental gradients in Sonoma County, California. *Remote Sensing of Environment*, *242*, 111779. https://doi.org/10.1016/J.RSE.2020.111779

ECOWAS. (2016). *Import and export | Economic Community of West African States(ECOWAS)*. https://www.ecowas.int/doing-business-in-ecowas/import-and-export/

El Hajj, M., Baghdadi, N., Bazzi, H., & Zribi, M. (2018). Penetration Analysis of SAR Signals in the C and L Bands for Wheat, Maize, and Grasslands. *Remote Sensing 2019, Vol. 11, Page 31*, *11*(1), 31. https://doi.org/10.3390/RS11010031

ESA. (2022). *ESA - The Sentinel missions*. https://www.esa.int/Applications/Observing_the_Earth/Copernicus/The_Sentinel_missions

EU. (2022). *EU Deforestation-free Regulation* (Vol. 2022, Issue December).

FAO. (2020). *Terms and Definitions FRA 2020*.

Federal Ministry for Economic Cooperation and Develpment (BMZ). (2020). *Climate Risk Profile : Côte d ' Ivoire*. https://www.pik-potsdam.de/en/institute/departments/climate-resilience/projects/project-pages/agrica/giz_climate-risk-profile-cote-d2019ivoire_en_final_2#:~:text=Depending on the scenario%2C temperature,north of Côte d'Ivoire.

Feliciano, D., Ledo, A., Hillier, J., & Nayak, D. R. (2018). Which agroforestry options give the greatest soil and above ground carbon benefits in different world regions? *Agriculture,*

Ecosystems and Environment, *254*, 117–129. https://doi.org/10.1016/J.AGEE.2017.11.032

Filella, guillem B. (2018). *Cocoa segmentation in Satellite images with deep learning*. ETH Zurich.

Fischer, R. A., Cottrell, E., Hauri, E., Lee, K. K. M., & Le Voyer, M. (2020). The carbon content of Earth and its core. *Proceedings of the National Academy of Sciences of the United States of America*, *117*(16), 8743–8749. https://doi.org/10.1073/PNAS.1919930117/-/DCSUPPLEMENTAL

Forkuor, G., Benewinde Zoungrana, J. B., Dimobe, K., Ouattara, B., Vadrevu, K. P., & Tondoh, J. E. (2020). Above-ground biomass mapping in West African dryland forest using Sentinel-1 and 2 datasets - A case study. *Remote Sensing of Environment*, *236*, 111496. https://doi.org/10.1016/J.RSE.2019.111496

Friedlingstein, P., O'Sullivan, M., Jones, M. W., Andrew, R. M., Gregor, L., Hauck, J., Le Quéré, C., Luijkx, I. T., Olsen, A., Peters, G. P., Peters, W., Pongratz, J., Schwingshackl, C., Sitch, S., Canadell, J. G., Ciais, P., Jackson, R. B., Alin, S. R., Alkama, R., … Zheng, B. (2022). Global Carbon Budget 2022. *Earth System Science Data*, *14*(11), 4811–4900. https://doi.org/10.5194/ESSD-14-4811-2022

Gao, Y., Skutsch, M., Paneque-Galvez, J., & Ghilardi, A. (2020). Remote sensing of forest degradation: a review. *Environmental Research Letters*, *15*. https://doi.org/10.1088/1748-9326/abaad7

Genuer, R., Poggi, J. M., & Tuleau-Malot, C. (2015). VSURF: An R package for variable selection using random forests. *R Journal*, *7*(2), 19–33. https://doi.org/10.32614/rj-2015-018

GFOI. (2018). *A Layman's Interpretation Guide to L-band and C-band Synthetic Aperture Radar data*.

Ghosh, S. M., & Behera, M. D. (2021). Aboveground biomass estimates of tropical mangrove forest using Sentinel-1 SAR coherence data - The superiority of deep learning over a semi-empirical model. *Computers & Geosciences*, *150*, 104737. https://doi.org/10.1016/J.CAGEO.2021.104737

Giacco, F., Thiel, C., Pugliese, L., Scarpetta, S., & Marinaro, M. (2010). Uncertainty analysis for the classification of multispectral satellite images using SVMs and SOMs. *IEEE Transactions on Geoscience and Remote Sensing*, *48*(10), 3769–3779. https://doi.org/10.1109/TGRS.2010.2047863

GIZ. (2020). *Strengthening governance and sustainable management of natural resources in the Comoé and Taï regions*. https://www.giz.de/en/worldwide/30013.html

Gomes, L. C., Bianchi, F. J. J. A., Cardoso, I. M., Fernandes, R. B. A., Filho, E. I. F., & Schulte, R. P. O. (2020). Agroforestry systems can mitigate the impacts of climate change on coffee production: A spatially explicit assessment in Brazil. *Agriculture, Ecosystems and Environment*, *294*(January), 106858. https://doi.org/10.1016/j.agee.2020.106858

GVR. (2019). *Cocoa Beans Market Size, Analysis | Global Industry Report, 2019-2025*. https://www.grandviewresearch.com/industry-analysis/cocoa-beans-market

Gytarsky, J. P., Hiraishi, T., Krug, T., Kruger, D., Pipatti, R., Buendia, L., Miwa, K., Ngara, T., Tanabe, K., & Wagner, F. (2015). Good Practice Guidance for Land Use, Land-Use Change and Forestry. In *Comptes Rendus - Biologies* (Vol. 338, Issue 2). https://doi.org/10.1016/j.crvi.2014.11.004

Hall-Beyer, M. (2017). *GLCM Texture: A tutorial v.3.0 March 2017*. http://www.ucalgary.ca/UofC/nasdev/mhallbey/research.htm

Hirata, Y., Takao, G., Sato, T., & Toriyama, J. (2012). *REDD-plus Cookbook. REDD Research and Development center, Forestry and Forest Products Research Institute Japan*.

Houghton, R. A., House, J. I., Pongratz, J., Van Der Werf, G. R., Defries, R. S., Hansen, M. C., Le Quéré, C., & Ramankutty, N. (2012). Carbon emissions from land use and land-cover change. *Biogeosciences*, *9*(12), 5125–5142. https://doi.org/10.5194/BG-9-5125-2012

Howard, S., & Nair, R. (1988). Agroforestry - A Decade of Development. Edited by H. A. Steppler and P. K. R. Nair. Nairobi: International Council for Research in Agroforestry (1987), pp. 335, $30.00. *Experimental Agriculture*, *24*(3), 393–393. https://doi.org/10.1017/s0014479700016252

Huang, X., Ziniti, B., Torbick, N., & Ducey, M. J. (2018). Assessment of Forest above Ground Biomass Estimation Using Multi-Temporal C-band Sentinel-1 and Polarimetric L-band PALSAR-2 Data. *Remote Sensing 2018, Vol. 10, Page 1424*, *10*(9), 1424. https://doi.org/10.3390/RS10091424

ICRC. (2021). *Burkina Faso: climate fact sheet*. https://www.climatecentre.org/wp-content/uploads/RCCC-ICRC-Country-profiles-Burkina_Faso.pdf

ILO. (2017). *Global estimates of child labour: Results and trends, 2012-2016 International Labour Office (ILO), Geneva, 2017 ISBN: 978-92-2-130152-3 (print) ISBN: 978-92-2-130153-0.*

International Anti-slavery. (2004). The cocoa industry in West Africa: a history of exploitation. In *Thomas Clarkson House*. https://doi.org/10.1038/164306b0

IPCC. (2018). *Global warning of 1.5°C: An IPCC Special Report on the impacts of global warming of 1.5°C above pre-industrial levels and related global greenhouse gas emission pathways, in the context of strengthening the global response to the threat of climate change* . https://doi.org/10.1017/9781009157940.008

IPCC. (2019). *2019 Refinement to the 2006 IPCC Guidelines for National Greenhouse Gas Inventories, Calvo Buendia, E., Tanabe, K., Kranjc, A., Baasansuren, J., Fukuda, M., Ngarize, S., Osako, A., Pyrozhenko, Y., Shermanau, P. and Federici, S. (eds).* www.ipcc-nggip.iges.or.jp

Jones Kachamba, D., Ørka, H. O., Gobakken, T., Eid, T., Mwase, W., Melgani, F., Nex, F., Moreno, J., Atzberger, C., & Thenkabail, P. S. (2016). Biomass Estimation Using 3D Data from Unmanned Aerial Vehicle Imagery in a Tropical Woodland. *Remote Sensing 2016, Vol. 8, Page 968*, *8*(11), 968. https://doi.org/10.3390/RS8110968

Kanmegne, J. (2004). *Slash and Burn Agriculture in the Humid Forest Zone of Southern Cameroon: Soil Quality Dynamics, Improved Fallow Management and Farmers' Perceptions*. University of Wageningen.

Kanmegne Tamga, D., Latifi, H., Ullmann, T., Baumhauer, R., Bayala, J., & Thiel, M. (2022).

Estimation of Aboveground Biomass in Agroforestry Systems over Three Climatic Regions in West Africa Using Sentinel-1, Sentinel-2, ALOS, and GEDI Data. *Sensors 2023, Vol. 23, Page 349*, *23*(1), 349. https://doi.org/10.3390/S23010349

Kanmegne Tamga, D., Latifi, H., Ullmann, T., Baumhauer, R., Thiel, M., & Bayala, J. (2022). Modelling the spatial distribution of the classification error of remote sensing data in cocoa agroforestry systems. *Agroforestry Systems*. https://doi.org/10.1007/s10457-022-00791-2

Kirkland, L.-A., Kanfer, F., & Millard, S. (2015). Lasso Tuning parameter selection. *Proceedings of the 57th Annual Conference of SASA*, 49–56. https://www.researchgate.net/publication/287727878_LASSO_Tuning_Parameter_Selection

Knauer, K., Gessner, U., Fensholt, R., Forkuor, G., & Kuenzer, C. (2017). Monitoring agricultural expansion in Burkina Faso over 14 years with 30 m resolution time series: The role of population growth and implications for the environment. *Remote Sensing*, *9*(2). https://doi.org/10.3390/rs9020132

Koné, M. (2010). *Analysis of the Cashew Sector Value Chain in Côte d ' Ivoire*. 67pp.

Lasky, J. R., Uriarte, M., Boukili, V. K., Erickson, D. L., John Kress, W., & Chazdon, R. L. (2014). The relationship between tree biodiversity and biomass dynamics changes with tropical forest succession. *Ecology Letters*, *17*(9), 1158–1167. https://doi.org/10.1111/ELE.12322

Leakey, R. R. B. (2017). Agroforestry Tree Products (AFTPs): Targeting Poverty Reduction and Enhanced Livelihoods: This chapter was previously published in Leakey, R.R.B., Tchoundjeu, Z., Schreckenberg, K., Shackleton, S., Shackleton, C., 2005. International Journal of Agricultural Sustainability, 3, 1–23, with permission of Taylor & Francis. *Multifunctional Agriculture*, 123–138. https://doi.org/10.1016/B978-0-12-805356-0.00013-1

Leite, R. V., Silva, C. A., Broadbent, E. N., Amaral, C. H. do, Liesenberg, V., Almeida, D. R. A. de, Mohan, M., Godinho, S., Cardil, A., Hamamura, C., Faria, B. L. de, Brancalion, P. H. S., Hirsch, A., Marcatti, G. E., Dalla Corte, A. P., Zambrano, A. M. A., Costa, M. B. T. da, Matricardi, E. A. T., Silva, A. L. da, … Klauberg, C. (2022). Large scale multi-layer fuel load characterization in tropical savanna using GEDI spaceborne lidar data. *Remote Sensing of*

Environment, *268*, 112764. https://doi.org/10.1016/J.RSE.2021.112764

Lin, Y., Zeng, Z., Chen, L., & Deng, Z. (2023). *The Relation Between the CO 2 Concentration Levels and the Temperature*. *03014*.

Lindner, T., Guo, H., Wang, H., Song, X., & Ruan, Z. (2023). Anomaly Detection of Remote Sensing Images Based on the Channel Attention Mechanism and LRX. *Applied Sciences 2023, Vol. 13, Page 6988*, *13*(12), 6988. https://doi.org/10.3390/APP13126988

Lone, J. M., Sivasankar, T., Pebam, R., Sarma, K. K., Qadir, M. A., & P.L.N. (2018). *(PDF) Comparison of C-band Sentinel-1 and L-band ALOSPALSAR-2 data for Aboveground Forest biomass estimation over Nongkhyllem Forest Reserve and Wildlife Sanctuary, Meghalaya,India*. https://www.researchgate.net/publication/325144897_Comparison_of_C-band_Sentinel-1_and_L-band_ALOSPALSAR-2_data_for_Aboveground_Forest_biomass_estimation_over_Nongkhyllem_Forest_Reserve_and_Wildlife_Sanctuary_MeghalayaIndia

Loosvelt, L., Peters, J., Skriver, H., Lievens, H., Van Coillie, F. M. B., De Baets, B., & Verhoest, N. E. C. (2012). Random Forests as a tool for estimating uncertainty at pixel-level in SAR image classification. *International Journal of Applied Earth Observation and Geoinformation*, *19*(1), 173–184. https://doi.org/10.1016/J.JAG.2012.05.011

Lundgren, B., Raint, J., & Director, ee. (1983). *Sustained Agroforestry*.

Madden, M. G. ;, Munroe, D. T., & Madden, M. G. (2005). *Multi-Class and Single-Class Classification Approaches to Vehicle Model Recognition from Images*. https://aran.library.nuigalway.ie/handle/10379/191

Maesano, M., Santopuoli, G., Valerio Moresi, F., Matteucci, G., Lasserre, B., & Scarascia Mugnozza, G. (2022). Above ground biomass estimation from UAV high resolution RGB images and LiDAR data in a pine forest in Southern Italy. *Biogeosciences and Forestry*, *15*, 451–457. https://doi.org/10.3832/ifor3781-015

Malhi, R. K. M., Anand, A., Srivastava, P. K., Chaudhary, S. K., Pandey, M. K., Behera, M. D., Kumar, A., Singh, P., & Sandhya Kiran, G. (2022). Synergistic evaluation of Sentinel 1 and

2 for biomass estimation in a tropical forest of India. *Advances in Space Research*, *69*(4), 1752–1767. https://doi.org/10.1016/J.ASR.2021.03.035

Marsh, R., & van Sebille, E. (2021). Ocean currents, heat transport, and climate. *Ocean Currents*, 497–520. https://doi.org/10.1016/B978-0-12-816059-6.00010-3

Meng, X., Zhu, Y., Yin, M., & Liu, D. (2021). The impact of land use and rainfall patterns on the soil loss of the hillslope. *Scientific Reports 2021 11:1*, *11*(1), 1–10. https://doi.org/10.1038/s41598-021-95819-5

Milenković, M., Reiche, J., Armston, J., Neuenschwander, A., De Keersmaecker, W., Herold, M., & Verbesselt, J. (2022). Assessing Amazon rainforest regrowth with GEDI and ICESat-2 data. *Science of Remote Sensing*, *5*, 100051. https://doi.org/10.1016/J.SRS.2022.100051

Minang, P. A., Duguma, L. A., Bernard, F., Mertz, O., & van Noordwijk, M. (2014). Prospects for agroforestry in REDD+ landscapes in Africa. In *Current Opinion in Environmental Sustainability* (Vol. 6, Issue 1, pp. 78–82). https://doi.org/10.1016/j.cosust.2013.10.015

Mitchell, A. L., Rosenqvist, A., & Mora, B. (2017). Current remote sensing approaches to monitoring forest degradation in support of countries measurement, reporting and verification (MRV) systems for REDD+. *Carbon Balance and Management*, *12*(1), 1–22. https://doi.org/10.1186/S13021-017-0078-9/TABLES/2

MONGABAY. (2020). *Forest data: Total Africa Deforestation Rates and Related Forestry Figures*. https://rainforests.mongabay.com/deforestation/archive/Total_Africa.htm

Musthafa, M., & Singh, G. (2022). Forest above-ground woody biomass estimation using multi-temporal space-borne LiDAR data in a managed forest at Haldwani, India. *Advances in Space Research*, *69*(9), 3245–3257. https://doi.org/10.1016/J.ASR.2022.02.002

Naidoo, L., Mathieu, R., Main, R., Kleynhans, W., Wessels, K., Asner, G., & Leblon, B. (2015). Savannah woody structure modelling and mapping using multi-frequency (X-, C- and L-band) Synthetic Aperture Radar data. *ISPRS Journal of Photogrammetry and Remote Sensing*, *105*, 234–250. https://doi.org/10.1016/j.isprsjprs.2015.04.007

Nair, P. K. R., Kumar, B. M., & Nair, V. D. (2009). Agroforestry as a strategy for carbon

sequestration. *Journal of Plant Nutrition and Soil Science*, *172*(1), 10–23. https://doi.org/10.1002/jpln.200800030

Nair, P. R., & Nair, V. D. (2014). Solid-fluid-gas: The state of knowledge on carbon-sequestration potential of agroforestry systems in africa. *Current Opinion in Environmental Sustainability*, *6*(1), 22–27. https://doi.org/10.1016/j.cosust.2013.07.014

Nayak, A. K., Rahman, M. M., Naidu, R., Dhal, B., Swain, C. K., Nayak, A. D., Tripathi, R., Shahid, M., Islam, M. R., & Pathak, H. (2019). Current and emerging methodologies for estimating carbon sequestration in agricultural soils: A review. *Science of The Total Environment*, *665*, 890–912. https://doi.org/10.1016/J.SCITOTENV.2019.02.125

Negash, M., & Kanninen, M. (2015). Modeling biomass and soil carbon sequestration of indigenous agroforestry systems using CO2FIX approach. *Agriculture, Ecosystems and Environment*, *203*, 147–155. https://doi.org/10.1016/j.agee.2015.02.004

NFI. (2023). *When was Photography Invented? - Everything you need to know - NFI*. https://www.nfi.edu/when-was-photography-invented/

NISAR. (n.d.). *Overview | Get to Know SAR – NASA-ISRO SAR Mission (NISAR)*. Retrieved January 17, 2023, from https://nisar.jpl.nasa.gov/mission/get-to-know-sar/overview/

Numbisi, F. N., Van Coillie, F. M. B., & De Wulf, R. (2019). Delineation of cocoa agroforests using multiseason sentinel-1 SAR images: A low grey level range reduces uncertainties in GLCM texture-based mapping. *ISPRS International Journal of Geo-Information*, *8*(4). https://doi.org/10.3390/ijgi8040179

Nuthammachot, N., Askar, A., Stratoulias, D., & Wicaksono, P. (2020). *Combined use of Sentinel-1 and Sentinel-2 data for improving above-ground biomass estimation*. https://doi.org/10.1080/10106049.2020.1726507

Owusu, S., Anglaaere, L. C. N., & Abugre, S. (2018). Aboveground Biomass and Carbon content of a cocoa –Gliricida sepium agroforestry system in Ghana. *Ghana Journal of Agricultural Science*, *53*(0), 45. https://doi.org/10.4314/gjas.v53i1.4

PALSAR. (2022). *PALSAR Overview - Earth Online*.

https://earth.esa.int/eogateway/instruments/palsar/description

Pesola, L., Cheng, X., Sanesi, G., Colangelo, G., Elia, M., & Lafortezza, R. (2017). Linking above-ground biomass and biodiversity to stand development in urban forest areas: A case study in Northern Italy. *Landscape and Urban Planning*, *157*, 90–97. https://doi.org/10.1016/J.LANDURBPLAN.2016.06.004

Pineda Jaimes, N. B., Bosque Sendra, J., Gómez Delgado, M., & Franco Plata, R. (2010). Exploring the driving forces behind deforestation in the state of Mexico (Mexico) using geographically weighted regression. *Applied Geography*, *30*(4), 576–591. https://doi.org/10.1016/J.APGEOG.2010.05.004

Pourshamsi, M., Xia, J., Yokoya, N., Garcia, M., Lavalle, M., Pottier, E., & Balzter, H. (2021). Tropical forest canopy height estimation from combined polarimetric SAR and LiDAR using machine-learning. *ISPRS Journal of Photogrammetry and Remote Sensing*, *172*, 79–94. https://doi.org/10.1016/j.isprsjprs.2020.11.008

Propastin, P. (2012). Modifying geographically weighted regression for estimating aboveground biomass in tropical rainforests by multispectral remote sensing data. *International Journal of Applied Earth Observation and Geoinformation*, *18*(1), 82–90. https://doi.org/10.1016/J.JAG.2011.12.013

Qureshi, A., Pariva, Badola, R., & Hussain, S. A. (2012). A review of protocols used for assessment of carbon stock in forested landscapes. *Environmental Science & Policy*, *16*, 81–89. https://doi.org/10.1016/J.ENVSCI.2011.11.001

Ramachandran Nair, P. K., Nair, V. D., Mohan Kumar, B., & Showalter, J. M. (2010). Carbon sequestration in agroforestry systems. In *Advances in Agronomy* (Vol. 108, Issue C). Academic Press. https://doi.org/10.1016/S0065-2113(10)08005-3

Rege, A., Warnekar, S. B., & Lee, J. S. H. (2022). Mapping cashew monocultures in the Western Ghats using optical and radar imagery in Google Earth Engine. *Remote Sensing Applications: Society and Environment*, *28*, 100861. https://doi.org/10.1016/J.RSASE.2022.100861

Riezebos, E. P., Vooren, A. P., & Guillaumet, J. L. (1994). *Le Parc National de Taï, Côte d'Ivoire.*

I: Synthesis of knowledge. II: Bibliography.

Roodposhti, M. S., Aryal, J., Lucieer, A., & Bryan, B. A. (2019). Uncertainty assessment of hyperspectral image classification: Deep learning vs. random forest. *Entropy*, *21*(1), 1–15. https://doi.org/10.3390/e21010078

Rosati, A., Paoletti, A., Al Harir, R., & Famiani, F. (2018). Fruit production and branching density affect shoot and whole-tree wood to leaf biomass ratio in olive. *Tree Physiology*, *38*(9), 1278–1285. https://doi.org/10.1093/TREEPHYS/TPY009

Ruf, F., Schroth, G., & Doffangui, K. (2014). Climate change, cocoa migrations and deforestation in West Africa: What does the past tell us about the future? *Sustainability Science 2014 10:1*, *10*(1), 101–111. https://doi.org/10.1007/S11625-014-0282-4

Sabas, B. Y. S., Danmo, K. G., Madeleine, K. A. T., & Jan, B. (2020). Cocoa Production and Forest Dynamics in Ivory Coast from 1985 to 2019. *Land 2020, Vol. 9, Page 524*, *9*(12), 524. https://doi.org/10.3390/LAND9120524

Schwaab, J., Meier, R., Davin, E. L., & Bürgi, C. (2021). *The role of urban trees in reducing land surface temperatures in European cities*. *2021*, 1–11. https://doi.org/10.1038/s41467-021-26768-w

Shahbandeh, M. (2021). *Cocoa production by country 2019/2020 | Statista*. https://www.statista.com/statistics/263855/cocoa-bean-production-worldwide-by-region/

Shahidan, M. F., Salleh, D. E., & Mohd Shariff, M. K. (2006). The influence of tree canopy on the thermal environment in a tropical climate : A preliminary study. *INTA Conference-Harmony in Culture and Nature, January 2006*.

Shao, Z., & Zhang, L. (2016). Estimating Forest Aboveground Biomass by Combining Optical and SAR Data: A Case Study in Genhe, Inner Mongolia, China. *Sensors (Basel, Switzerland)*, *16*(6). https://doi.org/10.3390/S16060834

Silva, C. A., Duncanson, L., Hancock, S., Neuenschwander, A., Thomas, N., Hofton, M., Fatoyinbo, L., Simard, M., Marshak, C. Z., Armston, J., Lutchke, S., & Dubayah, R. (2021). Fusing simulated GEDI, ICESat-2 and NISAR data for regional aboveground biomass

mapping. *Remote Sensing of Environment*, *253*. https://doi.org/10.1016/J.RSE.2020.112234

Somarriba, E., Cerda, R., Orozco, L., Cifuentes, M., Dávila, H., Espin, T., Mavisoy, H., Ávila, G., Alvarado, E., Poveda, V., Astorga, C., Say, E., & Deheuvels, O. (2013). Carbon stocks and cocoa yields in agroforestry systems of Central America. *Agriculture, Ecosystems and Environment*, *173*, 46–57. https://doi.org/10.1016/j.agee.2013.04.013

Stehman, S. V. (1997). Selecting and interpreting measures of thematic classification accuracy. *Remote Sensing of Environment*, *62*(1), 77–89. https://doi.org/10.1016/S0034-4257(97)00083-7

Steppler, H. A., & Ramachandran Nair, P. K. (1987). *Agroforestry a decade of development*.

Tadese, S., Soromessa, T., Bekele, T., Bereta, A., & Temesgen, F. (2019). Above Ground Biomass Estimation Methods and Challenges: A Review. *Journal of Energy Technologies and Policy*, *9*(8), 12–25. https://doi.org/10.7176/jetp/9-8-02

Thangata, P. H., & Hildebrand, P. E. (2012). Carbon stock and sequestration potential of agroforestry systems in smallholder agroecosystems of sub-Saharan Africa: Mechanisms for "reducing emissions from deforestation and forest degradation" (REDD+). *Agriculture, Ecosystems and Environment*, *158*, 172–183. https://doi.org/10.1016/j.agee.2012.06.007

Tiwari, A. K., & Singh, J. S. (1984). Mapping forest biomass in India through aerial photographs and nondestructive field sampling. *Applied Geography*, *4*(2), 151–165. https://doi.org/10.1016/0143-6228(84)90019-5

Tondoh, J. E., Kouamé, F. N. guessa., Martinez Guéi, A., Sey, B., Wowo Koné, A., & Gnessougou, N. (2015). Ecological changes induced by full-sun cocoa farming in CÔte d'Ivoire. *Global Ecology and Conservation*, *3*, 575–595. https://doi.org/10.1016/j.gecco.2015.02.007

Tschora, H., & Cherubini, F. (2020). Co-benefits and trade-offs of agroforestry for climate change mitigation and other sustainability goals in West Africa. *Global Ecology and Conservation*, *22*, e00919. https://doi.org/10.1016/j.gecco.2020.e00919

UNDP. (2022). *Report 2021/2022*.

Vatandaşlar, C., & Abdikan, S. (2022). Carbon stock estimation by dual-polarized synthetic

aperture radar (SAR) and forest inventory data in a Mediterranean forest landscape. *J. For. Res*, *33*, 827–838. https://doi.org/10.1007/s11676-021-01363-3

Vizzari, M. (2022). PlanetScope, Sentinel-2, and Sentinel-1 Data Integration for Object-Based Land Cover Classification in Google Earth Engine. *Remote Sensing*, *14*(11), 2628. https://doi.org/10.3390/RS14112628/S1

Von Maillot, A. (2020). *Tackling Deforestation We are committed to ending deforestation in our cocoa supply chain, and preserving and restoring existing forests Contents*.

Wadudu, A., Mohammed, A.-, Baah-Ennumh, T., Rahim, Y., & Abdulai, A. (2016). Role of the Shea Industry in the Socio-economic Lives of Women in the West Mamprusi District of Northern Ghana. *JOURNAL OF SOCIAL SCIENCE RESEARCH*, *10*(1), 1968–1977. https://doi.org/10.24297/JSSR.V10I1.4756

Wagner, F. H., Dalagnol, R., Silva-Junior, C. H. L., Carter, G., Ritz, A. L., Hirye, M. C. M., Ometto, J. P. H. B., & Saatchi, S. (2023). Mapping Tropical Forest Cover and Deforestation with Planet NICFI Satellite Images and Deep Learning in Mato Grosso State (Brazil) from 2015 to 2021. *Remote Sensing 2023, Vol. 15, Page 521*, *15*(2), 521. https://doi.org/10.3390/RS15020521

Wang, D., Wan, B., Liu, J., Su, Y., Guo, Q., Qiu, P., & Wu, X. (2020). Estimating aboveground biomass of the mangrove forests on northeast Hainan Island in China using an upscaling method from field plots, UAV-LiDAR data and Sentinel-2 imagery. *International Journal of Applied Earth Observation and Geoinformation*, *85*. https://doi.org/10.1016/J.JAG.2019.101986

Warren-Thomas, E., Nelson, L., Juthong, W., Bumrungsri, S., Brattström, O., Stroesser, L., Chambon, B., Penot, É., Tongkaemkaew, U., Edwards, D. P., & Dolman, P. M. (2020). Rubber agroforestry in Thailand provides some biodiversity benefits without reducing yields. *Journal of Applied Ecology*, *57*(1), 17–30. https://doi.org/10.1111/1365-2664.13530

Widdicombe, S., & Spicer, J. I. (2008). Predicting the impact of ocean acidification on benthic biodiversity: What can animal physiology tell us? *Journal of Experimental Marine Biology and Ecology*, *366*(1–2), 187–197. https://doi.org/10.1016/J.JEMBE.2008.07.024

WPR. (2023). *Cashew Production by Country 2023*. https://worldpopulationreview.com/country-rankings/cashew-production-by-country

Wulder, M., Hermosilla, T., White, J., & Coops, N. (2020). Biomass status and dynamics over Canada's forests: Disentangling disturbed area from associated aboveground biomass consequences. *Environmental Research Letters*, *15*. https://doi.org/10.1088/1748-9326/ab8b11

Yemefack, M. (2005). *Modelling and Monitoring Soil and Land Use Dynamics Within Shifting Agricultural Landscape Mosaic Systems in Southern Cameroon*. University of Twente, ITC.

Yin, L., Ghosh, R., Lin, C., Hale, D., Weigl, C., Obarowski, J., Zhou, J., Till, J., Jia, X., You, N., Mao, T., Kumar, V., & Jin, Z. (2023). Mapping smallholder cashew plantations to inform sustainable tree crop expansion in Benin. *Remote Sensing of Environment*, *295*, 113695. https://doi.org/10.1016/J.RSE.2023.113695

Zhang, W., Brandt, M., Wang, Q., Prishchepov, A. V., Tucker, C. J., Li, Y., Lyu, H., & Fensholt, R. (2019). From woody cover to woody canopies: How Sentinel-1 and Sentinel-2 data advance the mapping of woody plants in savannas. *Remote Sensing of Environment*, *234*, 111465. https://doi.org/10.1016/j.rse.2019.111465

Zhao, M., A, G., Liu, Y., & Konings, A. G. (2022). Evapotranspiration frequently increases during droughts. *Nature Climate Change 2022 12:11*, *12*(11), 1024–1030. https://doi.org/10.1038/s41558-022-01505-3

Zomer, R. J., Bossio, D. A., Trabucco, A., Van Noordwijk, M., & Xu, J. (2022). Global carbon sequestration potential of agroforestry and increased tree cover on agricultural land. *Circular Agricultural Systems*, *2*(3). https://doi.org/10.48130/CAS-2022-0003

Zoungrana, A., De Cannière, C., Cissé, M., Bationo, B. A., Traoré, S., & Visser, M. (2023). Does the social status of farmers determine the sustainable management of agroforestry parklands located near protected areas in Burkina Faso (West Africa)? *Global Ecology and Conservation*, *44*, e02476. https://doi.org/10.1016/J.GECCO.2023.E02476

Zvoleff, A. (2020). *glcm: Calculate Texture from Grey-Level Co-Occurence Matrices (GLCMs).*

R package version 1.6.5. htpps://cran.r-project.org/package=glcm

Acknowledgments

Alles vermag ich in dem, der mich kräftigt

The present work would have not been possible without the contribution and support from third parties that I would like to acknowledge in this section. I am grateful to:

- The German Federal Ministry of Education and Research (BMBF) for the financial support via the project carrier at the German Aerospace Centre (DL projektträger) through the research project: WASCAL-DE-Coop (FKZ: 01LG1808A).
- The Graduate School of Science and Technology (GSST) of the University of Würzburg for the opportunity I have been granted to carry my research as a PhD student.
- The World Agroforestry Centre (ICRAF-Abidjan) for supporting my field work activities. I am thankful to my supervisor at ICRAF Dr Jules Bayala, who has contributed actively to the publications from this research. to Dr Alain Atangana who helped me in the organization of the operations on the field; To Augustin Yra and Michael Kouame who assisted me during field campaign in Côte d'Ivoire.
- My supervisors Prof. Dr. Tobias Ullmann, PD Dr. Hooman Latifi and Prof. Dr. Roland Baumhauer for their support and mentoring during my PhD research. Thank you for your support in designing and publishing the results of my research.
- My colleagues from the WASCAL-DE-Coop project: Dr Michael Thiel (project leader), Dr Sarah Schönbrodt-Stitt, and Sabine Oppmann for their support and mentoring both in my academic and private life.
- My colleagues from the Department of Remote Sensing of the University of Würzburg for the nice environment that prevailed during my time there. I am thinking of Dr Martin Weggmann, Dr Mirjana Bevanda, Dr Insa Otte, Christine Linge and Dagmar Tepass
- My PhD fellows, namely Boris Ouattara, Alexandra Bell, Itohan-Osa, Adomas Liepa, Maninder Singh Dhillon, Jakob Schwalb-Willmann, and Steven Hill for the nice time we shared together during my time in Würzburg. I wish you all the best in life guys.
- My family, without whom I could not have completed this work. I am thinking of my thinking of my lovely wife Sandrine Foka Kanmegne for her love, to my mother Michelle

Solange Medjoda for the encouragement and moral support, and to my sisters Grace Tchemtchoua, Ann Mboudou and Carmen Kanmegne for their availability and kindness.

- My mentors Pr Eric Smaling, Pr Lijbert Brussard and Dr Fabrice Tiba, who helped me to grow as a scientist and as a man. I am thankful for the advice and guidance that you have always provided.
- The family of my friends in Germany and in France. I am thinking of the family of Mbama Boniface, William Massoma, Emmanuel Mbo, Christian Tsamo and Alain Ngaha, Jules-Rodrigue Nuemo, Yannick Yami, Georges Ngako and Nicaise Nguetse.
- The mothers I met, who were very supportive. I am thinking of Amina, Alice, Dr Laura Kouam and Michelle Ngoube
- My friends in Würzburg Kevin Yomi, Alexi Nana, Glory Amougou and Leaticia Fakam, just to name a few.

"If everyone played the drums, there would be no one to dance". I would like to thank those who participated in one way or another in the realization of this work, those who played and those who danced. May God reward you a hundredfold.

Affidavit

I hereby confirm that my thesis entitled "**Modelling Carbon Sequestration in Agroforestry Systems in West Africa using Remote Sensing",** is the result of my own work. I did not receive any help or contribution form commercial consultants. All sources and / or materials applied are listed and specified in the thesis.

Furthermore, I confirm that this thesis has not yet been submitted as part of another examination process neither in identical nor in similar form.

Place, Date: Signature

Eidesstattliche Erklärung

Hiermit erkläre ich an Eides statt, die Dissertation ***Modellierung der Kohlenstoffbindung von agroforstwirtschaftlichen Systemen in Westafrika mit Fernerkungdung*** eigenständig, d.h. insbesondere selbständig und ohne Hilfe eines kommerziellen Promotionsberaters, angefertigt und keine anderen als die von mir angegebenen Quellen und Hilfsmittel verwendet zu haben.

Ich erkläre außerdem, dass die Dissertation weder in gleicher noch in ähnlicher Form bereits in einem anderen Prüfungsverfahren vorgelegen hat.

Ort, Datum: Unterschrift